

DRAINAGE DESIGN
BASED UPON AERATION

by
Harold R. Duke

June 1973



HYDROLOGY PAPERS
COLORADO STATE UNIVERSITY
Fort Collins, Colorado

DRAINAGE DESIGN BASED UPON AERATION

**By
Harold R. Duke**

**HYDROLOGY PAPERS
COLORADO STATE UNIVERSITY
FORT COLLINS, COLORADO 80521**

June 1973

No. 61

TABLE OF CONTENTS

<u>Chapter</u>	<u>Page</u>
ABSTRACT	iv
ACKNOWLEDGMENTS	iv
INTRODUCTION	1
REVIEW OF LITERATURE	2
Soil Aeration	2
Classical Drainage Theories	2
Parameters Describing Capillary Properties	3
Significance of the Capillary Fringe	4
ANALYSIS OF THE PROBLEM	7
Equivalent Permeable Height	7
Equivalent Saturated Height	11
Height of Zone of Insufficient Aeration	12
EXPERIMENTAL PROCEDURES	14
Physical Model Experiments	14
Numerical Evaluations	14
RESULTS AND DISCUSSION	16
Inadequacy of Classical Drainage Theories	16
Influence of Soil Parameters Upon Capillary Phenomena	17
Verification of the Numerical Model	20
Shape and Position of the Water Table	21
Region of Aeration	25
CONCLUSIONS AND RECOMMENDATIONS	29
LITERATURE CITED	30
APPENDIX A - ONE-DIMENSIONAL NUMERICAL MODEL	32
The Finite-Difference Equations	32
Boundary and Initial Conditions	33
Solution Technique	33
Program FLODF	34
APPENDIX B - PHYSICAL PROPERTIES OF SOILS AND FLUID	41
APPENDIX C - COMPUTED SATURATION PROFILES	42
APPENDIX D - SCALED EFFECTIVE PERMEABLE AND SATURATED HEIGHTS	43
APPENDIX E - COMPARISON OF EXPERIMENTAL AND NUMERICAL RESULTS	44
APPENDIX F - RESULTS OF NUMERICAL ANALYSES	48

ABSTRACT

The effects of soil aeration requirements on permissible drain spacing were analyzed for both equilibrium and transient drainage problem. The presence of a zone of insufficient aeration above the water table requires that drain spacing must be narrower than is calculated by classical techniques if the plant root zone is maintained adequately aerated.

A one-dimensional model was developed to simulate drainage in soils where the flow and storage in the capillary region are significant. The contribution of the capillary region was described analytically in terms of the measureable soil properties and the rate of percolation to the water table. Drainage tests conducted in a sand-filled flume confirmed that the numerical model adequately described the total flow system.

Further analyses were conducted using the numerical model to determine the effects of bubbling pressure head and pore-size distribution on the position of the water table. These analyses showed that the water table is always lower than predicted by methods that ignore the capillary region. The lowering of the water table by the presence of the capillary region is increased by a higher bubbling pressure, a wider distribution of pore sizes, and a larger percolation rate.

It was shown that the region of inadequate aeration is always thicker than the amount by which capillary flow lowers the water table. As a result, the depth of aerated soil is always less than predicted by the classical drainage equations.

ACKNOWLEDGMENTS

This paper is based on the Ph.D. dissertation entitled "Drainage Design Based upon Aeration" prepared by H. R. Duke. The author wishes to express his appreciation to the members of his graduate committee: Drs. R.E. Danielson, Arnold Klute, D. B. McWhorter and especially to Dr. A. T. Corey, for their guidance and suggestions throughout this study.

The Agricultural Research Service of the U. S. Department of Agriculture provided financial support for this study.

DRAINAGE DESIGN BASED UPON AERATION^{1/}

by Harold R. Duke^{2/}

INTRODUCTION

Although aeration of the crop root zone is one of the primary objectives of agricultural drainage, present methods of design consider this factor only insofar as the depth of water table is specified. Any mathematical description of the partially saturated region above the water table so complicates the differential equations of flow that analytical solutions in closed form are impractical. Yet, in many situations, the region of capillary flow has a significant, if not dominant, effect upon the performance of agricultural drains. This is particularly true in areas having fine-textured soils and relatively shallow aquifers.

The equations resulting from considering flow in the partially saturated region are highly nonlinear, second-order partial differential equations. The recent generation of high-speed, large-capacity digital computers has opened the way for practical solutions to equations of this type.

This study utilizes a mathematical model based upon the Dupuit-Forchheimer assumptions to analyze the combined effects of saturated and partially saturated flow upon the performance of drains in shallow aquifers.

The primary objectives of this study are:

1. To evaluate the effect of soil capillary parameters upon the depth of soil above the water table which has sufficiently low saturation to permit adequate soil aeration. This evaluation requires determining the effects of capillarity upon the flow and storage of water above the water table as well as upon the shape and position of the water table.
2. To illustrate, for the specific conditions analyzed, how consideration of soil aeration could influence the design of drainage systems.

3. To develop a computer solution that permits objectives (1) and (2) to be achieved and at the same time is sufficiently simple and economical to be practical.

Current technology could provide a more rigorous mathematical approach than has been attempted here, since this approach accepts the Dupuit-Forchheimer approximation. However, it is questionable whether present techniques of field evaluation justify a more rigorous approach. The predicted performance is shown to agree quite well with experimental data. This observation is accepted as evidence of the adequacy of the approach used.

This study is limited to shallow, horizontal aquifers underlain at uniform depth by an impermeable boundary. The drainage systems considered are restricted to fully penetrating parallel open ditches of sufficient length that fluxes have components in only two dimensions. The soils are assumed to be homogeneous, isotropic, and stable with time.

Under these conditions, the positions of the water table and the locus of points at an arbitrary saturation are evaluated as affected by the depth of tailwater in the ditch, rate of uniform infiltration, bubbling pressure head, and distribution of pore sizes in the soil.

These analyses are ultimately extended to show the magnitude of spacing error resulting from neglecting capillary flow and aeration requirements. The height of the zone of insufficient aeration is determined for a predetermined drain spacing. Since the classical analyses assume that drainage is complete above the water table, the height of insufficient aeration is assumed equal to the height of the water table resulting from the classical analyses. This height is used to calculate the spacing, assuming no capillary flow. The comparison of these two spacings indicates the magnitude of spacing error resulting from neglecting capillary flow and aeration requirements.

^{1/} Contribution from the Western Region, Agricultural Research Service, USDA, in cooperation with the Colorado State University Experiment Station.

^{2/} Agricultural Engineer, USDA, Fort Collins, Colorado.

Soil Aeration

The adequacy of soil aeration is one of the most important factors in determining soil productivity. The carbohydrates produced by photosynthesis are transported to all living tissue of the plant to supply the energy for growth. Release of this stored energy is dependent upon oxidation within the plant cell. Except for such specialized plants as rice, agricultural plants cannot transport oxygen through the plant tissue from the aerial parts fast enough to provide adequate respiration in the roots. Thus, adequate root growth is dependent upon an external path of oxygen transfer (Hillel, 25).

Gases can enter the root environment either in the gaseous phase or dissolved in the liquid phase. Hagan, et al. (22, p. 942) give the respective diffusion coefficients of oxygen in air and in water as 1.13×10^1 and 1.54×10^{-3} cm²/min. Thus, the exchange of oxygen between plant roots and the atmosphere is achieved much more readily through soil having an interconnected gas-filled space than through a soil having only entrapped gases.

Gaseous exchange between soil and atmosphere can occur either by convection or by diffusion. Diffusion is generally accepted as the principal transport mechanism (Hillel, 25). Stolzy and Letey (43) suggest that an oxygen diffusion rate (ODR) of 40×10^{-8} g cm⁻²min⁻¹ may be taken as a safe minimum necessary for optimum plant growth.

The diffusion rate of gases in soil is dependent upon the fraction of the pore space occupied by a continuous air phase, and according to Penman and Marshall (in Hillel, 25) to a lesser extent upon the size distribution of air-filled pores. In experiments to determine the adequacy of soil aeration during sprinkler irrigation, Stegman, et al. (42) used a platinum electrode to evaluate ODR as a function of saturation. They concluded that, for a given soil, a unique saturation exists below which the critical ODR cannot be supplied. The ODR remained very low until the capillary pressure exceeded what Brooks and Corey (10) defined as the bubbling pressure. As capillary pressure further increased, the ODR increased rapidly. The critical saturation for four soils tested ranged between 75 and 92.5 percent. The effective saturation (as defined by Brooks and Corey, 10) averaged about 80 percent at the critical ODR for these soils.

Classical Drainage Theories

The exact solution of the differential equations describing drainage problems is usually quite difficult. In fact, attempts at such exact solutions have been successful in only the most simplified cases. Each of the developments reviewed in this section is based upon the assumption that the water table effectively bounds the permeable region and, where applicable, that drainage is instantaneous and complete as the water table passes a given point. Van Schilfgaarde (36) pointed out that the solutions resulting from these, and other simplifying assumptions can be of considerable value if carefully used, but emphasized the need for constant awareness of their limitations.

Van Schilfgaarde credited Colding, a Danish engineer, as having been the first to present, in 1872, a mathematical solution to a drainage problem. This

solution, describing the water table profile in equilibrium with a constant, uniform infiltration rate, is commonly called the ellipse, Hooghoudt, or Donnan equation as it has been developed independently by a number of researchers.

The ellipse equation is based upon the Dupuit assumptions, namely 1) that all streamlines in a system of gravity flow toward a shallow sink are horizontal, and 2) that the velocity along these streamlines is proportional to the slope of the free water surface but independent of depth. In this first development of the equation, drainage is assumed to terminate in open ditches which penetrate to the impermeable layer and which are shallow compared to their spacing. Although gradients near the centerline between drains are essentially vertical, certainty to the Dupuit assumptions, this equation appears to be a reliable approximation provided the other assumptions are valid.

In the years following the development of the ellipse equation, many attempts were made to account for the vertical components of potential gradients existing near the outflow region. Hooghoudt (van Schilfgaarde, 36), among others, replaced the Dupuit assumptions with the concept of radial flow toward the sink to determine the potential distribution for a number of specialized boundary conditions. The so-called "equivalent depth" correction to the ellipse equation was proposed by Hooghoudt to account for the lack of complete penetration of drains to the impermeable layer. Van Deemter, and Luthin and Gaskell (van Schilfgaarde, 36), presented details of a relaxation technique for solution of the problem. Other approaches, too numerous to mention, have been developed.

Although these steady-state solutions are of considerable use where rainfall or irrigation are sufficiently frequent that percolation to the water table can be considered uniform, the existence of steady-state conditions is the exception rather than the rule. Thus, many investigators have sought to develop solutions for the case of transient flow.

Boussinesq (van Schilfgaarde, 36) and Glover (Dumm, 19) applied the Dupuit assumptions to the transient flow situation, and found a solution for the case of drains on an impermeable boundary without resort to linearization. Glover (Dumm, 19) later extended his solution to the case of drains above an impermeable boundary by assuming that the depth through which flow occurs is invariant with time, thus effectively linearizing the differential equation.

As in the case of steady-state solutions, many investigators have attempted to more accurately account for initial conditions or changing boundary conditions. Kemper (van Schilfgaarde, 36), compared electrical analog data with results from Glover's equation and found that better agreement could be obtained by introduction of an empirical correction factor to Glover's equation. This correction resulted in a greater value of the dimensionless time factor, or slower drainage. This was in agreement with the fact that Glover's equation neglects convergence, resulting in an overestimate of the effectiveness of a drainage system.

Werner (48) employed the methods of Laplace transformation to evaluate a number of transient flow drainage situations, involving sloping aquifers, variable replenishment rates, and changing tailwater levels.

Dagan (17) presented an analysis of water table fluctuations in response to variable recharge. He linearized the free surface boundary condition to reduce the problem to a solution of a Volterra integral equation of the first kind. This equation was solved numerically and the results were presented in both tabular and dimensionless graphical form.

Hornberger, et al. (26) developed a numerical model based upon the Dupuit-Forchheimer assumptions to evaluate aquifer response to changes in stream stage. Capillary flow was neglected, and the results were compared with the exact solution of Boussinesq under appropriate boundary conditions. As one would expect, this comparison was quite precise where the initial condition was assumed to be a curved water table. This initially curved water table reduces the effects of large vertical gradients at early times, which occur when the initial water table is flat as assumed by Glover (Dumm, 19).

The preceding discussion is not intended to provide a complete history of the development of solutions to the flow equations. Such intensive reviews of the literature have been provided by van Schilf-gaarde (36), Childs (16) and others. Rather, it serves to illustrate the degree of mathematical sophistication that has been applied to the drainage problem while retaining the assumptions of negligible influence of capillary flow. Situations certainly exist in which these assumptions are justified. On the other hand, one can readily visualize situations in which the improvement achieved by mathematical sophistication is far outweighed by neglecting the capillary flow region. The succeeding sections review some significant attempts to treat flow in the capillary region.

Parameters Describing Capillary Properties

Scientists of many disciplines, including soil physics and chemical, petroleum and agricultural engineering have sought parameters characteristic of a porous body by which the capillary properties could be described. One such characterization of capillary conductivity, described by Gardner (21), is widely accepted by soil physicists. Gardner found that the relationship between capillary conductivity and capillary pressure head for many soils seemed to fit an equation of the type

$$K = \frac{a}{(P_c/\rho g)^n + b} \quad (1)$$

where K is the unsaturated conductivity, $P_c/\rho g$ is the capillary pressure head, n is a constant for a given soil, and a and b are constants such that a/b is the saturated hydraulic conductivity.

Brooks and Corey (10) presented a method for characterizing porous media based upon the nomenclature of petroleum technology. They used the terms permeability, capillary pressure, and saturation, rather than the hydraulic conductivity, tension, and water content familiar to the soil physicist. The relationships between these terms are discussed later. The relationships developed by Brooks and Corey express the functional dependence of permeability and saturation upon capillary pressure in terms of only

two soil parameters. The resulting power functions are somewhat easier to manipulate mathematically than Gardner's relation. Furthermore, empirical relationships such as equation (1) are obtained on small laboratory samples. Such data indicate a significant reduction in saturation and permeability at capillary pressures less than the bubbling pressure. The results of studies by White, et al. (49) indicate that this probably would not be the case in the field where the volume of soil relative to its atmospheric boundary is large. The relationship presented by Brooks and Corey (10), which is used here, assumes that air will not penetrate the interior of a soil volume until the capillary pressure reaches the bubbling pressure on the drainage cycle.

The basis for the Brooks and Corey relations is their observation that a large number of experimental data seem to fit the relation

$$S_e = (P_b/P_c)^\lambda \quad \text{for } P_c \geq P_b \quad (2)$$

The effective saturation, S_e , is defined by

$$S_e = (S - S_r)/(1 - S_r) \quad (3)$$

where S_r , the residual saturation, is the saturation at which the theory assumed the permeability is zero. The two soil parameters involved in the Brooks and Corey theory are bubbling pressure, P_b , and the pore-size distribution index, λ . The bubbling pressure is defined as the minimum capillary pressure on the drainage cycle at which a continuous nonwetting phase exists. The pore-size distribution index was shown to be a measure of the relative distribution of pore sizes, and was defined by equation (1), i.e., the negative slope of the straight-line portion of a plot of $\log S_e$ as a function of $\log P_c/\rho g$.

Brooks and Corey showed that the relative permeability, k_r , is given by

$$k_r = (P_b/P_c)^\eta \quad \text{for } P_c \geq P_b \quad (4)$$

where k_r is the ratio of effective permeability to saturated permeability. The exponent η was shown to be related to λ by

$$\eta = 2 + 3\lambda \quad (5)$$

Capillary pressure, P_c , may be expressed in terms of the capillary potential on a weight basis, commonly called pressure head, h , by

$$P_c = -\rho gh \quad (6)$$

where ρ and g are the liquid density and gravitational acceleration, respectively. The saturation, S , defined as the fraction of the pore space filled by the liquid phase, is related to volumetric water content, θ , by

$$S = \theta/\phi \quad (7)$$

where ϕ is the total porosity.

The term permeability is used as a measure of capacity of the soil to transmit a fluid, independently of fluid properties. Thus, the term is explicitly restricted to systems in which the solid matrix and fluid do not interact. Such is usually not the case in soil-water systems.

The polar nature of water and the electrical charge associated with clays in most soils result in adsorption of water onto the clay particles. This adsorption can cause swelling of clays, and in fine-textured materials or at low saturation may result in changes in the physical properties of water. In materials where these effects can be neglected, permeability, k , is related to hydraulic conductivity by

$$K = \frac{k \rho g}{\mu} \quad (8)$$

where K is hydraulic conductivity and μ is dynamic viscosity. It is apparent that relative hydraulic conductivity, K_r , is also given by equation (4) since the viscosity, density, and gravitational acceleration appear in both numerator and denominator.

Significance of the Capillary Fringe

Although most investigators have acknowledged the possibility of an influence of the capillary fringe on the performance of drains, only in recent years have significant efforts been made to analyze the phenomena. This section reviews the development of methods of treating the capillary region.

In 1947, Donnan (van Schilfgaarde, 36) demonstrated by sand tank experiments that the ellipse equation could be modified to give closer agreement with experimental results. He utilized an equation of the form

$$Q_d L / 2K = (Y_c + Y_f)^2 - (Y_d + Y_f)^2 \quad (9)$$

where Q_d is the total drain outflux, L is drain spacing, K is conductivity of the saturated sand, Y_c and Y_d are water table elevations at the midpoint and at the drain outlet, respectively. The height of the capillary region, Y_f , was assumed to be the height above the water table at which the soil first began to desaturate. Van Schilfgaarde (36), however, considered Donnan's approach inadequate. He pointed out that, in general, there is no well-defined capillary fringe, and the hydraulic conductivity decreases gradually with increased tension.

Despite this shortcoming, this approach remained the principal method of accounting for capillary flow for several years. Swartzendruber and Kirkham (44, 45) used the Swartz-Christoffel theorem to solve the case of steady horizontal flow through a rectangular slab. They also considered that capillary flow was confined to the zone that is essentially saturated. It was concluded that for their boundary conditions where the water table was one-tenth as high as it was long, the fringe contribution could reach a maximum of 170 percent of the flow beneath the water table as the soil thickness increased.

Chapman (12) considered the effects of the capillary region upon discharge, height of the seepage face, and shape of the free surface for a similar steady-state flow problem. Applying the same description of the capillary region he used Green's theorem to develop an equation describing the flux. Chapman's conclusions, based upon comparisons between his equation and the results of an electrical analog, were essentially the same as those of Swartzendruber and Kirkham.

Childs (13) modified van Deemter's hodograph solution to account for the presence of a capillary region. He considered the case of steady-state drainage

in equilibrium with a uniform infiltration rate, assuming that capillary flow occurred solely in that region remaining fully saturated. Childs considered that the height of this saturated zone is influenced by the infiltration rate. It was assumed that this increase in capillary fringe height was 1 percent when the ratio of infiltration rate to saturated conductivity was 0.01, and negligible at lower infiltration rates. He concluded:

"...for thick fringes, the bulk of the thickness of the fringe is accommodated above the water table which is not depressed in proportion below the level appropriate to the absence of a fringe."

Bouwer (4,5) utilized both numerical and electrical analog techniques to evaluate the influence of the "capillary fringe" upon the steady-state performance of drains. He defined a "critical tension" as the tension at the center of the range over which conductivity decreases rapidly. The capillary fringe was then defined as the region between the water table and the elevation of this critical tension. Since flow rates in the capillary fringe are usually small compared with the conductivity, Bouwer assumed that the pressure distribution in the fringe was essentially a static distribution. He emphasized that if the water table is near the surface, or the water content-tension curve shows a gradual change, then the application of a constant specific yield may be objectionable. Bouwer's analysis indicated that flatter water tables could be expected under conditions where the capillary flow was considered.

In analyses using hypothetical soil data, Bouwer concluded that neglecting the flow above the capillary fringe, as defined in his study, contributed little error to the solution. However, he conceded that such might not be the case for soils exhibiting a gradual reduction of conductivity with increasing tension.

Bouwer postulated that, so long as the capillary fringe did not extend to the surface, lowering the impermeable boundary by an amount numerically equal to the capillary fringe height would have approximately the same effect upon discharge as would the addition of the capillary fringe above the water table. Such an assumption would allow the use of Hooghoudt's "equivalent depth" concept for analyzing the capillary flow problem. Bouwer presented comparisons between the flux computed from such an analysis and the results of electrical analog solutions. From these results, he concluded that the comparison was quite satisfactory. However, an analysis of his published results indicates that the differences between these two solutions increase with increases in both the critical tension and the saturated thickness of the aquifer. One might expect such increased deviations, since lowering the impermeable boundary may result in longer streamlines than would exist in the equivalent capillary fringe. These longer streamlines would result in smaller potential gradients than in the capillary fringe and a lower flow rate.

Luthin (29) and Luthin and Worstell (31) attempted to account for the change in specific yield with depth in a problem of transient drainage. The value of specific yield used in these calculations was simply the arithmetic mean of the specific yields at the initial and final water table depths. It was assumed that the water content distribution was independent of water table velocity, thus these specific yields were evaluated from water content-tension curves. The

investigators concluded that significant errors were introduced by neglecting the change of specific yield with depth of the water table when the water table was near the surface.

These rather simplified analyses have been followed by progressively more elaborate considerations of the capillary region. Childs (14) evaluated the effect of decline of the water table upon the specific yield. He showed that, depending upon the depth to the water table, the effective specific yield will range from essentially zero for very shallow water tables to a constant ultimate value when the water table is very deep. A similar analysis by Duke (18) presents a quantitative basis for evaluating the apparent specific yield as a function of depth to the water table.

In a subsequent publication, Childs and Poulouvalis (15) extended the previous analysis to consider the effect of water table celerity upon the shape of the water content-elevation curve. The investigators presented a theoretical description of the shape of the water content-elevation curve in the idealized case of a water table moving at a constant speed. They pointed out that in the initial stages of water table movement the water content profile continues to change its shape with time. After a sufficient length of time, the shape of the water content profile remains constant, and the profile rises or falls with the water table.

Youngs (50) presented a hodograph analysis of steady-state drainage in equilibrium with a constant infiltration rate, taking into account the effect of the capillary fringe. Although he assumed capillary flow to be confined to the region remaining fully saturated, Youngs explicitly considered the effect of the percolation rate upon the height of the capillary fringe. Youngs presented the positions of both the water table and top of the capillary fringe at the centerline between drains. He concluded that the capillary fringe had little effect upon water table position midway between the drains, although one might question the validity of this conclusion after careful analysis of Youngs' results.

Kraijenhoff van de Leur (27) used uniform sand in a physical model to evaluate the effect of the capillary region upon the performance of drains subjected to step increments of rainfall. Again, he considered only the fully saturated region of the capillary zone, but considered the effects of both infiltration rate and rate of water table movement upon the height of this zone. For the conditions studied, he concluded that the effects of water table celerity did not sufficiently influence the shape of the capillary zone to affect the results. The capillary zone in his study was about 15 cm thick, a significant portion of the 60-cm depth of sand.

Brutsaert, et al. (11) applied a method of successive series of steady states to evaluate the shape and positions of a transient water table. This analysis was analogous to that of Kirkham and Gaskell (van Schilfgaarde, 37), but introduced capillary flow and a specific yield dependent upon water table depth. The functional relationship between water table depth and specific yield was obtained experimentally from measurements of total outflow volume and water table position in a series of model studies. As the rate of water table decline approached zero, this relation was expected to approach the water content-tension relation for the soil. The effects of permeability above the water table were considered by adding a

depth equivalent to the thickness of the essentially saturated region above the water table. Subsequent analyses were made with regard to the "depth of the upper boundary of the capillary fringe" rather than "depth of the water table."

Schmid and Luthin (38), in an analysis of drainage of sloping forest lands in the pre-Alps of Switzerland, applied the approach of Hooghoudt to the problem of a water table in equilibrium with rainfall on a sloping hillside. Although they did not explicitly evaluate flow above the water table, they pointed out its possible significance and suggested a method of accounting for the effects of capillary conductivity. They suggested integrating the area under the conductivity-capillary pressure curve from zero to the pressure at the soil surface, then dividing by the saturated conductivity to obtain an equivalent depth to be added to the waterlogged flow region. It must be realized, however, that the pressure-elevation relation is affected by the rainfall rate, and must be taken into account in such an integration procedure.

Schmid and Luthin (38) suggested that the solutions obtained from noncapillary considerations represented the upper limit of the flow region. That is to say, the actual water table will be lower than the values given by an amount equal to the equivalent depth as calculated above. As shown later in this paper, this is not the general case, especially for systems in equilibrium with rainfall. Certainly, such an assumption will give grossly erroneous results in the immediate vicinity of the drain.

Bouwer (6) presented the method of accounting for capillary flow mentioned by Schmid and Luthin (38). That is, he considered that the entire capillary region could be represented by a step-function analogous to the critical tension concept. Bouwer evaluated the thickness, Z_e , of this fictitious capillary fringe as

$$Z_e = \frac{1}{K} \int_0^H k(Z) dZ \quad (10)$$

where H represents the depth of the water table; K , the saturated hydraulic conductivity; $k(Z)$ the capillary conductivity; and Z is the vertical distance measured from the water table. Bouwer credited Myers and van Bavel (34) with development of this concept.

Hedstrom, et al. (24) utilized this concept, and a similar one related to capillary storage implied by Childs (14) to evaluate the effects of both capillary flow and changing specific yield upon the performance of transient drainage systems. The relationships developed by Hedstrom, et al. will be discussed in detail later.

Talsma (46) attempted to utilize the effective capillary fringe concept of Myers and van Bavel along with Childs' (13) concept of the influence of percolation rate to evaluate steady-state drainage. He was primarily concerned with the influence of capillary flow upon design spacing of drains in the Murrumbidgee irrigation area of Australia. The field conditions investigated were shallow drains with an essentially impermeable layer from 0.1 to 1.8 m beneath the drain, and the water table from 50 to 100 cm below the soil surface. The soils studied by Talsma showed no region of saturation above the water table, but began to desaturate immediately as tension increased. Thus, the values he obtained for Z_e were

small, of the order of 10 cm. Using Childs (14) method of analysis, Talsma calculated that the water table would be about 8 cm lower than the 50 cm calculated by neglecting capillary flow. He concluded that the spacing error introduced by neglecting capillary flow was less than 6 percent and that for soils in the study area the capillary flow could be safely ignored.

It is apparent from the preceding discussion that methods have been devised to treat the partially saturated as well as saturated flow regions in soil drainage systems. It is also apparent that the mathematical complexities involved limit the use of analytical methods to idealized boundary conditions, simplified capillary flow considerations, or both. It has been argued that the uncertainties of field data are sufficient to outweigh the errors introduced by these assumptions. However, digital computer technology has encouraged many investigations using numerical solution techniques for studying the effects of the capillary flow region. The reader is referred to the works of Bittinger, et al. (3), Rubin (35), Breitenbach, et al. (7, 8, 9) and Amerman (1) for details of finite difference equations, methods of approximating boundary conditions, and merits of the many matrix solution techniques. The following paragraphs describe some such investigations as they pertain to the problem of evaluating capillary flow in drainage systems.

Luthin and Day (30) conducted experiments in a sand-filled tank designed to evaluate the contribution of the capillary region to the total soil water flux during steady flow. They analyzed the flow by numerical solution of a nonlinear two-dimensional form of the continuity equation. Values of capillary conductivity were taken from a separate laboratory determination of the tension-conductivity characteristics of the soil used. It was concluded that the comparison of experimental and computed results substantiated the validity of the nonlinear continuity equation.

Sewell and van Schilfgaarde (39) developed a two-dimensional computer model to simulate flow in the saturated and unsaturated regions for steady-state tile drainage and subirrigation problems. Because the numerical model was written in two dimensions and solved in terms of potential, it was not necessary to approximate the effects of the capillary region by techniques such as Bouwer (6) used. The relation between capillary conductivity and tension was utilized directly from the conductivity-tension curves. The conductivity was determined from the equation proposed by Gardner, that is,

$$k = \frac{a}{(P_c/\rho g)^n + b} \quad (11)$$

where n , a , and b are constants, and $P_c/\rho g$ is the capillary pressure head, for each grid in the network. Results were compared with comparable solutions to the ellipse equation. For large drain spacings, the ellipse equation severely underestimated the flux from the drains because of the contribution of the capillary region.

Rubin (35) developed a two-dimensional numerical model capable of consistently evaluating the transient potential distribution in both the saturated

and partially saturated regions of an agricultural drainage system. This model utilized measured relationships between water content and tension and between conductivity and tension for calculating the coefficients of the model matrices. Rubin was able to show the distribution of Darcian velocities throughout the profile, as well as to define the potential distribution. This approach accounted for the influence of nonequilibrium water distribution as well as the effects of capillarity upon flux distribution. Rubin concluded that flow in the partially saturated region may profoundly affect the progress of the water-table decline.

Verma and Brutsaert (47) examined the effects of the Dupuit assumptions and the assumption of no-flow above the water table upon the rate of outflow during transient drainage. These investigators compared the results of one- and two-dimensional numerical models to evaluate the effects of the Dupuit assumptions. They concluded that, except for small time, the Dupuit assumptions resulted in less than 10 percent error in outflow rates if the ratio of drain spacing to aquifer depth was at least eight. The rate of outflow decreased significantly with increases in the parameter related to capillary fringe height, but was relatively insensitive to small changes in the parameter related to pore-size distribution. Increases in both drain spacing and water level in the ditch increased the error in outflow rate resulting from neglecting capillary flow.

Freeze (20) utilized a three-dimensional model to evaluate the effects of the capillary region upon both steady and transient flow through earth dams. He used exaggerated soil properties to emphasize the effects of the partially saturated region, therefore, his results are only qualitative. Freeze observed that a significant number of streamlines did cross the water table, a direct contradiction to the classical approach. He also observed that neglecting unsaturated flow caused larger errors in the transient cases than in steady-state problems. In a later section of this paper, it is shown that such results are expected, since the storage coefficient, which is related to capillary phenomena, does not enter into steady-state solutions. Freeze admitted the limited applicability of a three-dimensional model because of its complexity and the uncertainties of field data.

Although previous investigations have been concerned with various aspects of flow in the capillary region, these studies are related only indirectly to the effects of capillary properties upon the location of the aerated zone. Little attention has been given to a systematic evaluation of the relative influence of capillary conductivity and capillary storage upon the shape and position of the water table.

Before the full value of the previous investigations can be realized, each of these capillary parameters must be evaluated thoroughly and their relative importance determined. Only then will these investigations provide quantitative information of practical use to field design personnel.

The remaining sections of this paper provide one such evaluation. However, the current investigation is restricted in scope and the results can be interpreted quantitatively only for the specific boundary conditions evaluated.

ANALYSIS OF THE PROBLEM

The design of drains to achieve a predetermined depth of water table has been a classical problem of agricultural drainage. In reality, the position of the water table is of little direct importance. What is important is the effect of the water table upon the movement of water and air within the partially saturated root zone. The results of investigations by Stegman, et al. (42) imply that adequate soil aeration may be achieved by maintaining the effective saturation below some critical value within the root zone.

Thus, besides determining the position of the water table (considering both saturated and partially saturated flow), the water content in the soil above the water table should be evaluated in regard to its effect on soil aeration. Before proceeding with the analysis of this problem, the assumptions used are presented as follows:

1. Water flux is solely in response to gradients of mechanical potential in the liquid phase.
2. Hysteresis is absent, thereby restricting the analysis to drainage only.
3. The medium is homogeneous and isotropic, so that saturated hydraulic conductivity can be considered a scalar constant.
4. The celerity of the water table is sufficiently small that the shape of the saturation profile above the water table can be considered a function of the soil parameters and vertical flux only.
5. The soil and fluid properties remain constant with time. That is, the soils considered do not shrink or swell.
6. The conductivity and saturation are described, in terms of capillary pressure, by the Brooks-Corey equations.

Most of this study is concerned with the use of a numerical model based upon the Dupuit-Forchheimer assumptions to predict the performance of open ditch drains. The Dupuit-Forchheimer approach has been modified to incorporate the flow and storage of capillary water in a one-dimensional flow model.

Based upon the Dupuit-Forchheimer assumptions and the assumptions enumerated above, the mass continuity equation is expressed as

$$\phi_e \frac{\partial Y_s}{\partial t} = \frac{\partial}{\partial x} \left(K Y_k \frac{\partial Y}{\partial x} \right) + Q \quad (11)$$

where ϕ_e is the effective, or drainable, porosity; K is the saturated hydraulic conductivity; Q is the strength of the distributed water source (used here to simulate the surface boundary condition); x is the horizontal space coordinate; and t is time. The horizontal component of the free surface gradient, $\partial Y / \partial x$, (Y is the water table elevation referred to the impermeable lower boundary) is assumed to be uniform along a vertical line, both above and below the water table. If this equation is to represent both partially saturated and saturated flow, the storage term, Y_s , and horizontal flow term, Y_k , must account for the effects of capillary storage and

capillary conductivity, respectively. Since the flow problem is analyzed as a one-dimensional problem, the effect of the capillary region is incorporated in the form

$$Y_k = Y + H_k \quad (12)$$

where H_k is a fictitious depth of saturated soil having the same capacity for horizontal flow as the capillary zone, and

$$Y_s = Y + H_s \quad (13)$$

where H_s is a fictitious depth of saturated soil having a volume of drainable water equal to that in the capillary zone. The concepts of an equivalent permeable height, as suggested by Myers and van Bavel (Bouwer, 6), and of an equivalent saturated height used by Hedstrom, et al. (24) are used. Because of their pertinence to this study, these concepts are developed in detail in this section. In addition, a theory is presented for evaluating the depth of soil above the water table at which an effective saturation in excess of some arbitrarily selected value exists.

Equivalent Permeable Height

The effectiveness of the capillary region in conducting water horizontally toward a drain is given by an expression suggested by Myers and van Bavel (Bouwer, 6) as

$$H_k = \frac{1}{K} \int_0^H K_e dz \quad (14)$$

where H_k is the effective permeable height, a fictitious height of saturated soil having the same capacity to transmit water as does the partially saturated region above the water table. The saturated hydraulic conductivity is denoted by K ; K_e is the capillary conductivity as a function of capillary pressure; Z is elevation above the water table, and H is the distance from the water table to the soil surface. When H is less than the bubbling pressure head, $P_b / \rho g$, the soil remains saturated to the surface and $H_k = H$. If $H > P_b / \rho g$, the conductivity is dependent upon elevation and any vertical flux that may exist. The equations for H_k (where the soil water is in static equilibrium with the water table and where both steady, uniform downward and upward fluxes occur) are developed in the following sections.

Static equilibrium. When the soil profile is in static equilibrium with the water table, $Z = P_c / \rho g$, where $P_c / \rho g$ is the capillary pressure head (See Fig. 1). Under these conditions, the Brooks-Corey equation for effective conductivity K_e can be written

$$K_e = K \quad \text{for } Z \leq P_b / \rho g \quad (15)$$

and

$$K_e = \left(\frac{P_b / \rho g}{Z} \right)^n \quad \text{for } Z > P_b / \rho g \quad (16)$$

Substituting equations (15) and (16) into (14) gives

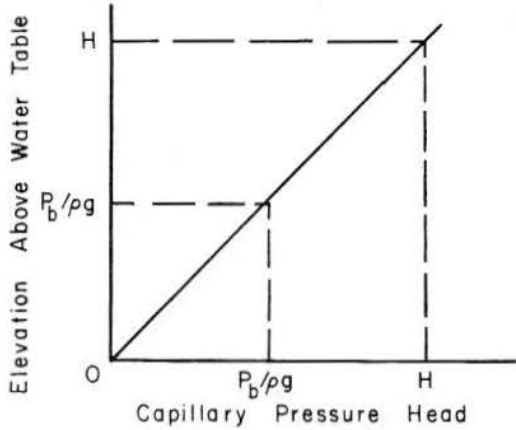


Figure 1. Capillary pressure profile in soil in static equilibrium with a water table.

$$H_k = \frac{1}{K} \left[\int_0^{P_b/\rho g} K dz + \int_{P_b/\rho g}^H (P_b/\rho g)^\eta z^{-\eta} dz \right] \quad (17)$$

which, when integrated, is simplified to

$$H_k = \frac{P_b}{\rho g} \left(\frac{n - H^{1-n} (P_b/\rho g)^{n-1}}{n-1} \right) \quad (18)$$

Dimensionless variables, H_k and H , are defined by dividing H and H_k by the bubbling pressure head, a characteristic parameter of dimensionless length, such that

$$H_k = H / (P_b/\rho g) \quad (19)$$

and

$$H_k = H_k / (P_b/\rho g) \quad (20)$$

Substituting equations (19) and (20) into (18) gives the equation for scaled permeable height, that is,

$$H_k = \frac{n - H_k^{1-n}}{n-1} \quad (21)$$

Equation (21) is equivalent to equation (17) developed by Hedstrom, et al. (24).

Steady downward flow. During steady percolation to a water table, the capillary pressure head is, at every point, less than the elevation above the water table. It is apparent from Figure 2 that the relation between capillary pressure head and elevation above the water table exhibits three separate regions delineated by Z' , Z'' , and H . Before equation (14) can be applied to this case, it is necessary to evaluate these elevations and their corresponding capillary pressures. In the region between the water table and the point at which the capillary pressure equals the bubbling pressure, ($0 < Z < Z'$), the hydraulic conductivity remains constant at the saturated value (see Figure 2).

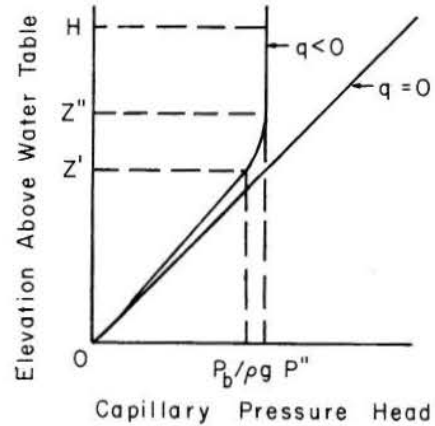


Figure 2. Capillary pressure profile in a soil with a steady downward flux of water.

For this region, Darcy's equation can be written in one-dimensional form as

$$q = -K_e \frac{d\psi}{dz} \quad (22)$$

where q is the volumetric flux rate, positive upward; K_e is the effective hydraulic conductivity; ψ is the hydraulic head; and elevation Z is defined positive upward. Since both q and K are constant at capillary pressures less than $P_b/\rho g$, the gradient of hydraulic head in this region is constant, because the pressure gradient is constant. Expanding equation (22) in terms of the components of hydraulic head, i.e., elevation and pressure heads, gives

$$q/K = - \frac{d(Z - P_c/\rho g)}{dz} \quad (23)$$

Defining a dimensionless flux by $q = q/K$, gives

$$dz = \frac{d(P_c/\rho g)}{1+q} \quad (24)$$

The elevation Z' at which $P_b/\rho g$ is the capillary pressure in the soil is given by

$$Z' = \int_0^{P_b/\rho g} \frac{d(P_c/\rho g)}{1+q} \quad (25)$$

Performing the indicated integration gives

$$Z' = \frac{P_b/\rho g}{1+q} \quad (26)$$

or, defining a scaled elevation $Z.' \equiv Z'/(P_b/\rho g)$,

$$Z.' = \frac{1}{1+q} \quad (27)$$

As elevation increases above Z' , capillary pressure increases, and conductivity decreases. Thus

the gradient of capillary pressure must decrease. If the soil profile is sufficiently deep, the hydraulic conductivity continues to decrease with increasing elevation until it approaches the flux in magnitude. That elevation at which

$$K_e = -\epsilon q \quad (28)$$

is defined as Z'' where ϵ is a constant greater than, but arbitrarily close to unity. The capillary pressure head at Z'' is denoted by P'' , and it is assumed that $K_e = -\epsilon q$ for $Z > Z''$. In the region $Z > Z'$,

$$q = -K_e \frac{d(Z - P_c/\rho g)}{dZ} \quad (29)$$

Substituting the Brooks-Corey expression for K_e , equation (28) becomes

$$q = -K(P_b/\rho g)^\eta (P_c/\rho g)^{-\eta} [1 - d(P_c/\rho g)/dZ] \quad (30)$$

Defining a scaled capillary pressure $P = P_c/P_b$, and employing the definition of q , equation (30) is written as

$$q = P^{-\eta} [(P_b/\rho g) \frac{dP}{dZ} - 1] \quad (31)$$

or

$$dZ = \frac{P_b}{\rho g} \frac{dP}{1 + q.P^\eta} \quad (32)$$

In the region $Z'' < Z < H$, $P_c/\rho g = P''$, and

$$\epsilon q = -K[(P_b/\rho g)/P'']^\eta \quad (33)$$

or

$$P'' = \frac{P_b}{\rho g} (-\epsilon q)^{-1/\eta} \quad (34)$$

The elevation at which P'' occurs can be evaluated by integrating equation (32) between the limits $Z = Z'$ at $P = 1$ and $Z = Z''$ at $P = P''$, where $P'' = P''/(P_b/\rho g)$, which yields

$$Z'' = Z' + \frac{P_b}{\rho g} \int_1^{P''} \frac{(-\epsilon q)^{-1/\eta} dP}{1 + q.P^\eta} \quad (35)$$

Substituting equation (26) into (35), and defining $Z'' = Z''/(P_b/\rho g)$ gives

$$Z'' = \frac{1}{1 + q} + \int_1^{P''} \frac{(-\epsilon q)^{-1/\eta} dP}{1 + q.P^\eta} \quad (36)$$

The closed form solution of equation (36) is difficult for $\eta > 3$. McWhorter (33) has pointed out that the integral can be expressed in terms of the incomplete Beta function. In the study reported here, numerical techniques were utilized to evaluate these integrals.

After evaluating the elevations Z' and Z'' at which the conductivity function changes form, the equivalent permeable height is evaluated from equation (14). Equation (14) can be expressed as

$$H_k = \frac{1}{K} \left[\int_0^{Z'} K dZ + \int_{Z'}^{Z''} K_e dZ + \int_{Z''}^H (-\epsilon q) dZ \right] \quad (37)$$

or, integrating directly the first and third terms and substituting the scaled form of the Brooks-Corey expression

$$K_e = KP^{-\eta} \quad (38)$$

into the second integral, equation (37) can be expressed as

$$H_k = Z' + \int_{Z'}^{Z''} P^{-\eta} dZ - \epsilon q.(H-Z'') \quad (39)$$

In the region $Z > Z'$, dZ is given by equation (32). Substituting this expression into equation (39) and noting that $Z = Z'$ when $P = 1$ and $Z = Z''$ when $P = (-\epsilon q)^{-1/\eta}$, (39) becomes

$$H_k = Z' - \epsilon q.(H-Z'') + \frac{P_b}{\rho g} \int_1^{(-\epsilon q)^{-1/\eta}} \frac{P^{-\eta} dP}{1 + q.P^\eta} \quad (40)$$

Equation (40) can be expressed in terms of scaled variables, after substituting for Z' , as

$$H_k = \frac{1}{1 + q} - \epsilon q.(H-Z'') + \int_1^{(-\epsilon q)^{-1/\eta}} \frac{dP}{P^\eta(1 + q.P^\eta)} \quad (41)$$

Substituting equation (36) into (41), and assuming

$$\frac{1 + \epsilon q}{1 + q} = 1 \quad (42)$$

equation (41) becomes

$$H_k = 1 - \epsilon q.H + \int_1^{(-\epsilon q)^{-1/\eta}} \frac{dP}{P^\eta(1 + q.P^\eta)} + \int_1^{(-\epsilon q)^{-1/\eta}} \frac{\epsilon q.P dP}{1 + q.P^\eta} \quad (43)$$

Combining the integrands gives

$$H_k = 1 - \epsilon q.H + \int_1^{(-\epsilon q)^{-1/\eta}} \frac{1 + \epsilon q.P^\eta}{P^\eta(1 + q.P^\eta)} dP \quad (44)$$

Note that if $H < Z''$, the second term in equation (41) does not exist, and the upper limit on the third term is $P_s < (-\epsilon q)^{-1/\eta}$ where P_s is the scaled capillary pressure at the soil surface. In this case,

$$H_k = \frac{1}{1+q} + \int_1^{P_s} \frac{dP}{P^\eta (1+q \cdot P^\eta)} \quad (45)$$

It is important to emphasize that q is defined positively upward, so that for the case considered here, values of q are negative.

Steady upward flow. Upward flow of water from the water table may be induced by evaporation at the soil surface, or by root extraction. In the one-dimensional problem analyzed, both of these terms may be approximated as pseudo-sink terms. Neither of these terms is truly steady state; both are subject to diurnal fluctuations. They are not plane sinks either, as root extraction or vaporization may be distributed over a substantial depth. However, over a long period of time, the flux may be approximated by steady flow. It may be valid to assume some fictitious mean depth at which liquid phase flux can be considered to terminate. Based upon such concepts, the influence of upward flux upon the equivalent permeable height can be evaluated in a manner analogous to that of the previous section.

This analysis is subject to a further limitation as described by Anat, et al. (2). That is, for a given set of soil parameters and depth to the water table, there is a maximum rate of upward flow that can be induced. The following analysis assumes that q is physically possible for the situation described, which implies that the surface capillary pressure is finite.

Since the water content, and consequently the hydraulic conductivity, decrease in the direction of flow, the capillary pressure gradient must increase continuously with elevation above the water table. In the limit, as H approaches the maximum depth, H_{max} , at which a given flux can occur, this capillary pressure gradient approaches infinity as shown in Figure 3.

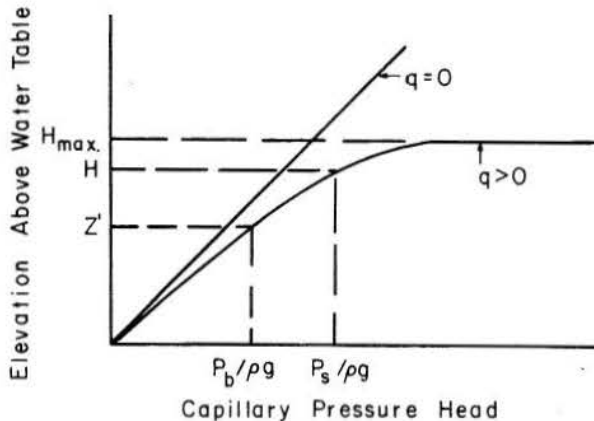


Figure 3. Capillary pressure profile in a soil with a steady upward flux of water.

Thus, assuming that $H < H_{max}$, the elevation at which the bubbling pressure head occurs is given by equation (26). It is important to remember that for the case of upward flow being considered, q is a positive value. For the case of steady upward flow, the capillary pressure head-elevation relation exhibits only two separate regions as indicated in Fig-

ure 3. The elevation of Z' and the surface capillary pressure must be evaluated before equation (15) can be evaluated.

In the region $Z' < Z \leq H_{max}$, $P_b < P_c < \infty$, and the flux is given by Darcy's equation

$$q = -K_e \frac{d(Z - P_c/\rho g)}{dZ} \quad (46)$$

Following the logic of the preceding section, it can be shown that

$$dZ = \frac{P_b}{\rho g} \frac{dP}{1 + q \cdot P^\eta} \quad (47)$$

Defining $P_s = P_s/P_b$, the limits of integration of equation (47) are $P = 1$ at $Z = Z'$ and $P = P_s$ at $Z = H$, $H \leq H_{max}$. Integrating equation (47) between these limits gives

$$H - Z' = \int_1^{P_s} \frac{dP}{1 + q \cdot P^\eta} \quad (48)$$

or, substituting equation (27) for Z' ,

$$H - \frac{1}{1+q} = \int_1^{P_s} \frac{dP}{1 + q \cdot P^\eta} \quad (49)$$

Since it is assumed that H , q , and η are known for a given situation, equation (49) is solved by numerical procedures to determine the surface pressure, P_s . Having thus determined the surface pressure and the elevation Z' , equation (14) can be expressed

$$H_k = \frac{1}{K} \left[\int_0^{Z'} K dZ + \int_{Z'}^H K_e dZ \right] \quad (50)$$

Substituting the appropriate pressures in the limits of the second integral, applying the Brooks-Corey expression for K_e , and equation (47) for dZ , equation (50) becomes

$$H_k = \frac{1}{K} \left[\int_0^{Z'} K dZ + \frac{P_b}{g} \int_1^{P_s} \frac{P^{-\eta} dP}{1 + q \cdot P^\eta} \right] \quad (51)$$

Integrating, substituting equation (26) for Z' , and expressing the result in terms of scaled variables gives

$$H_k = \frac{1}{1+q} + \int_1^{P_s} \frac{dP}{P^\eta (1+q \cdot P^\eta)} \quad (52)$$

Equations (21), (44), or (52) provide a basis for evaluating the contribution of the capillary region to horizontal flow toward the drain. The value of H_k is highly dependent upon η , and (except for relatively deep water tables and small vertical flux) is dependent upon the depth to the water table. When water tables are shallow and the depth to the water table changes significantly with either space or time, a single value of H_k may provide a poor correction to account for the capillary flow region. In the case of steady downward flux, this approximation

can be especially poor, since the hydraulic conductivity is nowhere less than the magnitude of the flux.

Equivalent Saturated Height

When the water table depth varies significantly with time, the capillary region influences the flow in a second way. The volume of water released from storage for a unit decline of the water table is dependent upon the depth to the water table. This dependence has been discussed by Childs (14), Duke (18), and others. Such a dependence of the specific yield upon depth to the water table can be treated in a manner analogous to the previously discussed effective permeable height. A fictitious column of saturated soil of height H_s , which contains the same volume of drainable water as the partially saturated soil profile is defined by

$$H_s = \int_0^H S_e dZ \quad (53)$$

where S_e , the effective saturation, is defined by $S_e = (S - S_r)/(1 - S_r)$. The volume of drainable water per unit area of soil in this fictitious column is given by

$$V_d = \phi(1 - S_r)H_s \quad (54)$$

where V_d is the total water volume, ϕ is total porosity, and S_r is the residual saturation. Volume V_d is equal to the volume of drainable water in a unit area of soil of height, H , above the water table. Thus the volume of water, V_r , released per unit area from the soil by a unit decline in the water table is given by

$$V_r = \phi[1 + (H_s)_H - (H_s)_{H+1}] \quad (55)$$

where the subscripts refer to the depth to water table at which H_s is evaluated.

By applying the Brooks-Corey expression

$$S_e = (P_b/P_c)^\lambda \quad (56)$$

where λ is the pore size distribution index, with the appropriate limits on equation (53), the effective saturated height is evaluated. The pressure profiles illustrated in Figures 1 through 3 are applicable for the cases of equilibrium, steady downward flow, and steady upward flow, respectively. Therefore, the elevations at which the description of the pressure gradient changes its form are the same as those elevations calculated in the analyses of the effective permeable height.

Static equilibrium. When the soil water is in static equilibrium with the water table, the capillary pressure head is equal to the elevation head. Since S_e is unity for $P_c < P_b$, equation (53) can be written

$$H_s = \int_0^{P_b/\rho g} dZ + \int_{P_b/\rho g}^H S_e d(P_c/\rho g) \quad (57)$$

Substituting equation (56) and integrating gives

$$H_s = \frac{P_b}{\rho g} + \frac{P_b}{\rho g} \left(\frac{(P_b/\rho g)^{\lambda-1} H^{1-\lambda} - 1}{1-\lambda} \right) \quad (58)$$

or, in terms of scaled variables,

$$H_{s.} = \frac{\lambda - H.^{1-\lambda}}{\lambda - 1} \quad (59)$$

for $H. \geq 1$, otherwise $H_{s.} = H.$

Since $\eta = 2 + 3\lambda$ (according to Brooks and Corey, 10), $H_{s.}$ is always greater than $H_k.$ for a given soil and water table depth. This means that the effect of differences in depth to the water table is more significant with respect to the effective storage height than to the effective permeable height.

Steady downward flow. During steady percolation to a water table the effective saturation throughout the profile attains a minimum value $S_e > S_r$ dependent upon the flux. In a manner identical with the evaluation of the effective permeable height, three pressure regions can be identified, such that

$$H_s = \int_0^{Z'} dZ + \int_{Z'}^{Z''} S_e dZ + \int_{Z''}^H S_e dZ \quad (60)$$

where Z' is given by equation (26) and S_e by equation (56). Substituting these expressions, using equation (32) to describe dZ in the second integral, and substituting equation (34) for the pressure at Z'' gives

$$H_s = \frac{(P_b/\rho g)}{1+q.} + \frac{P_b}{\rho g} \int_1^{(-cq.)^{-1/\eta}} \frac{P.^{-\lambda} dP.}{1+q.P.^{\eta}} + \int_{Z''}^H [(-cq.)^{-1/\eta}]^{-\lambda} dz \quad (61)$$

Integrating the right-hand term of equation (61) and expressing the result in terms of scaled variables, gives

$$H_{s.} = \frac{1}{1+q.} + (-cq.)^{\lambda/\eta} (H.-Z.'') + \int_1^{(-cq.)^{-1/\eta}} \frac{dP.}{P.^{\lambda}(1+q.P.^{\eta})} \quad (62)$$

Substituting equation (39) for Z'' and combining the integrands gives

$$H_{s.} = \frac{1}{1+q.} + (-cq.)^{\lambda/\eta} H. - \frac{(-cq.)^{\lambda/\eta}}{1+q.} + \int_1^{(-cq.)^{-1/\eta}} \frac{P.^{-\lambda} (-cq.)^{\lambda/\eta}}{1+q.P.^{\eta}} dP. \quad (63)$$

or, combining terms,

$$H_{s.} = \frac{1 - (-cq.)^{\lambda/\eta}}{1+q.} + (-cq.)^{\lambda/\eta} H. + \int_1^{(-cq.)^{-1/\eta}} \frac{P.^{-\lambda} - (-cq.)^{\lambda/\eta}}{1+q.P.^{\eta}} dP. \quad (64)$$

By using the relation between η and λ , equation (64) could be reduced to an equation involving only one of these soil parameters. This reduction is not shown, because of the added complexity of the equations caused by introducing further fractional exponents. It is re-emphasized that for this case, $q.$ is negative.

Note that if $H. < Z''$, the surface pressure $P_s. < P_b$ and equation (64) reduces to

$$H_s. = \frac{1}{1+q.} + \int_1^{P_s.} \frac{dP.}{P.^{\lambda}(1+q.P.^{\eta})} \quad (65)$$

Steady upward flow. When the water flux is steady in the positive direction, i.e., upward, and less than the limiting upward flux discussed previously, equation (53) may be written as

$$H_s = \int_0^{Z'} dZ + \int_0^{Z'} \frac{P_s./\rho g}{Z'} S_e dZ \quad (66)$$

where Z' and $P_s./\rho g$ were defined previously. Substituting the value of Z' from equation (26) S_e from equation (56), and dZ from equation (32) into equation (66) gives

$$H_s = \frac{(P_b./\rho g)}{1+q.} + \frac{P_b.}{\rho g} \int_1^{P_s.} \frac{P.^{-\lambda} dP.}{1+q.P.^{\eta}} \quad (67)$$

which, in terms of scaled variables, is

$$H_s. = \frac{1}{1+q.} + \int_1^{P_s.} \frac{P.^{-\lambda} dP.}{1+q.P.^{\eta}} \quad (68)$$

where $P_s.$ is evaluated from equation (49).

Equations (59), (64), and (68) provide a theoretical basis for evaluating the effect of the capillary region upon the specific yield of the soil. The comments regarding the influence of soil parameters and flux discussed previously with regard to $H_k.$ are also applicable to $H_s.$

Height of Zone of Insufficient Aeration

The preceding sections have illustrated how the effects of capillary conductivity and capillary storage can be evaluated from measurable soil properties. This analysis provides a method by which the flux of water in both the saturated and partially saturated regions can be taken into account, using an analysis based upon the Dupuit-Forchheimer assumptions. Thus by applying an appropriate solution technique, the shape and position of the water table can be evaluated even when the capillary region significantly influences the distribution of flux.

For a given soil and flux of water, the ability of the soil to support a significant rate of gaseous diffusion is severely restricted for some distance above the water table. In fact, the gaseous phase is not continuous below the elevation at which the capillary pressure equals the bubbling pressure. Above this elevation, Z' , the fraction of air increases with elevation. At some distance above the water table, Z_A , the air phase may reach a magnitude such that gaseous transfer with the atmosphere is sufficient to maintain plant growth.

At least two methods may be used to evaluate the degree of aeration at which a sufficient rate of gaseous exchange can take place. The first, and probably most consistent, method is to evaluate the gaseous diffusion constant of the soil profile as a function of height above the water table. All points above which the diffusion is greater than some predeter-

mined minimum value can be considered sufficiently aerated.

The second method, and the easiest to apply, is to assume that the portion of the profile in which the effective saturation is less than some predetermined value, S_A , is sufficiently aerated. The second technique is utilized in this analysis to achieve the objective of the present study.

The critical saturation, S_A , may be expressed in terms of its corresponding critical capillary pressure, P_A , by the Brooks-Corey expression, equation (56) as

$$S_A = (P_b./P_A)^{\lambda} \quad (69)$$

Then

$$P_A./\rho g = (P_b./\rho g) S_A^{-1/\lambda} \quad (70)$$

and the problem is to determine the elevation, Z_A , above the water table at which P_A occurs.

Static equilibrium. When the soil water profile is in static equilibrium with the water table $Z = P_c./\rho g$, and equation (70) can be written

$$Z_A = \frac{P_b.}{\rho g} S_A^{-1/\lambda} \quad (71)$$

or, employing the previous scaling criteria, i.e., $Z_A. = Z_A/(P_b./\rho g)$,

$$Z_A. = S_A^{-1/\lambda} \quad (72)$$

Note that this equation is valid only for $H. > 1$, since no air phase exists when $P_c. \leq P_b.$

Steady downward flow. With steady percolation toward the water table capillary pressures are reduced, and P_A occurs at a greater elevation (if at all) than in the case of static equilibrium. Since the surface capillary pressure decreases with increasing flow rate, P_A must be less than the surface capillary pressure if S_A exists within the soil profile. Thus, a maximum percolation rate exists, beyond which a suitable root environment is nonexistent. At this limit

$$-cq. \leq (P_b./P_A)^{\eta} \quad (73)$$

Substituting equation (70) into (73) gives

$$-cq. \leq \left(\frac{P_b.}{\rho g}\right)^{\eta} \left(\frac{P_b.}{\rho g}\right)^{-\eta} S_A^{\eta/\lambda} \quad (74)$$

or

$$-q. \leq \frac{S_A^{\eta/\lambda}}{\epsilon} \quad (75)$$

Assuming that this limitation of $q.$ is satisfied, and noting that Z_A can exist only in the region $Z' < Z_A \leq Z''$, then the relation between elevation and pressure is described by equation (32), i.e.,

$$dz = \frac{P_b}{\rho g} \frac{dP_c}{1 + q \cdot P_c^\eta} \quad (32)$$

Integrating equation (32) between the limits $P_c = 1$ at $Z = Z'$ and $P_c = S_A^{-1/\lambda}$ at $Z = Z_A$ gives

$$Z_A - Z' = \frac{P_b}{\rho g} \int_1^{S_A^{-1/\lambda}} \frac{dP_c}{1 + q \cdot P_c^\eta} \quad (76)$$

or substituting equation (26) for Z' and expressing the result in scaled variables,

$$Z_A = \frac{1}{1+q} + \frac{S_A^{-1/\lambda}}{1} \int_1^{S_A^{-1/\lambda}} \frac{dP_c}{1 + q \cdot P_c^\eta} \quad (77)$$

where q has a negative value.

Steady upward flow. During steady upward flow, capillary pressure head increases more rapidly than elevation head. Therefore the effective saturation

continually decreases with elevation above Z' , and S_A can be located at any point within the region $Z' < Z_A < H$. Since the surface capillary pressure increases with increasing flow rate, the only limitation on flux for this case is that the prescribed flux can exist for a particular water table depth.

The height of the zone of insufficient aeration is given by equation (77), where q has a positive value when flow is upward.

As mentioned previously, the effective permeable height and effective saturated height are incorporated into a numerical model of agricultural drainage systems based upon the Dupuit-Forchheimer assumptions. This model is used to evaluate the shape and position of the water table as influenced by flow in the partially saturated region. After the water table is located, equations (72) and (77) are used to determine the region of the soil having adequate aeration.

The details of the computer program are presented in Appendix A.

EXPERIMENTAL PROCEDURES

Physical Model Experiments

The objective of the laboratory experiments is to provide data regarding the shape and position of the water table from a physical system in which capillary flow contributes a significant portion of the total flow toward the drain. These data are utilized to determine the boundary conditions under which the numerical model accurately describes the physical system. The numerical model is assumed to be applicable to a hypothetical system, and the remainder of this study is concerned with analyzing the response of that hypothetical system.

Data collected from two physical drainage models are used to verify the numerical model. These models were described in detail by Hedstrom, et al. (24). The larger facility is a soil-filled flume 12.2 meters (40 feet) long, 1.22 m (4 feet) high, and 5.1 cm (2 inches) thick. The smaller one, constructed as a scaled model of the larger, is 5.1 cm thick, 36.6 cm high, and 3.66 m long. Both physical models are fitted with tensiometers to allow monitoring the distribution of capillary pressures throughout the profile. Transient experiments were initiated by saturating the soil to a predetermined height and allowing the water table to become level. The transient response was due solely to drainage of preexisting fluid; that is, no infiltration accompanied the transient experiments. The transient experimental data used in this study are those reported by Hedstrom, et al. (24).

Steady-state experiments were conducted with the larger model only. A rainfall simulator constructed and described by Smith (40) was used to maintain a steady uniform rate of infiltration at the soil surface. A constant outflow level was maintained in the fully penetrating ditches with an overflow device. The tensiometers were connected to a series of manometer banks and monitored periodically after infiltration began. The water table was assumed to be in equilibrium with the infiltration rate when capillary pressures ceased to change significantly. Some fluctuations in capillary pressure continued indefinitely because of the influence of temperature fluctuations on conductivity and flow through the rainfall simulator.

Although the free surface of the liquid phase is referred to as the water table, the wetting phase fluid used in the experimental studies was actually a hydrocarbon. This fluid was used rather than water to minimize changes in soil capillary properties due to swelling of the soil. Because of lower surface tension and density, this fluid also results in simulation of a water-filled model of approximately twice the dimensions of the physical model.

Except for periodic in situ determinations of saturated conductivity, all properties of the soils used in this study are those presented by Hedstrom (23). The reader is referred to that publication for detailed descriptions of the techniques of evaluating the soil properties. Properties of the soils and the hydrocarbon liquid are tabulated in Appendix B.

Numerical Evaluations

This study is not intended to compare analytic solutions with experimentally determined drain performance. Two such comparisons (one for equilibrium, the other for transient drainage) are presented only

to show that typical analytic solutions do not adequately describe drain performance if capillary flow is significant. The assumption of no capillary flow is represented by the numerical solution of the case where bubbling pressure is zero. This solution is used as a basis to which solutions accounting for capillary flow are compared.

Except for numerical models to simulate the experimental data, all numerical models simulate a hypothetical drainage system having arbitrarily selected dimensions. Table 1 shows the range of physical parameters used in these numerical models. A total of 156 numerical analyses were conducted, simulating various combinations of the parameters shown in Table 1. Each numerical value of these parameters is hereafter designated by its symbol and the column of Table 1 in which the value appears. For example, L(3) represents a drain spacing of 1500 units.

Table 1. Summary of Physical Parameters Used in Numerical Models

Parameter	Condition				
	1	2	3	4	5
Saturated hydraulic conductivity - K , [L/T]	0.002				
Effective porosity - ϕ_e , [n.d.]	0.3				
Depth to impermeable layer - D , [L]	100.				
Drain spacing - L , [L]	500.	1000.	1500.		
Water level in ditch - Y_d , [L]	0.	33.33	66.67		
Initial water table elevation - Y_i , [L]	33.33	66.67	100.		
Infiltration rate - q , [L/T]	0.	2×10^{-6}	1×10^{-5}	2×10^{-5}	4×10^{-5}
Bubbling pressure head - $P_b/\rho g$, [L]	0.	5.	10.	20.	40.
Pore-size distribution index - λ , [n.d.]	2/3	4/3	10/3		

Note: brackets indicate dimensions of parameter; L - length, T - time, n.d. - dimensionless.

The units of each of these parameters are arbitrary, so long as consistent units are used. Note that the boundary conditions simulated are very specific, with the soil thickness, D , being a constant throughout the study. Except for four series of models, the drain spacing was held constant at 1000 units (designated as L(2) to represent the second enumerated condition of spacing, L , of Table 1).

Steady-state models. Solutions to the condition of drainage in equilibrium with steady infiltration were achieved by simulating the transient problem until the position of the water table remained constant. The criterion of equilibrium was selected such that the water table elevation did not change in the third significant digit as time increased by a factor of $10^{0.25}$. This transient technique is not efficient for generating equilibrium solutions, but is probably as fast with respect to computer time as the iterative technique required to obtain an equilibrium solution directly. This technique also avoided develop-

ment of another computer program and provided analyses of transient responses to steady percolation.

For each infiltration rate greater than zero, i.e., infiltration conditions 2 through 5 in Table 1, $q(2-5)$, a series of analyses was made with each ditch level condition, $Y_d(1-3)$. Each of these series of analyses consisted of a group of runs to evaluate separately the effects of $P_b/\rho g$ and of λ . The conditions for evaluating the effects of bubbling pressure head were $P_b/\rho g(1-5)$, $\lambda(2)$ (see Table 1), and those used to evaluate the effects of pore-size distribution were $P_b/\rho g(4)$, $\lambda(1-3)$. The condition $P_b/\rho g(1)$ was used in each case as the basis for comparison of capillary effects, since $P_b/\rho g = 0$ implies (from the Brooks-Corey theory) that there are no capillary effects.

To evaluate qualitatively the effect of spacing upon drain performance, one series of analyses (i.e., using the range of $P_b/\rho g$ and λ as described above) was made with each of conditions $L(1)$ and $L(3)$, with $Y_d(1)$, $q(4)$.

Transient models. The transient response of drains was analyzed for the case of no infiltration, $q(1)$, only. Maintaining drain spacing, $L(2)$, constant, a series of analyses (i.e., varying $P_b/\rho g$ and λ as described above) was made for each of six combinations of boundary and initial conditions as shown in Table 2.

Table 2. Initial and Boundary Conditions on Transient Flow Models

Boundary Condition, Y_d	Initial Condition, Y_i		
	33.33	66.67	100.0
0	x	x	x
33.33		x	x
66.67			x

As with the equilibrium analyses, the condition of no capillary flow (as shown in Table 1) for each series of runs was $P_b/\rho g(1)$. Effects of drain spacing were evaluated for $P_b/\rho g(1-5)$, $\lambda(2)$, $Y_i(2)$ with $Y_d(1)$ and $Y_d(2)$ and drain spacings $L(1)$ and $L(3)$.

Zone of aeration. After evaluating the position and shape of the water table for each of the above-mentioned model runs, the height of the zone of insufficient aeration was calculated. This height was added to the water table height to determine the region (if any) in which the degree of saturation was less than some predetermined arbitrary value. Further analyses were conducted with $P_b/\rho g = 0$ to determine the spacing (based upon no capillary considerations) that would result in a water table equal in elevation to the elevation of this zone of insufficient aeration.

Results of these analyses are presented in the following section.

The primary objectives of this study were to evaluate the effects of capillarity upon the location of a zone of adequate aeration, and to evaluate the drain spacing necessary to provide a specified depth of aeration. These objectives were pursued by using a numerical model based upon the Dupuit-Forchheimer assumptions. The results presented in this section represent only a portion of the solutions generated, and are typical of all solutions obtained. The remainder of the results are shown in Appendices C through F.

It must be emphasized that the results cannot be extended to more general boundary conditions than those simulated in this study. These investigations must be extended considerably before they can serve as general guidelines for design of drainage systems.

Inadequacy of Classical Drainage Theories

The experiments were expected to be significantly affected by the capillary region. The primary objective of this study was to evaluate the effects of capillary properties on the location of an aerated region, rather than to evaluate the adequacy of classical drainage theories. Therefore, the experimental data are compared with only two analytical solutions; one typical of the classical solutions to equilibrium drainage and the other to transient drainage problems. The ellipse equation and Glover's equation for the case of the drain on the impermeable boundary are compared with experimental data to illustrate that neglecting the effects of the capillary region can lead to significant errors.

The ellipse equation, based upon the Dupuit-Forchheimer assumptions, is

$$Y_c = (L^2 q / 2 + Y_d^2)^{1/2} \tag{78}$$

where Y_c is the water-table height at the centerline, Y_d is the water level in the drains, q is the dimensionless infiltration rate (q/K), and L is the drain spacing. Figure 4 shows a comparison of the solution to equation (78)

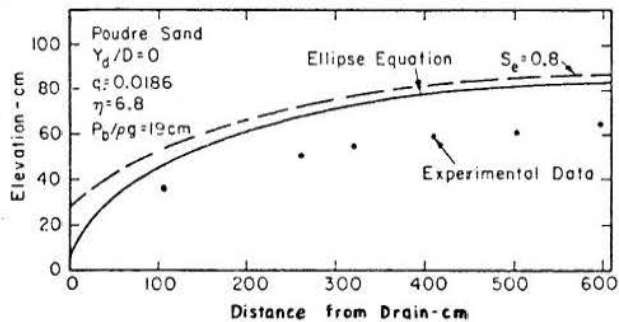


Figure 4. Comparison of solution to the ellipse equation with experimentally determined equilibrium water table position.

with the steady state water table measured in the large flume. The measured water table is lower at the centerline than predicted by the ellipse equation, which indicates that the ellipse equation underestimates the spacing that will maintain the desired water table position.

Figure 4 also shows the locus of points at which the effective saturation, S_e , is 0.8. This saturation was selected, based upon the work of Stegman, et al (42), to represent the limit of the region of adequate aeration. This zone is above the water table predicted by the ellipse equation, which indicates that the ellipse equation overestimates the spacing required to maintain the desired depth of aerated soil profile (assuming that the classical analysis considers the entire region above the water table to be aerated).

Glover's equation (Dumm, 19) for the case of drains on the impermeable boundary is also based upon the Dupuit-Forchheimer assumptions. This equation for transient drainage is

$$Y_c / Y_0 = L^2 / (L^2 + 9KY_0 t / 2\phi) \tag{79}$$

where t is time, ϕ is the drainable porosity, Y_0 is the initial drainable depth, and all other variables are as defined for the ellipse equation. Figure 5 compares the solution of equation (79) with the experimental data of Hedstrom, et al. (24). Glover's equation predicts a significantly slower decline of the water table than was observed experimentally. Thus, like the equilibrium equation, the classical equation for transient drainage underestimates the spacing for a given water table response.

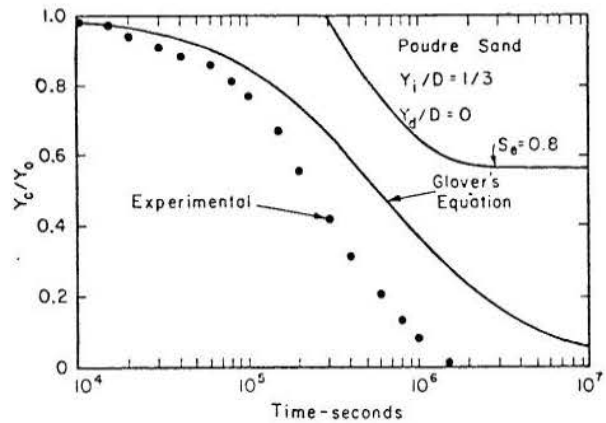


Figure 5. Comparison of solution to Glover's equation with experimentally observed decline of the water table.

The rate of decline of the surface at which $S_e = 0.8$ is much slower than predicted by Glover's equation as shown in Figure 5. In fact, the zone of adequate aeration can never come closer to the water level in the drain than the scaled height, Z_A , given by equation (72). Thus, Glover's equation also overestimates the drain spacing required to give a particular depth of aerated soil. The relative overestimation increases to infinity as the depth of desired aeration approaches the depth to water in the drain ditch.

The degree of deviation of experimental data from theory shown in Figures 4 and 5 may not be observed in field installations designed by an experienced drainage engineer. The design values of specific yield and water table depth are usually based

upon previous experience with similar drainage systems in similar soils. As a result, the value of specific yield used in design calculations is an artificial value, which forces the fit between experimental data and theory. Duke (18) discusses the hazard of using such artificial values of specific yield when the depth to water table differs significantly from that at which the specific yield was evaluated. Such "rule of thumb" practices undoubtedly give satisfactory results in areas where considerable past experience is available, but fail to give due consideration to those parameters that can result in significant differences in the flow situation.

Influence of Soil Parameters Upon Capillary Phenomena

Saturation profiles. In a previous section it was shown that the saturation profile is dependent upon the bubbling pressure head, pore-size distribution, and the magnitude and direction of vertical flux through the capillary region. Figure 6 illustrates the distribution of saturation with scaled height, Z , above the water table when the soil profile is in static equilibrium with the water table. As the distribution of pore sizes becomes more uniform (i.e., η increases) the volume of drainable water above the water table decreases. This volume of drainable water is represented by the area under the curves of Figure 6, evaluated from zero to a height, Z , corresponding to the water table depth. At large η the saturation approaches residual saturation ($S_e = 0$) at relatively small Z . Thus the partially saturated region has less influence upon drain performance if η is large. The shape of the saturation profile is less sensitive to changes in η for large values of η than for small values. Therefore, it is more important to evaluate η carefully for soils with a wide range of pore sizes (e.g., clays) than for soils with uniform pore sizes (e.g., clean sand).

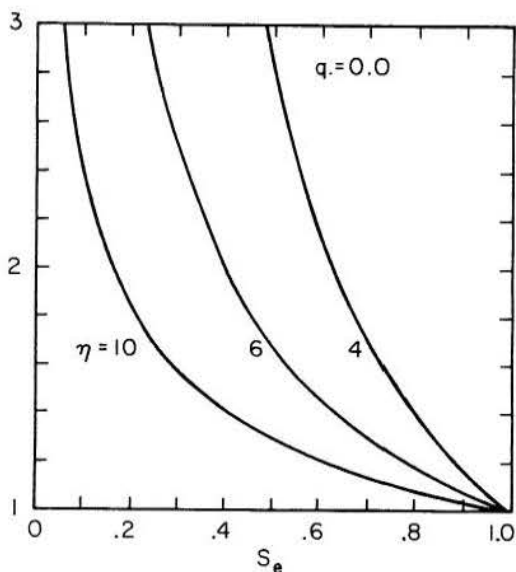


Figure 6. Saturation profile in static equilibrium with the water table.

The presence of a steady downward flux of water can significantly affect the shape of the saturation profile, as shown in Figure 7. For the flux shown here (i.e., one percent of the saturated conductivity) the saturation profile for low η values is little different from the equilibrium profile over the range

of Z shown. At high values of η , however, the saturation remains significantly higher. S_e approaches a minimum value corresponding to the saturation at which the hydraulic conductivity is equal in magnitude to the flux. It is apparent that a downward flux increases the volume of water in the capillary region and can be expected to increase the influence of the capillary region on drain performance. Saturation profiles for a range of downward fluxes are shown graphically in Appendix C.

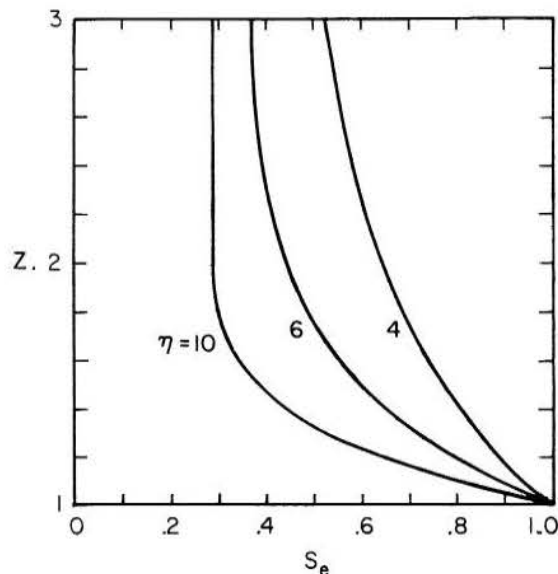


Figure 7. Saturation profile with steady downward flux ($q = -.01$).

When flux is upward, the pressure gradient increases rapidly with height above the water table. Because of these large gradients and the resulting high capillary pressures, the saturation decreases rapidly with Z , as shown in Figure 8. Anat, et al. (2) showed that a maximum height exists above which a given flux cannot be maintained from the water table. This limiting height is evidenced by the fact that S_e goes to zero at a finite elevation above the water table as shown in Figure 8.

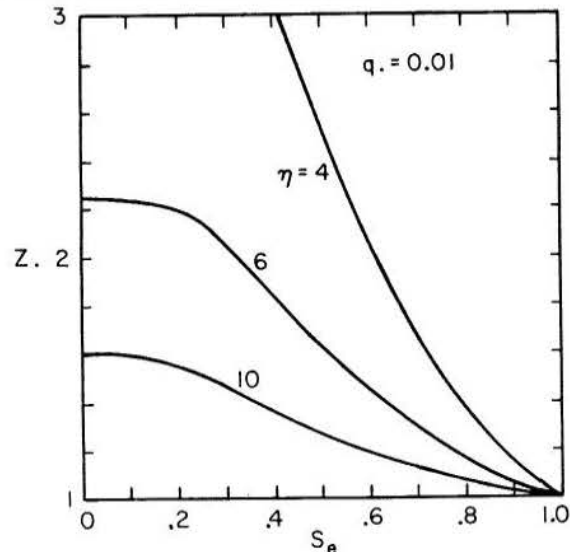


Figure 8. Saturation profile with steady upward flux ($q = .01$).

Since the areas under the curves of Figure 8 are less than in the corresponding equilibrium cases, upward flow can be expected to lessen the importance of horizontal flow in the capillary region. Such upward fluxes, which might result from evapotranspiration, are more pertinent to problems of subirrigation, and will not be considered further in this study.

Effective permeable height. Since the effective hydraulic conductivity is dependent upon saturation, the shape of the saturation profile strongly influences the ability of the capillary region to transmit water toward the drain. Figure 9 shows the effect of η and scaled depth to water table, H , upon the effective permeable height, H_k , for the static profiles of Figure 6. The curves of Figure 9 were calculated from equation (21). It is apparent that the major contribution to H_k occurs within a relatively short distance above the water table. H_k is influenced by water table depth to greater depth for small values of η and is more sensitive to changes in η for small values of η . Regardless of the value of η , H_k is never less than unity when $H > 1$.

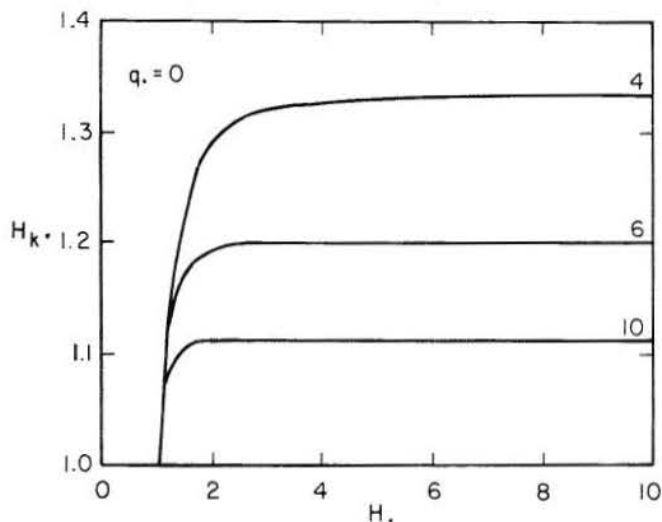


Figure 9. Scaled effective permeable height as a function of scaled water table depth, static equilibrium.

As previously mentioned, when the flux is downward, the hydraulic conductivity is nowhere less than the magnitude of the flux. Therefore, downward flux increases the effective permeable height, as indicated by equation (44) and shown graphically in Figure 10. The same general observations apply to this case as to the case of static equilibrium. However, H_k does not approach a constant as water-table depth increases. Rather, as indicated by the second term in equation (44), H_k increases linearly with H at higher values of H (i.e., $H > 2$). Therefore, the entire depth of profile can contribute to horizontal flow, and the water table depth becomes an important consideration in evaluating the total flow system.

Figure 11 shows the influence of q upon H_k for a selected value of H and η . The rate of increase of H_k with increasing q is not great except for relatively large q . This suggests that H_k can be calculated from the static equilibrium equation (equation 21) with little error so long as q is small. The rate of change of H_k with respect to q is also dependent upon η (and upon H .

for shallow water table depths). As η increases, the deviation from the equilibrium value increases. The relations between H_k and H for various flux ratios, from which Figure 11 is constructed, are presented in Appendix D.

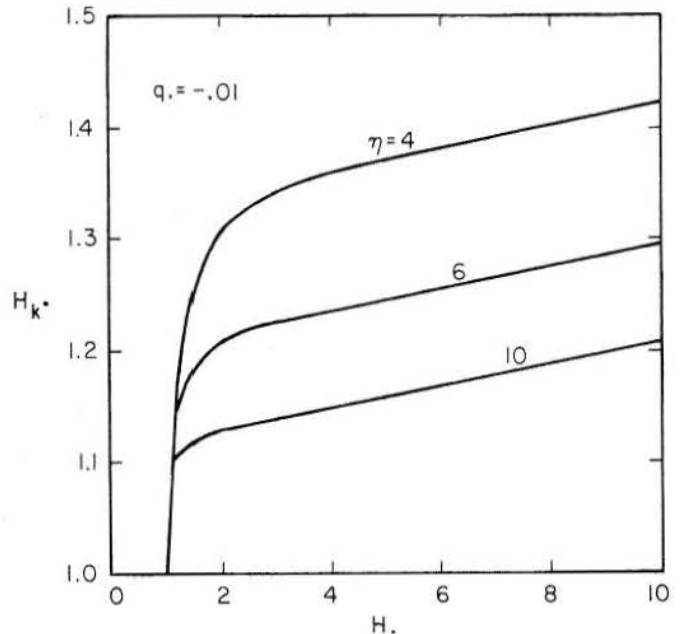


Figure 10. Scaled effective permeable height as a function of scaled water table depth, steady downward flux.

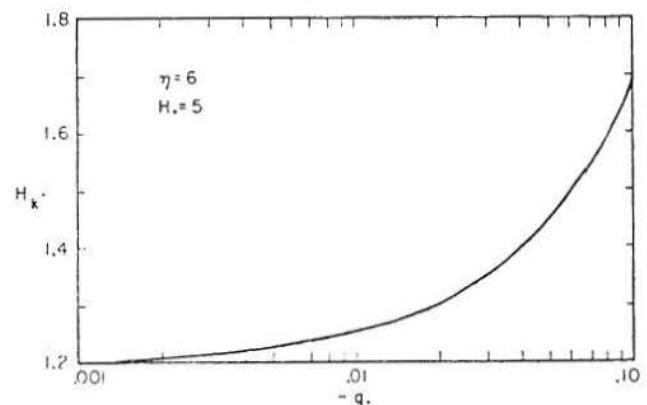


Figure 11. Effect of flux upon effective permeable height.

Effective saturated height. When the water table is in equilibrium with steady percolation, the effective permeable height is sufficient to describe the effects of the capillary region upon the flow system. In such a case, the saturation above the water table is invariant with time and release of water from storage does not enter into the consideration of flow. However, if the water table declines with time, at least part of the outflow is derived from soil storage, and changes in storage become important. The depth of water stored above the water table is indicated by the equivalent saturated height, H_s . Figure 12 illustrates the influence of water table depth, H , upon H_s , as computed from equation (59), when the soil profile is in static equilibrium with the water table. The scaled effective saturated height,

H_s , exhibits much the same relation to water table depth as does H_k . However, since the exponent of capillary pressure, P_c , is larger (i.e., a smaller negative number, $\lambda < \eta$) in the equation relating S_e to P_c than in the equation relating relative conductivity, K_r , to P_c , H_s is much larger than H_k at a particular water table depth. H_s is much more sensitive to H and to η than is H_k . Therefore, the effective specific yield continues to change as the water table declines to relatively large depths.

As in the case for H_k , a downward flux can significantly increase the magnitude of H_s . (Figure 13). Because of the magnitude of λ relative to η , H_s is influenced by the vertical flux more than is H_k . Therefore use of the equilibrium equation to calculate H_s may result in significant errors. Since the case of steady percolation in conjunction with a falling water table was not considered in this study, the effects of q upon H_s have not been evaluated in detail. The relations between H_s and H for a range of q are given in Appendix D, and are similar to Figures 12 and 13.

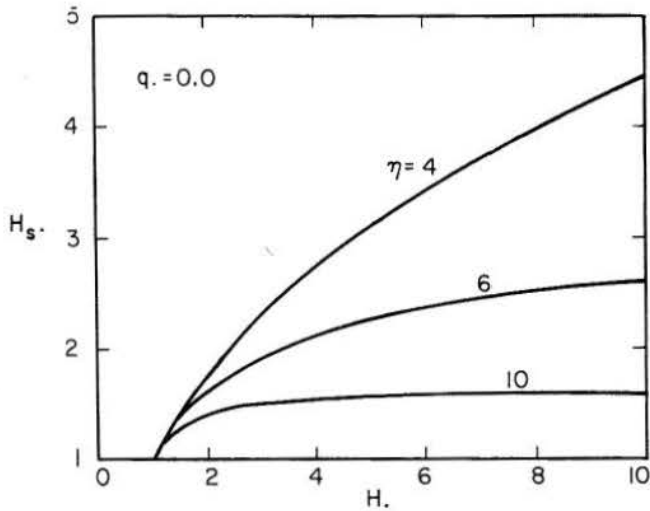


Figure 12. Scaled effective saturated height as a function of scaled water table depth, static equilibrium.

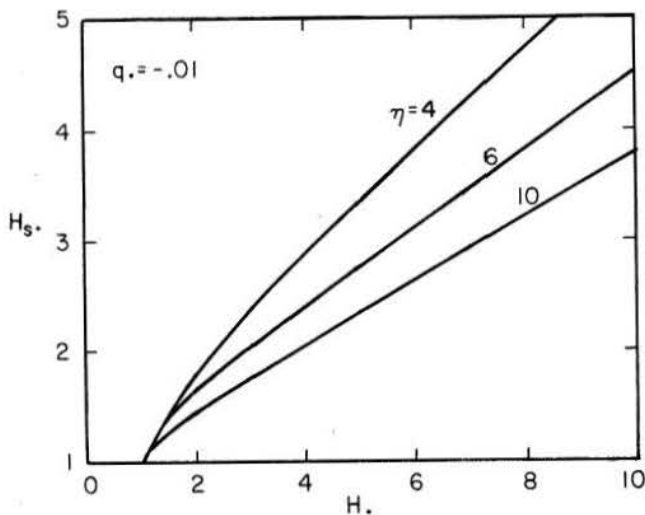


Figure 13. Scaled effective saturated height as a function of scaled water table depth, steady downward flow.

Zone of insufficient aeration. The concepts presented in the preceding sections provide a means to evaluate the contribution of capillary flow and storage in a Dupuit-Forchheimer analysis. Such an analysis will allow evaluation of the shape and position of the water table. The water table per se, however, is of indirect importance to the problem of maintaining a suitable degree of aeration within the root zone. Depending upon the distribution of pressure in the capillary region, the saturation remains quite high for some distance above the water table. It is of prime interest to evaluate the height above the water table at which the saturation is sufficiently low to permit adequate root aeration.

The scaled depth of insufficient aeration is given by equations (72) and (77) for static equilibrium and steady downward flow, respectively. Examination of these equations reveals that the scaled depth of insufficient aeration, Z_A , is simply that point on the saturation distribution curves (Figures 6 and 7) at which adequate aeration, S_A , occurs. Therefore, these two figures show, for their respective flux rates, Z_A as a function of any selected value of S_A .

It is apparent from Figures 6 and 7 that Z_A is dependent upon η . Figure 14 illustrates the effect of η upon Z_A when S_A is selected as 0.8. Z_A is very sensitive to changes in η for small η , but changes less than 20 percent as η increases from 6 to infinity. The effect of η upon Z_A is strongly dependent upon the selected value of S_A , as is apparent from Figure 6. At large S_A , η has little effect upon Z_A , but for smaller S_A , the variation of Z_A with η becomes very large.

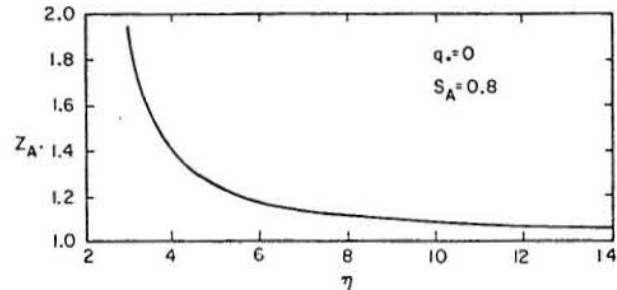


Figure 14. Effect of η upon scaled height of insufficient aeration, static equilibrium.

Comparing Figures 6 and 7 indicates that a downward flux increases the sensitivity of Z_A to η . Figure 15 shows the relation between Z_A and $-q$ for $S_A = 0.8$. From this figure, it is seen that Z_A differs from the static equilibrium value in excess of 10 percent only for $-q$ greater than about 0.07. Therefore, the static equilibrium value should be an adequate approximation to Z_A over a wide range of q . Again, however, this relationship between q and Z_A is dependent upon the selected value of S_A . For lower values of S_A , the range of q over which the equilibrium value is adequate is considerably smaller.

From Figure 7, it is evident that when a downward flux persists, there is a minimum saturation that can exist. Conversely, for any value of S_A and η there is a maximum downward flow rate beyond which the selected S_A cannot exist. This maximum flow rate, given by equation (75), is shown graphically as a function of η in Figure 16. The maximum flux is most sensitive to η at low values of η . Unless a

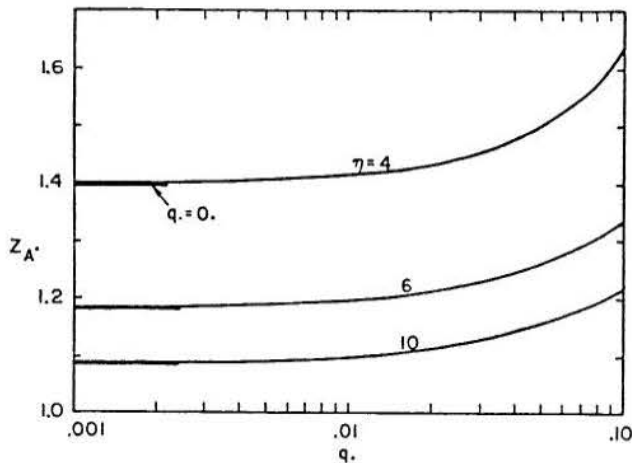


Figure 15. Effect of q . upon Z_A .

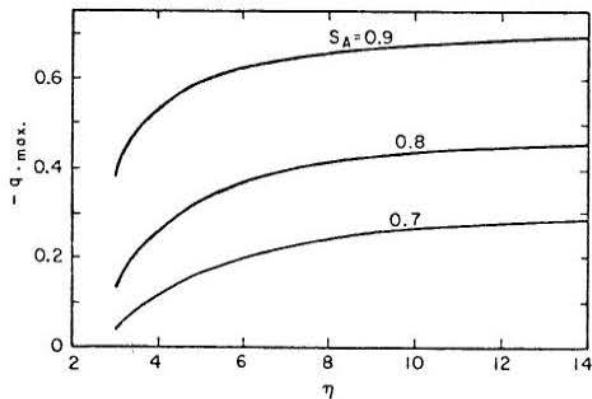


Figure 16. Effect of η upon the maximum downward flux at which a given S_A can exist.

very low S_A is required (or the saturated hydraulic conductivity is quite low) this restriction on q . is not likely to eliminate the zone of aeration under typical drainage conditions.

In the preceding discussions, it has been shown that the effects of η upon H_K , H_S , and Z_A are relatively small for large values of η . However, the same conclusion cannot be drawn regarding the effect of bubbling pressure head, $P_b/\rho g$. Since $P_b/\rho g$ is the scaling parameter for the dimensionless form of each of these terms, the effective permeable and saturated heights and the height of the zone of inadequate aeration are directly proportional to $P_b/\rho g$. Therefore, except for very low η values, such as may be characteristic of clay soils, the value of bubbling pressure head is expected to be a more important parameter than is η .

Verification of the Numerical Model

The numerical model developed in this study is based upon the Dupuit-Forchheimer assumptions and utilizes the concepts of equivalent permeable height and equivalent saturated height to account for the effects of the capillary region upon drain performance. Before this numerical model can be used to evaluate the effects of the various capillary parameters, it is necessary to demonstrate the adequacy of the model for predicting drain performance.

Steady state. When the water table is in equilibrium with steady infiltration, the specific yield of the soil does not influence drain performance, and the effective permeable height is a sufficient parameter to describe the effects of the capillary region. The numerical model used in this study, called FLODF, can be used to simulate the problem where capillary flow is neglected, simply by setting $H_K = 0$. Figure 17 shows the comparison of this numerical solution for no capillary flow with the solution of the ellipse equation. Since both solutions utilize the Dupuit-Forchheimer assumptions and both consider the nonlinearity in flow depth, the coincidence of the two solutions indicates that the size of finite increments used in the model is sufficiently small.

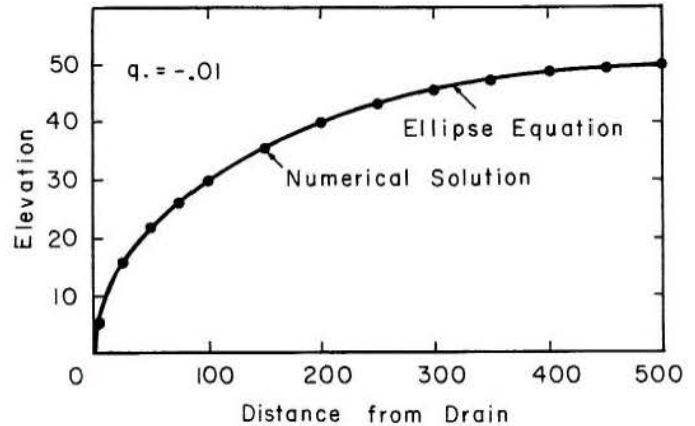


Figure 17. Comparison of solutions of numerical model and ellipse equation for steady state, no capillary flow considered.

The adequacy of the model to describe the problem where capillary flow is considered is shown in Figure 18. Local nonhomogeneity, as discussed by Smith (40), undoubtedly contributes to the scatter of the experimental data. Further comparisons, shown in Appendix E, indicate comparable agreement.

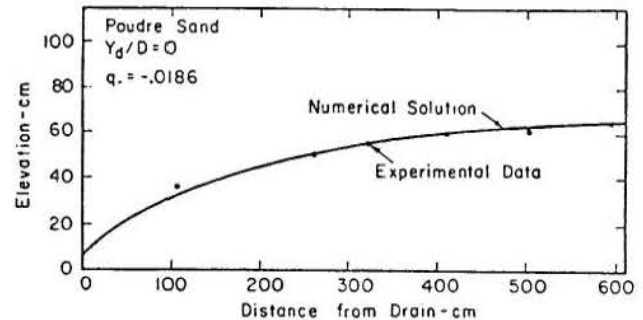


Figure 18. Comparison of numerical solution with experimental data, steady state.

Transient drainage. To verify the adequacy of FLODF to simulate the transient drainage problem neglecting capillary flow, the numerical solution is compared with Glover's solution for the drain on the boundary. Glover's equation for this case accounts for the nonlinearity in depth of flow. Because of the initially flat water table, however, Glover's solution is only an approximate solution to the differential equation. The comparison of these two solutions is shown in Figure 19. Except for early times,

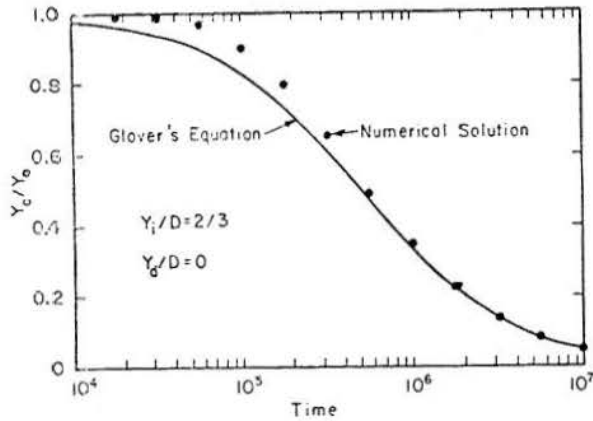


Figure 19. Comparison of solution of Glover's equation and numerical model, transient flow, no capillary flow considered.

the two solutions are quite close, which is accepted as evidence that the numerical solution is adequate. Figure 20 illustrates the adequacy of FLODF for simulating transient flow when the capillary region is significant. Except at very small times, which are usually of minor interest, FLODF adequately describes the rate of decline of the water table. Several factors undoubtedly contribute to the lack of agreement at early time. The numerical model does not consider the effect of vertical gradients, which are quite large at very early times. When the water table is falling rapidly, the celerity of the water table affects the shape of the saturation profile. Thus one would expect the water table to decline more rapidly than predicted until the rate of decline becomes sufficiently small.

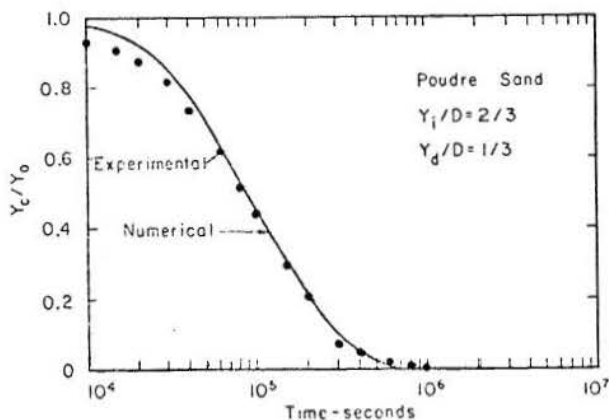


Figure 20. Comparison of transient numerical solution with experimental data, significant capillary flow.

For one series of experimental boundary conditions, the numerical model was not successful, as illustrated in Figure 20. When the water table was initially at the surface, the numerical model predicted a more rapid decline than was indicated by the experimental results, as shown in Figure 21.

It is apparent that the finite difference approach used is inadequate to accurately model this boundary condition. Under this initial condition, the soil remains saturated to the surface for some time after the water table begins to decline. Therefore, the water table will decline very rapidly

initially, with the initial outflow derived from expansion of the liquid phase and entrapped gases. Since the numerical model is based upon the assumption that the liquid is incompressible, the model cannot be expected to accurately evaluate this initial phase of drainage. As a result, the rate of decline is overpredicted. Therefore, further analyses of this initial boundary condition are not considered.

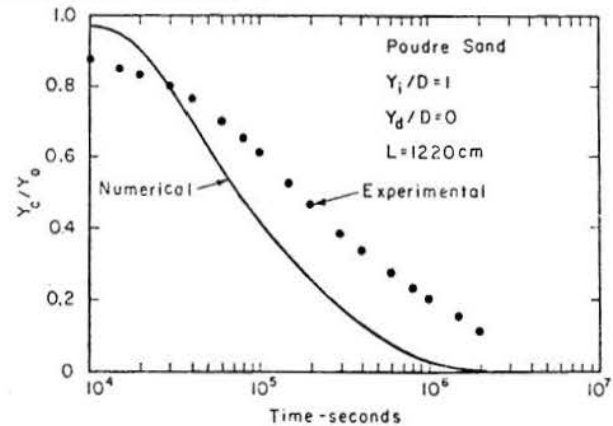


Figure 21. Comparison of experimental and predicted transient drain response, water table initially at soil surface.

Appendix E contains the comparison of experimental and predicted drain performance for all equilibrium and transient experiments in this study. All of these results are comparable to those presented in the text.

Except where the initial water table is at the surface, these comparisons between experimental and numerical results are considered sufficiently accurate to justify further use of the numerical model to evaluate the effects of capillary properties upon drain performance. The following sections describe the results of numerical model analyses conducted for a hypothetical soil, with a restricted range of boundary conditions. In all cases, the hydraulic conductivity is 2×10^{-3} , the effective porosity is 0.30, and the total depth of soil is 100. Except where specified otherwise, the drain spacing is 1000 units. The units of each parameter can be selected arbitrarily, so long as consistent units are used.

Shape and Position of the Water Table

The numerical model was used to simulate 156 combinations of boundary and initial conditions, soil properties, and infiltration rates. The numerical results discussed in the text of this paper represent typical examples of the cases evaluated. Appendix F contains the pertinent results of all analyses conducted.

Steady state. The effect of the capillary region upon the equilibrium position of the water table depends upon the effective permeable height of the capillary region. Figure 22 indicates the effect of increasing H_k by increasing the bubbling pressure head.

The upper curve of this figure represents the solution to the ellipse equation, i.e., capillary flow is neglected. As the effective permeable height, H_k , is increased, the area through which horizontal flow can occur is increased. Since the uniform flux is constant, the result of increasing H_k is that

smaller gradients are required and the water table becomes flatter. Since H_k is directly proportional to $P_b/\rho g$, the effect of increasing $P_b/\rho g$ is significantly reflected in the water table position.

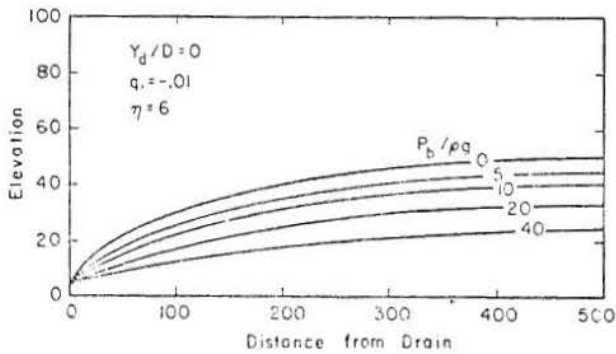


Figure 22. Effect of bubbling pressure head upon equilibrium water table position.

Figure 23 illustrates the effect of η upon water table position. The water table position is not nearly as sensitive to η as it is to $P_b/\rho g$, since H_k is affected relatively little by η .

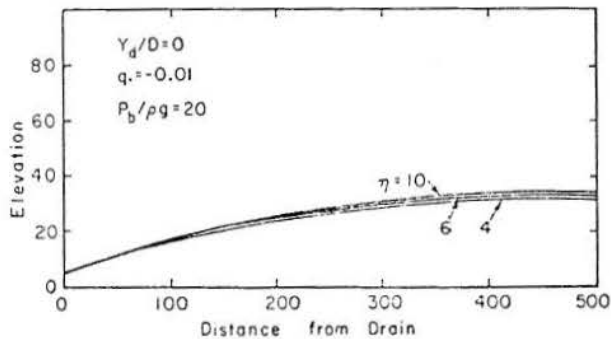


Figure 23. Effect of η upon equilibrium water table position.

The effect of infiltration rate upon water table elevation at the centerline, Y_c , is shown in Figure 24. The primary result of increased infiltration is to increase the water table elevation. This increase in water table elevation reduces the fraction of the flow moving through the capillary region by increasing the depth of saturated soil relative to H_k . H_k itself is little influenced by this increased flux, since increasing q tends to increase H_k while the higher water table results in a smaller distance from water table to soil surface and tends to decrease H_k . As a result, the magnitude of the error in water table elevation resulting from neglecting capillary flow is relatively independent of flux. The relative error, however, decreases as the infiltration rate is increased.

The tailwater level in the drain ditch has a significant effect upon the sensitivity of the water table to increased bubbling pressure head as shown in Figure 25. Increasing the ditch level increases depth available for saturated flow throughout the distance between drains. Thus the gradient necessary to attain a given flow is reduced. Although the gradient may be reduced in proportion to H_k (i.e. to $P_b/\rho g$), the effect upon water table position is substantially less at higher tailwater depths. These small gradients account for the minor change in Y_c with increasing $P_b/\rho g$ at $Y_d/D = 2/3$ (see Figure 25) while

Y_c changes by a factor of two over the range of $P_b/\rho g$ shown when $Y_d/D = 0$.

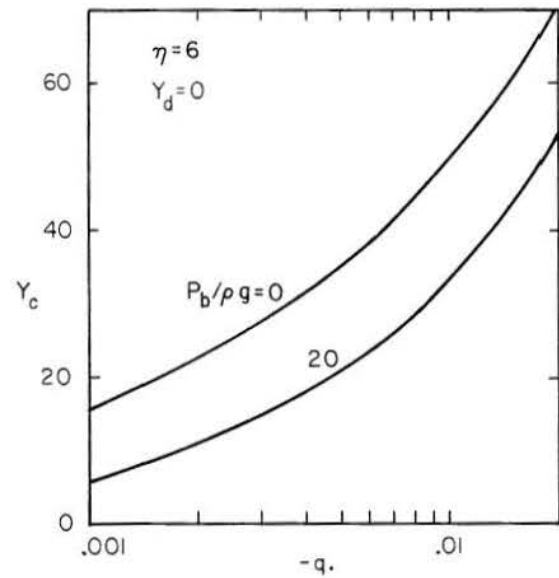


Figure 24. Effect of flux upon equilibrium water table position at centerline.

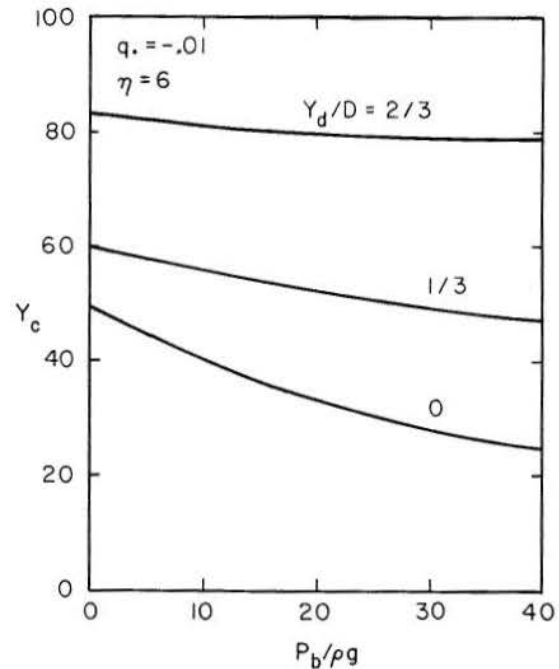


Figure 25. Effect of tailwater level upon relation between centerline water table height and bubbling pressure head.

Figure 26 indicates that drain spacing has little influence upon the magnitude of difference between the capillary and classical analyses of centerline water table elevation. Since the water table elevation at the centerline increases with increased drain spacing, the relative difference between the two analyses decreases with increasing drain spacing.

Transient flow. When the water table position changes with time, the contribution of the capillary region depends upon both the conductivity and the

saturation characteristics of the soil in the capillary zone. Hedstrom, et al. (24) demonstrated that the capillary region significantly affects transient performance of drains. Their techniques, however, did not allow evaluation of the relative effects of the effective permeable height, H_k , and the effective saturated height, H_s , upon transient drainage. The numerical model developed for this study is capable of such analyses. FLODF can simulate no capillary effects (H_k and H_s assumed zero), the influence of capillary conductivity only ($H_s = 0$), or the combined effects of capillary conductivity and capillary storage. Figure 27 shows one such analysis, considering each of the three alternatives for treating the capillary region.

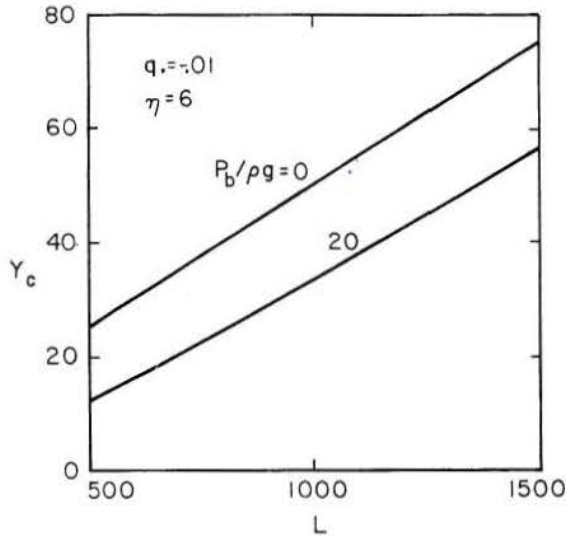


Figure 26. Effect of drain spacing upon influence of bubbling pressure head on equilibrium water table height.

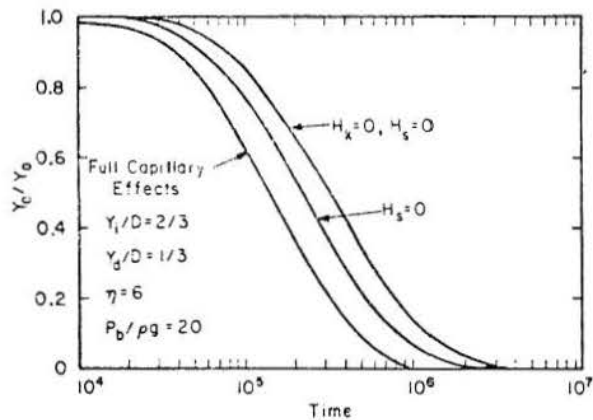


Figure 27. Comparison of the relative importance of capillary conductivity and capillary storage to decline of the water table at the centerline.

For the boundary conditions of the analysis shown, it is apparent that the effects of H_k and H_s are of the same order of magnitude. As in the steady-state problem, the capillary region tends to increase the depth through which flow can occur. This increased flow depth tends to increase the rate of flow, and consequently increases the rate of water table decline. Since H_s increases less rapidly than does

water table depth, the apparent specific yield increases with increasing water table depth. The low apparent specific yield at early time also increases the rate of water table decline, since a smaller volume of water must move through the soil to obtain a given water table decline.

The capillary flow is directly proportional to the magnitude of H_k . Therefore, since H_k approaches a constant at relatively shallow water table depth, the conductivity contribution of the capillary region is affected little by water table depth, so long as this depth is significantly greater than $P_b/\rho g$ (see Figure 9). On the other hand, H_s is quite sensitive to water table depth over a wide range. The influence of H_s upon release of capillary water is not dependent upon the magnitude of H_s , but rather upon dH_s/dH (i.e., rate of change of H_s with respect to water table depth). Since dH_s/dH is largest for small water table depth (see Figure 12), the effect of capillary storage is more pronounced when the water table is shallow. This water table depth dependence is illustrated by comparing Figures 27 and 28. The initial water table for Figure 27 was at $2/3$ the total soil depth, while that for Figure 28 was only $1/3$ the total soil depth. It is apparent that the capillary conductivity is more important than the capillary storage for this latter case.

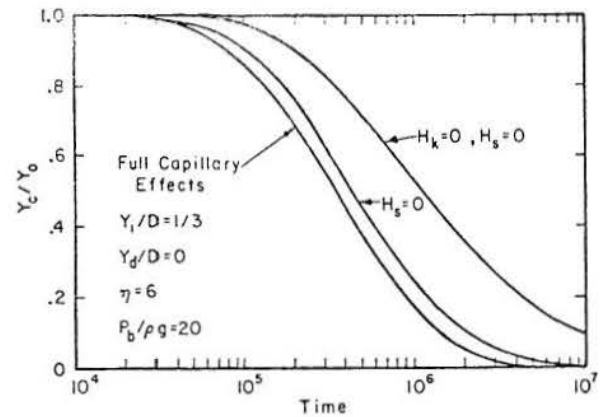


Figure 28. Comparison of the relative importance of capillary conductivity and capillary storage to decline of a deep water table.

The effects of increasing $P_b/\rho g$ upon the rate of water table decline are illustrated in Figure 29. As in the case of steady drainage, the capillary zone has a capacity to transmit flow toward the drain. As a result, increasing $P_b/\rho g$ increases the effective permeable height, H_k , and drainage is more rapid. Since H_s is also directly proportional to $P_b/\rho g$, the effect of capillary storage becomes more pronounced as $P_b/\rho g$ is increased. For the initial condition illustrated in Figure 29, the soil was initially saturated to the surface for $P_b/\rho g = 40$. As a result, the water table decline at the centerline was almost instantaneous to the point where the surface soil began to desaturate, thus accounting for the low water table at early time.

Figure 30 illustrates the effect of η upon the transient response. As indicated by equations (21) and (59) the rate of water table decline is not as sensitive to η as to $P_b/\rho g$. The sensitivity to changes in η decrease as η becomes large. So long as $P_b/\rho g$ is finite, the water table must drop more rapidly than indicated by the analysis neglecting capillary flow, regardless of the value of η . Note

that as $\eta \rightarrow \infty$, H_k and H_s approach $P_b/\rho g$ rather than zero.

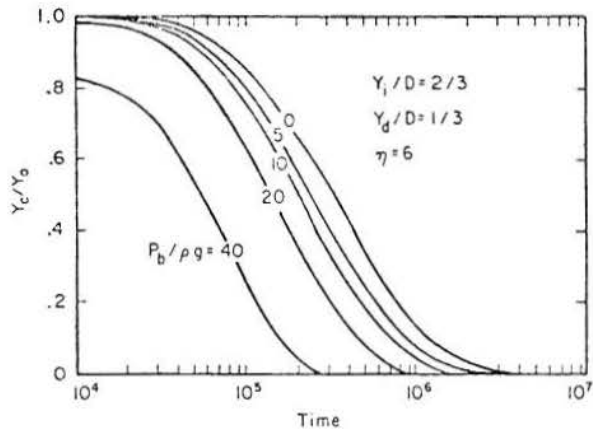


Figure 29. Effect of bubbling pressure head upon transient water table response.

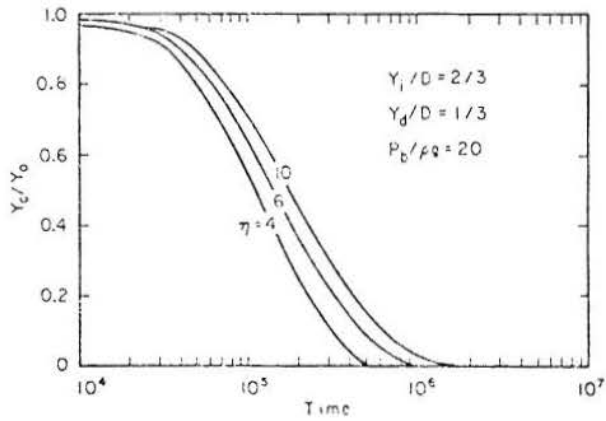


Figure 30. Effect of η upon transient water table response.

Because of differences in shape of the drawdown curves, it is rather impractical to compare the entire curve for various initial, boundary and capillary conditions. Further comparisons of water table response are based upon the time required to achieve an arbitrarily selected fraction of the total available drawdown. The relative drawdown, Y_c/Y_0 , selected for such comparisons is 0.8.

Figure 31 illustrates the effect of $P_b/\rho g$ upon the time at which the water table declines to 80 percent of its original height ($t_{.8}$). As $P_b/\rho g$ increases, the rate of change of $t_{.8}$ with respect to $P_b/\rho g$ decreases. This indicates that the relative effectiveness of the capillary zone in transmitting water toward the drain is reduced as $P_b/\rho g$ increases. Such an effect is expected if one considers the increased length of flow path and the increased convergence losses near the drain resulting from these large capillary effects.

Figure 32 illustrates the time to reach this 80 percent drainage relative to the corresponding time if capillary effects are neglected. Again, this figure illustrates the reduced effectiveness of the capillary region at high bubbling pressures. The extremely fast response at high bubbling pressure for the case $Y_i/D = 2/3$, $Y_d/D = 1/3$ is due to the fact

that the soil profile remains saturated to the surface during early time over a significant portion of the distance between drains.

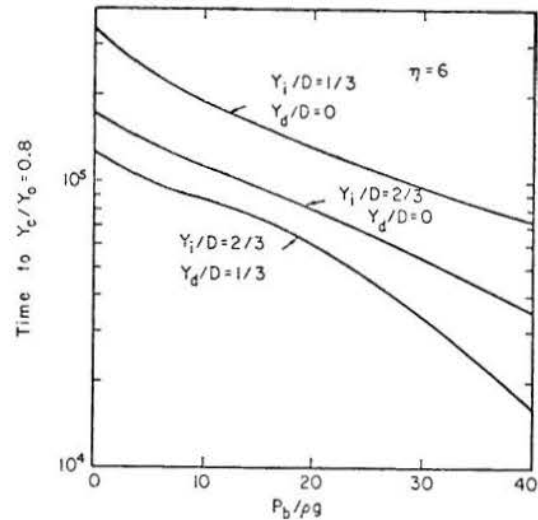


Figure 31. Effect of bubbling pressure head upon time required to lower water table to 80 percent of the initial drainable depth.

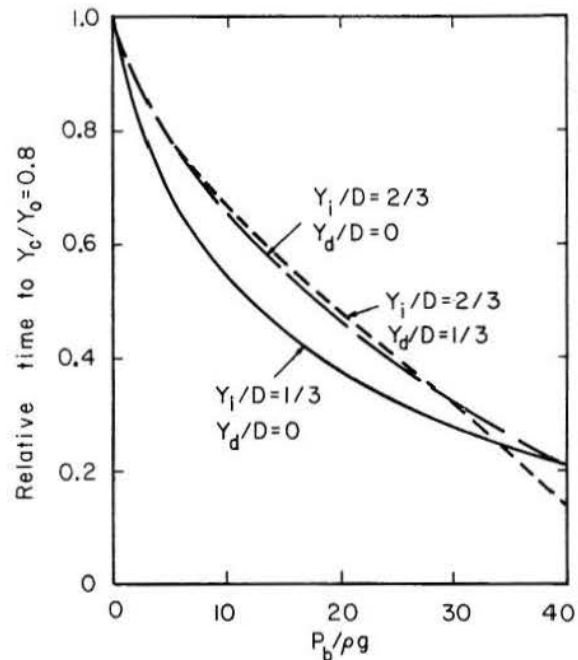


Figure 32. Effect of bubbling pressure head upon relative time required to lower water table to 80 percent of the initial drainable depth.

Figure 32 also illustrates the effect of the initial water table level upon drain response. At early time, the capillary region provides a larger flow area compared to the depth below the water table as the initial water table depth is decreased. This larger area for flow results in more rapid drawdown for the lower initial water table. As bubbling pressure head is increased, this difference in effective flow depths is offset by increased convergence losses in the capillary region. Figure 33 illustrates the effect of drain spacing upon the time required to

obtain 80 percent drawdown. The relative time used in Figure 33 is the time required for the spacing shown divided by the time to obtain the same drawdown with $L = 1000$. Drain spacing has little effect upon the relative significance of capillary flow except when the bubbling pressure head is large. When drain spacing is small, large values of $P_b/\rho g$ result in significant convergence losses, which reduce the effectiveness of the capillary region. On the other hand, when the spacing is increased, the effects of surface saturation at high bubbling pressure are significant over a larger proportion of the distance between drains. As a result, the rate of water table decline increases.

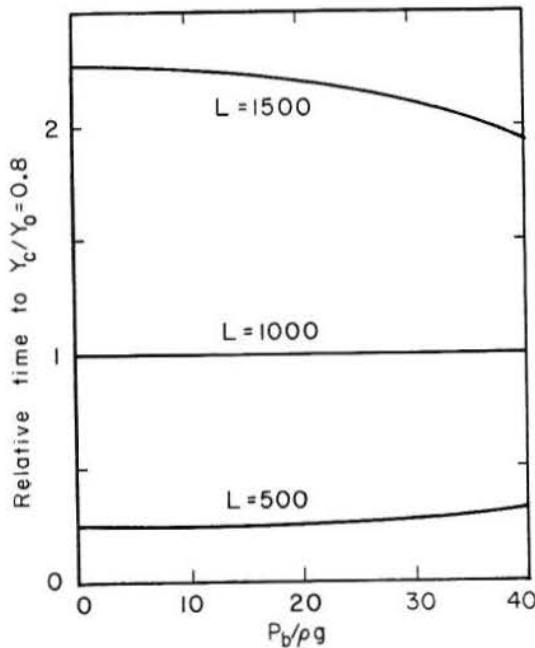


Figure 33. Effect of drain spacing upon time to obtain 80 percent drawdown relative to time at $L = 1000$.

Region of Aeration

The preceding sections have indicated the manner in which the capillary flow region affects the water table position. The water table position itself is of little direct importance to the problem of drainage, however. One important function of drainage is to maintain the water content within the root zone sufficiently low to permit adequate aeration. This section is devoted to a discussion of the effects of the region of insufficient aeration above the water table upon drain design. The effect of the capillary region upon design spacing of drains is evaluated by assuming that the upper limit of this zone of insufficient aeration satisfies the same aeration requirements as the water table calculated by neglecting capillary flow. Thus, an equivalent spacing is defined which will give a water table elevation (neglecting capillary flow) equal to the elevation of the zone of insufficient aeration. For this discussion, it is assumed that the soil is adequately aerated whenever the effective saturation is less than 0.8. Further numerical results are presented in tabular form in Appendix F.

Steady state. Figure 34 illustrates the equilibrium position of the surface where $S_A = 0.8$ for the water table profiles shown in Figure 22. In every

case, the height of the zone of insufficient aeration, Z_A , (calculated from equation 77) is greater than the depression of the water table resulting from capillary flow. As a result, increasing the bubbling pressure head results in a decreased depth of adequately aerated soil, even though the water table elevation is lowered.

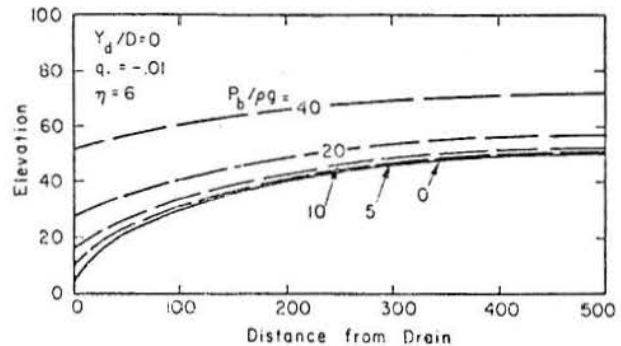


Figure 34. Effect of bubbling pressure head upon aeration profile, steady state drainage.

Figure 35 indicates that the effects of η upon the aerated region are more significant than the effects upon the water table position (see Figure 23). The sensitivity to changes in η decreases with increasing η , just as was the case regarding water table response. The position of the aerated zone is much less sensitive to η than to $P_b/\rho g$, as indicated by equation (77) (i.e., Z_A is directly proportional to $P_b/\rho g$).

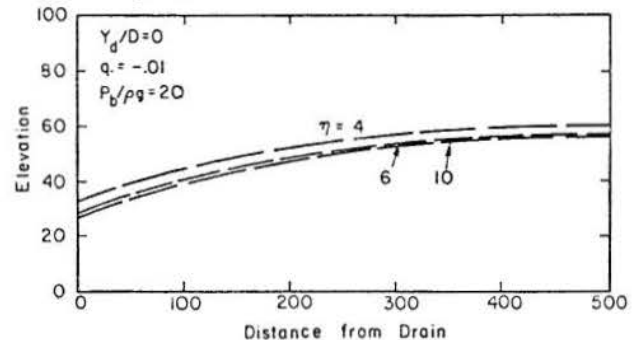


Figure 35. Effect of η upon equilibrium aeration profile.

Figure 36 illustrates the effects of $P_b/\rho g$ upon the height of the zone of insufficient aeration, Y_A , at the centerline between drains. Since the water table depression is always less than $P_b/\rho g$, Y_A continues to increase with increasing bubbling pressure head. The effect of $P_b/\rho g$ upon Y_A decreases somewhat as the water level in the ditch is decreased. This results from the increased effect of $P_b/\rho g$ upon water table elevation for small Y_d , as shown in Figure 25, and the fact that Z_A is independent of water table depth.

As evidenced by the curve for $Y_d/D = 2/3$, it is entirely possible that the soil will have no zone of adequate aeration at the centerline if the bubbling pressure is sufficiently large and the water table is near the surface.

The effects of the capillary region upon drain design are presented in terms of a relative spacing.

This relative spacing is the effective spacing (the spacing calculated by neglecting capillary flow which will result in a water table at the same elevation as Y_A calculated by considering capillary flow) divided by the actual drain spacing. Thus, this relative spacing is an indication of the spacing error resulting from neglecting the effects of the capillary region.

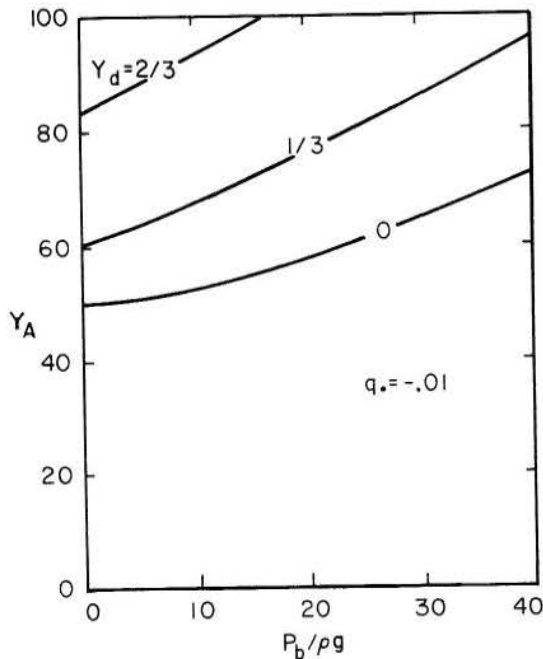


Figure 36. Effect of $P_b/\rho g$ upon height of zone of insufficient aeration at centerline.

Figure 37 illustrates the effect of bubbling pressure head and of tailwater level upon the relative spacing. Because of relatively small effects of capillary flow upon water table position, the relative spacing increases as depth of tailwater increases (i.e., as gradient decreases). The influence of convergence upon the effectiveness of the capillary zone is again apparent for $Y_d/D = 0$, since the rate of change of relative spacing with respect to $P_b/\rho g$ increases with increasing bubbling pressure head.

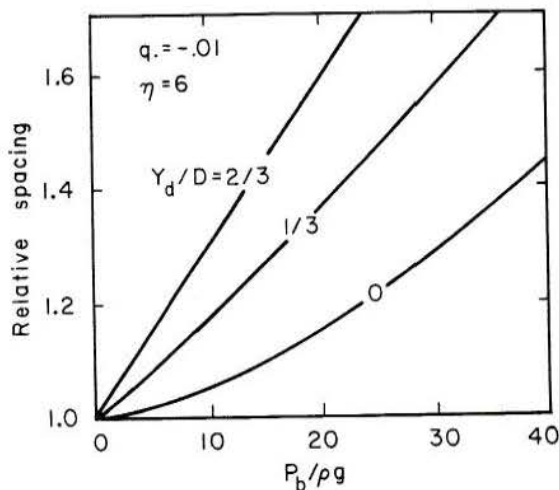


Figure 37. Effect of bubbling pressure head and tailwater level upon relative drain spacing.

The effects of drain spacing upon relative spacing are shown in Figure 38. Because of the increased significance of convergence losses, the relative spacing is larger for small drain spacing. The effects of drain spacing diminish as the spacing increases because these convergence losses become a progressively smaller fraction of the total head dissipated.

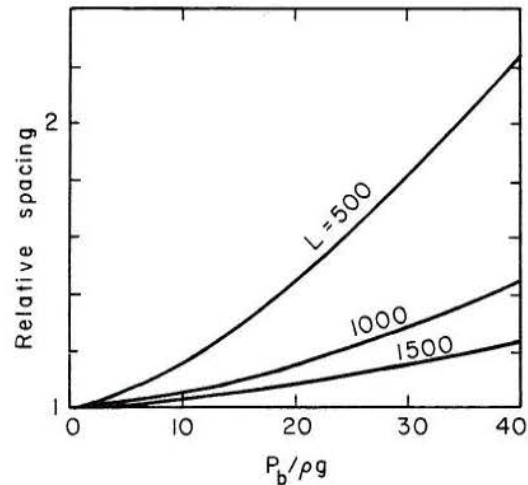


Figure 38. Effect of absolute drain spacing upon relative spacing, steady state.

The effects of infiltration rate and tailwater depth upon relative spacing are shown in Figure 39. The relative spacing is increased by either reducing the percolation rate or raising the tailwater level. Either of these changes results in smaller water table gradients. As discussed earlier, the effect of the capillary region upon the position of the water table is small when small water table gradients exist. Since Z_A is independent of water table gradient and depth to water table, it is these conditions where water table gradients are small that result in the greatest effects upon Y_A . Such small water table gradients exist whenever the infiltration rate is low or the tailwater depth (therefore the equivalent flow depth) is large.

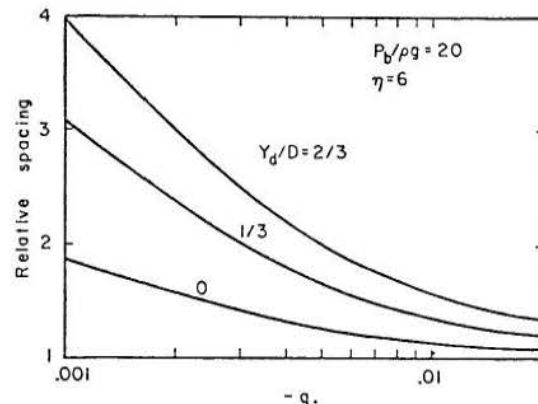


Figure 39. Effect of infiltration rate and tailwater depth upon relative spacing.

Transient drainage. During transient drainage, the zone of insufficient aeration above the water table is assumed to have a constant thickness with time. That is, Z_A is assumed to be the equilibrium value, given by equation (71). The basis for comparison of drain performance is arbitrarily selected as the time

required to reduce the zone of inadequate aeration at the centerline between drains, Y_A , to 0.8 the original drainable depth of the water table.

Figure 40 illustrates the effect of bubbling pressure head upon the rate of decline of the surface of aeration for the boundary conditions of Figure 29. Although the rate of decline of the water table is increased by large values of $P_b/\rho g$, the effect of the capillary zone upon position of the water table is not as large as the value of Z_A . As a result, increasing the bubbling pressure head delays the rate of decline of the zone of insufficient aeration. If Z_A is greater than the initial drainable depth, the aerated zone will never decline below the initial water table elevation, as is apparent for the case $P_b/\rho g = 40$ in Figure 40. As drainage progresses toward the final water table elevation, Y_d , the zone of inadequate aeration, Y_A , approaches the constant elevation, $Y_d + Z_A$.

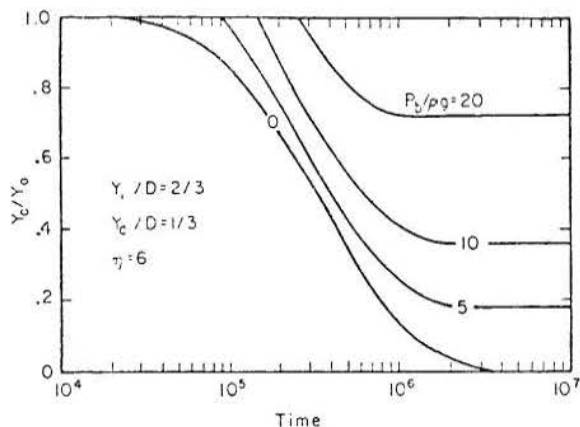


Figure 40. Effect of bubbling pressure head upon rate of decline of the zone of insufficient aeration.

Since the final water table elevation, Y_d , is independent of effects of the capillary region, the ultimate effects of η upon Y_A are somewhat larger than for the case of equilibrium, as shown in Figure 41. During early stages of aeration within the region considered, water table gradients are larger for large η . The resulting higher water table tends to compensate for small values of Z_A . As a result, the effects of η are initially small and tend to increase with time.

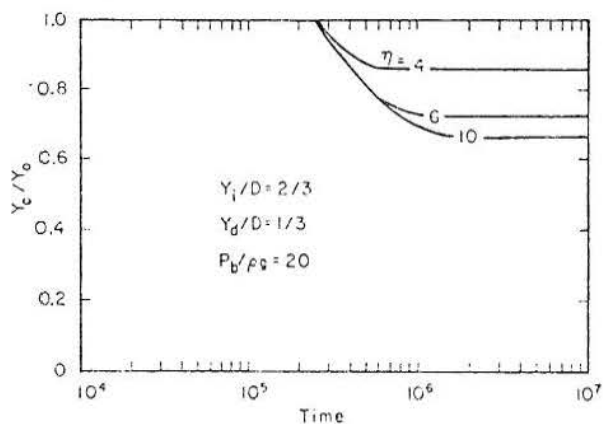


Figure 41. Effect of η upon rate of decline of zone of insufficient aeration.

From the discussion of equilibrium drainage, one would expect the relative spacing to increase as the drainable depth (i.e., $Y_i - Y_d$) decreases. Figure 42 illustrates the effect of the initial and final water table depths upon relative spacing. The effects of increased convergence losses, due to smaller saturated thickness are reflected in the slightly larger relative spacing shown for the case where the tail-water depth is zero.

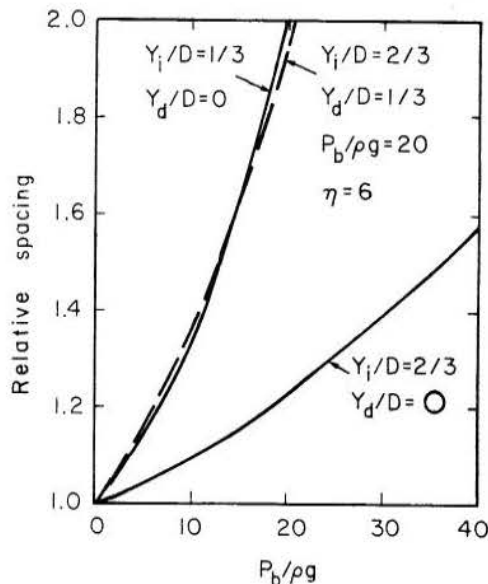


Figure 42. Effect of bubbling pressure head upon relative spacing for various initial and final boundary conditions.

The effect of drain spacing upon relative spacing is shown in Figure 43. Since the initial and final water table elevations are the same for all spacings shown, the average gradient decreases with increasing drain spacing. Such was not the case with the equilibrium drainage discussed previously. As a result, the effects of drain spacing upon relative spacing are small for transient drainage.

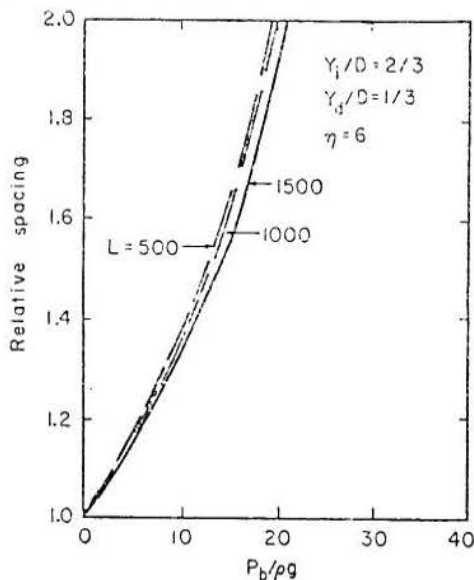


Figure 43. Effect of bubbling pressure head upon relative spacing as influenced by drain spacing.

It should be emphasized that the magnitude of the errors resulting from spacing calculations based upon the assumption of no capillary flow is dependent upon the degree of aeration required. If the effective saturation required for adequate aeration is less than the value (0.8) selected in this discussion,

the relative spacing will be even greater than that indicated. From the standpoint of drain design, this means that drains must be spaced even closer, and possibly deeper, to maintain an optimum environment for plant roots.

CONCLUSIONS AND RECOMMENDATIONS

The previous discussion has shown that neglecting the effects of the capillary region on drain performance can result in serious design deficiencies. Classical drainage theories always overestimate the maximum spacing. The degree of overestimation depends on the soil characteristics, the infiltration rate, initial and boundary conditions, and the degree of aeration required within the root zone.

The analyses performed for this study are insufficient to justify any general design criteria. They do, however, indicate the manner in which various parameters affect the error resulting from neglecting the capillary region.

The bubbling pressure head, $P_b/\rho g$, is the most significant soil property affecting the adequacy of classical drainage theories. As $P_b/\rho g$ increases, the classical theories provide a less accurate description of actual drain performance. The pore size distribution, n , is significantly less important in evaluating drain performance than is $P_b/\rho g$, especially for large values of n . This suggests that, if $P_b/\rho g$ can be determined accurately, then n (which is considerably more difficult to evaluate) could possibly be estimated with sufficient accuracy from a qualitative inspection of the particle size distribution.

In general, the classical theories provide the least adequate evaluation of drainage when water

table gradients are small. Such conditions may result from low infiltration rates, α , high hydraulic conductivity, K , (although large K is usually associated with small $P_b/\rho g$), a large saturated thickness of soil, or a large capillary region with respect to the total soil depth.

It is recommended that further investigation be conducted in the following areas:

1. The analyses presented here need to be extended to more boundary conditions so they will be useful in field design procedures,
2. The effects of capillary flow upon systems in which vertical gradients are significant (e.g., tile drains in thick aquifers) should be evaluated,
3. The effects of soil stratification upon the importance of the capillary region should be evaluated,
4. The possibility of developing correction factors to be applied to classical drainage theories should be investigated, and
5. Methods for field evaluation of bubbling pressure head and pore size distribution index need to be developed.

LITERATURE CITED

1. Amerman, C. R., Appendix 1, Numerical solution of the flow equation. In: Soil and water physical principles and processes, by Daniel Hillel, Academic Press, New York, pp. 241-254, 1971.
2. Anat, A., H. R. Duke and A. T. Corey, Steady upward flow from water tables. Colo. State Univ. Hydrology Paper No. 7, Fort Collins, Colo., 34 pp., 1965.
3. Bittinger, M. W., H. R. Duke, and R. A. Longenbaugh, Mathematical simulations for better aquifer management. Publ. No. 72 of the IASH, Symposium on Artificial Recharge and Management of Aquifers, Haifa, Israel, pp. 509-519, 1967.
4. Bouwer, H., Theoretical aspects of flow above the water table in tile drainage of shallow homogeneous soils. Proc. Soil Sci. Soc. Amer., 23: 260-263, 1959.
5. Bouwer, H., Theoretical aspects of unsaturated flow in drainage and subirrigation. Agr. Engr., pp. 395-400, 1959.
6. Bouwer, H., Unsaturated flow in ground-water hydraulics. J. of Hydr. Divn. Amer. Soc. Civil Engrs., HYS: 121-144, 1964.
7. Breitenbach, E. A., D. H. Thurnau, and H. K. van Poolen, Immiscible fluid flow simulator. Soc. Petr. Engr., AIME, Paper No. SPE2019, Dallas, Tex., April 22-23, 1968.
8. Breitenbach, E. A., D. H. Thurnau, and H. K. van Poolen, The fluid flow simulation equations. Soc. Petr. Engr., AIME, Paper No. SPE2020, Dallas, Tex., April 22-23, 1968.
9. Breitenbach, E. A., D. H. Thurnau, and H. K. van Poolen, Solution of the immiscible fluid flow simulation equations. Soc. Petr. Engr., AIME, Paper No. SPE2021, Dallas, Tex., April 22-23, 1968.
10. Brooks, R. H. and A. T. Corey, Hydraulic properties of porous media. Colo. State Univ. Hydrology Paper No. 3, Fort Collins, Colo., 27 pp., 1964.
11. Brutsaert, W., G. S. Taylor, and J. N. Luthin, Predicted and experimental water table drawdown during tile drainage. Hilgardia, 31: 389-418, 1961.
12. Chapman, T. G., Capillary effects in a two-dimensional groundwater flow system. Geotechnique, 10: 55-61, 1960.
13. Childs, E. C., A treatment of the capillary fringe in the theory of drainage. J. Soil Sci., 10: 83-100, 1959.
14. Childs, E. C., The nonsteady state of the water table in drained land. J. Geophys. Res., 65: 780-782, 1960.
15. Childs, E. C. and A. Poulouvasilis, The moisture profile above a moving water table. J. of Soil Sci., 13: 271-285, 1962.
16. Childs, E. C., An introduction to the physical basis of soil water phenomena. John Wiley and Sons, Ltd., London, 493 pp. 1969.
17. Dagan, G., Linearized solution of unsteady deep flow toward an array of horizontal drains. J. Geophys. Res., 69: 3361-3369, 1964.
18. Duke, H. R., Capillary properties of soils-influence upon specific yield. Trans. Amer. Soc. Agric. Engrs., (in press).
19. Dumm, L. D., Drain and spacing formula. Agr. Engr., 35: 726-730, 1954.
20. Freeze, R. A., Influence of the unsaturated flow domain on seepage through earth dams. Water Resources Res., 7: 929-941, 1971.
21. Gardner, W. R., Some steady-state solutions of the unsaturated moisture flow equation with application to evaporation from a water table. Soil Sci., 85: 228-233, 1958.
22. Hagan, R. M., H. R. Haise, and T. W. Edminister, Irrigation of Agricultural lands. Monograph No. 11, Amer. Soc. of Agron., Madison, Wis.,
23. Hedstrom, W. E., Models for subsurface drainage. Ph.D. dissertation submitted to Colo. State Univ., 149 pp., 1970.
24. Hedstrom, W. E., A. T. Corey, and H. R. Duke, Models for subsurface drainage. Colo. State Univ. Hydrology Paper No. 48, Fort Collins, Colo., 56 pp., 1971.
25. Hillel, Daniel, Soil and water physical principles and processes. Academic Press, New York, 288 pp., 1971.
26. Hornberger, G. M., J. Ebert, and I. Remson, Numerical solution of the Boussinesq equation for aquifer-stream interaction. Water Resources Res., 6: 601-608, 1970.
27. Kraijenhoff van de leur, D. A., Some effects of the unsaturated zone on nonsteady free-surface groundwater flow as studied in a scaled granular model. J. Geophys. Res., 67: 4347-4362, 1962.
28. Letey, J., L. H. Stolzy, and W. D. Kemper, Soil aeration. In: Irrigation of agricultural lands. Edited by R. M. Hagan, H. R. Haise, and T. W. Edminister. Amer. Soc. of Agron. Monograph No. 11, Madison, Wis., pp. 941-949, 1967.
29. Luthin, J. N., The falling water table in tile drainage-II. Proposed criteria for spacing tile drains. Trans. Amer. Soc. Agric. Engrs., 2: 44-45, 1959.

30. Luthin, J. N. and P. R. Day, Lateral flow above a sloping water table. Proc. Soil Sci. Soc. Amer., 19: 406-410, 1955.
31. Luthin, J. N. and R. V. Worstell, The falling water table in tile drainage-I. A laboratory study. Proc. Soil Sci. Soc. Amer., 21: 580-584, 1957.
32. Luthin, J. N. and R. V. Worstell, The falling water table in tile drainage-III. Factors affecting the rate of fall. Trans. Amer. Soc. Agric. Engrs., 2: 45-51, 1959.
33. McWhorter, D. B., Personal communication. Dept. of Agric. Engr., Colo. State Univ., 1971.
34. Myers, L. E. and C. H. M. van Bavel, Measurement and evaluation of water table elevations. Proc. 5th Congress, ICID, Toyko, Japan, Question 17, pp. 109-119, 1963.
35. Rubin, J., Theoretical analysis of two-dimensional transient flow of water in unsaturated and partly unsaturated soils. Proc. Soil Sci. Soc. Amer., 32: 607-615, 1968.
36. Schilfgaarde, J. van, Approximate solutions to drainage flow problems. In: Drainage of agricultural lands. Edited by J. N. Luthin, Amer. Soc. of Agron. Monograph No. 7, Madison, Wis., pp. 79-112, 1957.
37. Schilfgaarde, J. van, Design of tile drainage for falling water tables. J. of Irrig. and Drain. Divn., Amer. Soc. Civil Engrs., IR2: 1-11, 1963.
38. Schmid, P. and J. Luthin, The drainage of sloping lands. J. Geophys. Res., 69: 1525-1529, 1964.
39. Sewell, J. I. and J. van Schilfgaarde, Digital computer solutions of partially unsaturated steady-state drainage and subirrigation problems. Trans. Amer. Soc. Agric. Engrs., 6: 292-296, 1963.
40. Smith, R. E., Mathematical simulation of infiltrating watersheds. Ph.D. dissertation submitted to Colo. State Univ., 193 pp., 1970.
41. Soil Conservation Service, USDA, SCS national engineering handbook Section 16 - Drainage of agricultural land. Engr. Divn., Soil Cons. Serv., USDA, Washington, D. C., 430 pp., 1971.
42. Stegman, E. C., A. E. Erickson, and E. H. Kidder, Characterization of soil aeration during sprinkler irrigation. Summer Meeting, Amer. Soc. Agric. Engrs., Paper No. 66-214., 18 pp., 1966.
43. Stolzy, L. H. and J. Letey, Correlation of plant response to soil oxygen diffusion rates. Hilgardia, 35: 567-575, 1964.
44. Swartzendruber, D. and D. Kirkham, Capillary fringe and flow of water in soil. Soil Sci. 81: 473-484, 1956.
45. Swartzendruber, D. and D. Kirkham, Capillary fringe and flow of water in soil: II. Experimental results. Soil Sci., 82: 81-95 1956.
46. Talsma, T., The effect of flow above the water table on tile drain design in Murrumbidgee irrigation area soils. Aust. J. of Soil Res., 3: 23-30, 1965.
47. Verma, R. D. and W. Brutsaert, Similitude criteria for flow from unconfined aquifers. J. Hydr. Divn., Amer. Soc. Civil Engrs., HY9: 1493-1509, 1971.
48. Werner, P. W., Some problems in non-artesian ground-water flow. Trans. Amer. Geophys. Union, 38: 511-518, 1957.
49. White, N. F., D. K. Sunada, H. R. Duke, and A. T. Corey, Boundary effects in desaturation of porous media. Soil Sci., 113: 7-13, 1972.
50. Youngs, E. G., Hodograph solution of the drainage problem with very small drain diameter, Water Resources Res., 6: 594-600, 1970.

APPENDIX A

ONE-DIMENSIONAL NUMERICAL MODEL

The digital computer program utilized in this study employs a backward-difference-implicit scheme for solution of the system of finite-difference equations. The development of these equations, the techniques of solving the equations, and a copy of the computer program, FLODF, are presented in this section.

The Finite-Difference Equations

The partial differential equation describing mass continuity in flow of a solution through porous media has been given by many investigators as

$$\frac{\partial \rho_s}{\partial t} = -\nabla \cdot F + S \quad (A-1)$$

where ρ_s is the mass of solution per unit volume of porous medium, F is the mass flux of solution, S is the rate of production of mass per unit volume of porous medium, and t is time. Assuming that the density of the solution phase, ρ_L , is invariant in space and time, equation (A-1) can be reduced to

$$\frac{\partial \theta}{\partial t} = -\nabla \cdot Q + S_v \quad (A-2)$$

where θ is the volumetric solution content (ρ_s/ρ_L), Q is the volumetric flux rate (F/ρ_L), and S_v is the source strength on a volumetric basis (S/ρ_L).

As previously discussed, program FLODF utilizes a Dupuit-Forchheimer approach to the solution of equation (A-2). Figure A-1 illustrates the boundary conditions and symbols utilized in FLODF.

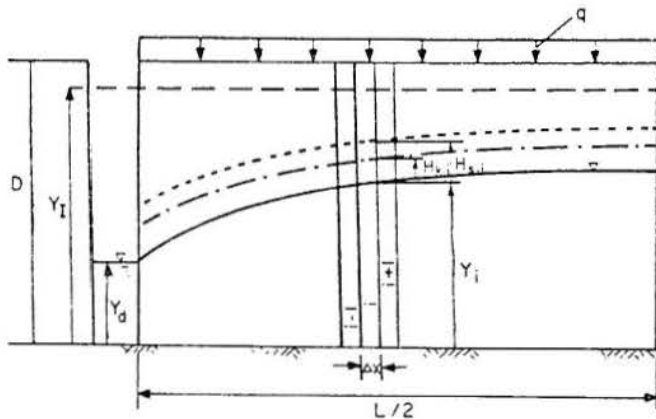


Figure A-1. Boundary conditions and symbolism used in FLODF.

Equation (A-2) can be written in one-dimensional form as

$$\phi \frac{\partial Y_s}{\partial t} = -\frac{\partial Q}{\partial x} + q \quad (A-3)$$

where x is the horizontal space coordinate, measured from the drain outlet, ϕ is the drainable porosity,

Y_s is the effective saturated thickness, and q is the uniform percolation rate. Assuming that the volumetric flux is described by Darcy's equation, equation (A-3) becomes

$$\frac{\partial}{\partial x} (K Y_k \frac{\partial Y}{\partial x}) = \phi \frac{\partial Y_s}{\partial t} - q \quad (A-4)$$

where Y_k is the depth available for horizontal flow and Y is the height of the water table. This depth of horizontal flow is the sum of the water table height and the effective permeable height, H_k , or

$$Y_k = Y + H_k \quad (A-5)$$

The effective saturated thickness, Y_s , is similarly given by

$$Y_s = Y + H_s \quad (A-6)$$

Both H_k and H_s are described in detail in the text, and are dependent upon soil properties and the rate of percolation through the partially saturated zone, q .

If the soil is homogeneous with respect to the saturated hydraulic conductivity, K , then equation (A-4) may be written

$$\frac{\partial}{\partial x} (Y_k \frac{\partial Y}{\partial x}) = \frac{\phi}{K} \frac{\partial Y_s}{\partial t} - \frac{q}{K} \quad (A-7)$$

By dividing the flow region into N equal increments in the x -direction, and applying a backward difference scheme, equation (A-7) can be written in finite-difference form for increment $i(i-2, N-1)$ as

$$\frac{Y_{k,i+1/2} (Y_{i+1}^{t+\Delta t} - Y_i^{t+\Delta t})}{\Delta x^2} - \frac{Y_{k,i-1/2} (Y_i^{t+\Delta t} - Y_{i-1}^{t+\Delta t})}{\Delta x^2} = \frac{\phi}{K} \frac{(Y_{s,i}^{t+\Delta t} - Y_{s,i}^t)}{\Delta t} - \frac{q_i^{t+\Delta t/2}}{K} \quad (A-8)$$

where the subscripts i , $i-1$ and $i+1$ represent the grid of interest and its two adjacent grids, respectively; t refers to a time level at which the solution has been determined, and Δt is the increment of time at the end of which a solution is desired. The implicit solution technique used places no restrictions upon the time increment to achieve stability of the solution. Other restrictions upon Δt will be discussed later.

As suggested by Breitenbach, et al. (7) the area through which flow may occur between adjacent grids (i.e., $Y_{k,i+1/2}$, $Y_{k,i-1/2}$) is taken as the area from which flow emanates. Breitenbach, et al. found such a technique to better simulate problems in which either a seepage face or irregular lower boundaries exist than does the mean flow area indicated by equation (A-8). Thus, equation (A-8) becomes

$$\frac{Y_{k,i+1}(Y_{i+1}^{t+\Delta t} - Y_i^{t+\Delta t})}{\Delta x^2} - \frac{Y_{k,i}(Y_i^{t+\Delta t} - Y_{i-1}^{t+\Delta t})}{\Delta x^2} = \frac{\phi}{K} \frac{(Y_{s,i}^{t+\Delta t} - Y_{s,i}^t)}{\Delta t} - \frac{q_i^{t+\Delta t/2}}{K} \quad (A-9)$$

With this simplification, equation (A-9) would be expected to give an accurate solution only when the difference between Y_k for adjacent grids is small with respect to Y_k (i.e., small gradient or large number of grids).

Since both Y_k and Y_s are functions of the dependent variable, Y , equation (A-9) remains non-linear. If the time increment, Δt , is sufficiently small that

$$|Y^{t+\Delta t} - Y^t| \ll Y^t \quad (A-10)$$

then $Y_k^{t+\Delta t}$ may be taken as Y_k^t , $H_s^{t+\Delta t}$ as H_s^t , and H_s^t as $H_s^{t-\Delta t}$ with little error. Then equation (A-9) may be written as

$$\begin{aligned} & (Y_{i+1}^t + H_{k,i+1}^t)(Y_{i+1}^{t+\Delta t} - Y_i^{t+\Delta t}) - \\ & (Y_i^t + H_{k,i}^t)(Y_i^{t+\Delta t} - Y_{i-1}^{t+\Delta t}) = \\ & \frac{\phi \Delta x^2}{K \Delta t} (Y_i^{t+\Delta t} + H_{s,i}^t - Y_i^t - H_{s,i}^{t-\Delta t}) - \frac{\Delta x^2}{K} q_i^{t+\Delta t/2} \end{aligned} \quad (A-11)$$

If q is a constant with time and space, the superscript and subscript may be dropped. The coefficients representing Y_k can be expressed as known constants at any given time step, such that

$$C_1 = Y_{i+1}^t + H_{k,i+1}^t \quad (A-12)$$

and

$$C_2 = Y_i^t + H_{k,i}^t \quad (A-13)$$

Expanding equation (A-11) and collecting like terms gives

$$\begin{aligned} C_1 Y_{i+1}^{t+\Delta t} - (C_1 + C_2 + \frac{\phi \Delta x^2}{K \Delta t}) Y_i^{t+\Delta t} + C_2 Y_{i-1}^{t+\Delta t} = \\ \frac{\phi \Delta x^2}{K \Delta t} (H_{s,i}^t - Y_i^t - H_{s,i}^{t-\Delta t}) - \frac{\Delta x^2}{K} q \end{aligned} \quad (A-14)$$

Thus, the differential equation has been approximated by a finite-difference equation reduced to a linear equation with three unknowns.

Boundary and Initial Conditions

The entire flow system is described by $N-2$ equations of the form of equation (A-14), with N heretofore unknown values of Y . Thus, at least two values of Y must be specified. The outflow boundary condition, Y_1 , is predetermined and held constant with time at the value Y_d , thus simulating a constant tailwater level in the outflow ditch.

The desired boundary condition at $i = N$ is that of a zero flux boundary, since this point represents the centerline between parallel drains. To achieve this no flux boundary between $i = N$ and $i = N-1$, the Darcy flux, Q must be zero, i.e.

$$Q_{N-1/2} = K Y_{k,N} \left(\frac{\partial Y}{\partial x} \right)_{N-1/2} = 0 \quad (A-15)$$

This zero flux can be achieved by setting any one of the terms to zero. Since K is assumed to be a constant, and Y_N is not known a priori, the flow area term is used to set the no flux boundary in FLODF. Since the flow area was taken as the area from which flow emanates, then

$$Y_N + H_{k,N} = 0 \quad (A-16)$$

is a sufficient no-flux boundary condition, and the absolute value of Y_N is irrelevant.

In each case presented, the initial condition is that of a level water table, i.e., $\partial Y_i / \partial x = 0$, ($i = 2, N-1$), with $Y_1 = \text{constant}$, $t > 0$. Because of the method of linearization used to develop equation (A-14), and the large initial gradients for small i , the solution is expected to be least accurate at early times.

The volumetric source term in equation (A-14), where applicable, is the rate of percolation through the unsaturated region, taken positive downward. Thus, the source term serves as a pseudo-boundary condition of uniform flux for this one-dimensional problem.

Solution Technique

Since equation (A-14) is linear in Y , and the entire flow system can be described by $N-2$ such equations in $N-2$ unknowns, the solution at any succeeding time can be obtained directly, without resort to iterative techniques. FLODF utilizes a Gaussian elimination solution to the matrix equation

$$|C| |Y| = |R| \quad (A-17)$$

where $|C|$ is the coefficient matrix, $|Y|$ the solution matrix, and $|R|$ the matrix of coefficients representing the right-hand side of equation (A-14).

For this one-dimensional problem, the coefficient matrix is a tri-diagonal matrix of dimension $(N-2) \times (N-2)$. The solution sub-routine (GELIM) reduces the matrix storage requirement to dimension $(N-2) \times (3)$, which allows the use of a large number of grids.

The number of grids required to give an accurate solution was evaluated by trial. Where the gradients were largest (i.e., initial water level at the soil surface and zero ditch level), the solution was obtained for successively larger numbers of grids (i.e., smaller Δx). When any two successive solutions were obtained that agreed within three significant figures, the grid size was considered sufficiently small. For the problems studied here, 100 active grids ($N=102$) were sufficient to satisfy these accuracy criteria.

A similar analysis was performed to determine the optimum time increment between successive solutions. Since the decline of the water table is approximately linear with respect to log time, the time increment is calculated by an equation of the form

$$\Delta T = 10^b T \quad (A-18)$$

where b is a constant less than unity, and T is the total simulated solution time. By trial, it was determined that $b = 0.25$ satisfied the accuracy criteria described above, when the first solution was obtained at $T = 1$. Thus, solutions of the system were obtained to a simulated time of 10^7 in only 29 steps. This ability to use large values of Δt as drainage progresses is the major difference between FLODF and the computer program developed by Hedstrom, et al. (1971).

Program FLODF

The computer program is written in Fortran IV, specifically for the Scope 3.3 compiler system of the CDC 6400 computer at the Colorado State University Computer Center, Fort Collins, Colorado. A Fortran

listing of this program, for the case of zero infiltration, is presented in this section. Where the infiltration rate is finite, the effective permeable, and saturated depths are calculated by a subroutine similar to program EFFECT, which is also presented.

```

PROGRAM FLODF(INPUT,OUTPUT,TAPES=INPUT,TAPE6=OUTPUT)
C EVALUATE TRANSIENT FLOW TOWARD A FULLY PENETRATING DITCH BASED UPON DUPUIT
C -FORCHHEIMER ASSUMPTIONS, CONSIDERING EFFECTS OF CAPILLARY PERMEABILITY(IOP=1)
C AND SATURATION(IOP=2)
COMMON Y(200),YP(200),YE(200),SH(250),PH(250),SE(200),SEP(200),
IRHS(200),CM(200,3),YM(500),TSQ(500),TTL(500),QTT(500),RAT(500)
READ(5,1) Y1,YI,TL,TH,NAM1,NAM2,NAM3,CON
1 FORMAT(4F10.6,3A5,F10.6)
READ(5,2) PHI,PBOG,PSDI,SR,TT,NC
2 FORMAT(5F15.7,I5)
READ(5,3) Q,IOP
3 FORMAT(F15.7,I4)
C INPUT PARAMETERS DEFINED AS FOLLOWS (DIMENSIONS)-
C Q= UNIFORM INFILTRATION RATE, POSITIVE DOWNWARD (L/T)
C PHI= ULTIMATE DRAINABLE POROSITY (ND)
C CON= SATURATED HYDRAULIC CONDUCTIVITY (L/T)
C YI = INITIAL SATURATED THICKNESS (L)
C Y1 = DEPTH OF WATER IN DITCH AT T.GT.0 (L)
C TL = DRAIN SPACING (L)
C TH = TOTAL SOIL DEPTH (L)
C PBOG=BUBBLING PRESSURE HEAD (L)
C PSDI=PORE SIZE DISTRIBUTION INDEX- COREYS LAMBDA (ND)
C TT = TOTAL SOLUTION TIME TO BE SIMULATED (T)
C NC = NUMBER OF GRID COLUMNS IN MODEL (ND)
C NAM= FIFTEEN CHARACTER DESCRIPTION OF SOIL USED
C IOP= CAPILLARY SIMULATION DESIRED
C 0= NO CAPILLARY EFFECTS
C 1= PERMEABILITY EFFECTS ONLY
C 2= PERMEABILITY AND SATURATION EFFECTS
C SR = RESIDUAL SATURATION (ND)
C ARRAY NAMES DEFINED AS FOLLOWS-
C Y - WATER TABLE ELEVATION
C YP - WATER TABLE ELEVATION AT END OF PREVIOUS TIME STEP
C YE - EFFECTIVE PERMEABLE HEIGHT
C SH - EFFECTIVE SATURATED HEIGHT AS FUNCTION OF ELEVATION
C PH - EFFECTIVE PERMEABLE HEIGHT AS FUNCTION OF ELEVATION
C SE - EFFECTIVE SATURATED HEIGHT
C SEP - EFFECTIVE SATURATED HEIGHT AT PREVIOUS TIME STEP
C RHS - VALUE OF RIGHT-HAND SIDE OF FINITE DIFFERENCE EQUATION
C CM - VALUE OF COEFFICIENTS OF PRESSURE
C YM - RELATIVE HEIGHT OF WATER TABLE AT MIDPOINT
C TSQ - FRACTION OF DRAINABLE VOLUME REMOVED
C TTL - TIME AT WHICH SOLUTION IS OBTAINED
C QTT - CUMULATIVE VOLUME DRAINED
C RAT - FLOW RATE
PBPH=PBOG*PHI
EXP=0.25
XIN= 1.0/EXP +0.001
INX=XIN
C CALCULATE TIME INCREMENT MULTIPLIER
TC=10.0**(EXP)-1.0
NA=NC-2
C (CALCULATE EFFECTIVE PERMEABLE HEIGHT AND EFFECTIVE SATURATED HEIGHT)
CALL SKEF(PBOG,PSDI,SR)
NC1=NC-1
FNC=NA
X=TL/(2.0*FNC)
K=TH-Y1
L=TH-YI
FK=K
FL=L
C CALCULATE INITIAL DRAINABLE VOLUME (DRAIN)
IF(L.LT.1) L=1
IF(K.LT.1) K=1
DI=TH-YI-FL
DF=TH-YI-FK

```

```

DRAIN=TL*PHI*(YI+SH(L)+DI*(SH(L+1)-SH(L))-YI-SH(K)-DF*(SH(K+1)-
ISH(K)))/2.0
4 T=0.0
DT=1.0
KT=0
THAL=0.0
IF(IOP.LT.2) DRAIN =TL*PHI*(YI-YI)/2.0
SQ=0.
VOLP=0.0
YP(1)=YI
YF(1)=0.
C CALCULATE MATRIX COEFFICIENTS (CM,RHS)
DO 5 I=1,200
YE(I)=0.
Y(I)=0.
CM(I,1)=0.
CM(I,2)=0.
CM(I,3)=0.
5 RHS(I)=0.0
Y(I)=YI
WRITE(6, 6) NAM1,NAM2,NAM3,PBOG,PSDI,TL,TH,YI,YI,CON,PHI,NA,TT,Q,
IDRAIN
6 FORMAT(1H1,30X,* DUPUIT-FORCHHEIMER APPROXIMATION TO TWO DIMENSION
IAL FLOW TOWARD DRAINS* /// 10X,* SOIL IS *,3A5,/ 10X,* BUBBLE PRES
2S. HEAD = *,F5.1,* CM* / 10X,* PORE SIZE DIST. INDEX = *,F5.2, /
310X,* DRAIN SPACING = *,F5.0,* CM* / 10X,* SOIL DEPTH = *,F6.0,* C
4M* / 10X,* INITIAL WT THICKNESS = *,F5.0,* CM* / 10X,* DITCH LEVEL
5 = *,F5.0,* CM* / 10X,* HYDRAULIC CONDUCTIVITY = *,E12.3,* CM/SEC*
6/ 10X,* POROSITY = *,F5.3 / 10X,* NO. COLUMNS = *,I5 / 10X,* TOTA
7L SOLUTION TIME = *,E12.3,* SEC* / 10X,* INFILTRATION RATE = *,E12
8.7,* CM/SEC* / 10X,* DRAINABLE VOLUME = *,E12.3,* ML*)
STFC1=5H NONE
STFC2=5H
IF(IOP.EQ.1.OR.IOP.EQ.2) STEC1=5H PERM
IF(IOP.EQ.?) STEC2= 5H -SAT
WRITE(6, 7) STEC1,STEC2
7 FORMAT(1H ,10X,* PARAMETERS OF UNSAT. FLOW--*, 2A5 ///)
8 KT=KT+1
IF(T.EQ.0.0) GO TO 23
9 IF(IOP.EQ.?) 14,10
10 DO 13 I=1,NC
IF(IOP.EQ.1) 12,11
11 YE(I)=0.
12 SE(I)=0.
SEP(I)=0.
13 CONTINUE
14 DO 19 J=1,NA
RHS(J)=0.
CM(J,2)=0.
CM(J,1)=(Y(J)+YE(J)+Y(J+1)+YE(J+1))/2.0
CM(J,3)=(Y(J+1)+YE(J+1)+Y(J+2)+YE(J+2))/2.0
IF(J.EQ.1.OR.J.EQ.NA) 15,18
15 IF(J.EQ.NA) 16,17
16 CM(J,?)=0.
GO TO 18
17 CM(J,1)= Y(J+1)+Y(J)
RHS(J)=RHS(J)- CM(J,1)*YI
CM(J,2)= CM(J,2)-CM(J,1)
CM(J,1)=0.0
18 CM(J,2)=CM(J,2)-CM(J,1)-CM(J,3)- X**2*PHI/(CON*DT)
RHS(J)= RHS(J)+PHI*X**2*(SE(J+1)-YP(J+1)-SEP(J+1))/(CON*DT)-X**2*Q
2/CON
19 CONTINUE
20 CALL GELIM(NA,CM,RHS)
DO 21 J=2,NC1
SEP(J)=SE(J)
Y(J)=RHS(J-1)
IF(Y(J).GT.TH) Y(J)=TH
21 CONTINUE
Y(NC)=Y(NC1)
22 T= T+DT
YQ=YE(?)

```

```

23 DO 25 I=2,NC1
    IF(T.GT.0.0) GO TO 24
    FIY= TH-YI
    IY=FIY
    IF(IY.GT.249) IY=249
    IF(IY.LT.1) IY=1
    YP(I)= YI
    SEP(I)=SH(IY)
    VOLP=VOLP +X*(YP(I)+SEP(I))*PHI
    Y(I)=YP(I)
24 FIY= TH-Y(I)
    IF(IOP.LT.1) GO TO 25
    IY=FIY
    FY=IY
    COPR= TH- Y(I)-FY
    IF(IY.LT.1) IY=1
    YE(I)= PH(IY)+ CORR*(PH(IY+1)-PH(IY))
    IF(IOP.LT.2) GO TO 25
    SE(I)= SH(IY)+ CORR*(SH(IY+1)-SH(IY))
25 CONTINUE
    Y(NC)=Y(NC1)
    YP(NC)=YP(NC1)
    YE(NC)=YE(NC1)
    IF(T.EQ.0.0) GO TO 9
    QT=CON*DT*(YP(2)+Y1)*(Y(2)-Y1)/X
    SQ= SQ+ QT
    VOL=0.
    DO 26 I=2,NC1
    YP(I)=Y(I)
26 VOL= VOL + PHI*(SE(I)+Y(I))*X
    BAL= VOLP-VOL-QT+Q*DT*0.5*TL
    TBAL= TBAL+BAL
    VOLP=VOL
    RVOL= BAL/VOL
    RATE= QT/DT
    YM(KT)=(Y(NC1)-Y1)/(YI-Y1)
    TSQ(KT)= SQ/DRAIN
    TTL(KT)= T
    QTT(KT)= SQ
    RAT(KT)=RATE
    DT = T*TC
    KTM1=((KT-1)/INX)*INX -KT+1
    IF(KTM1.EQ.0) 27,32
27 WRITE(6,28) BAL,TBAL,RVOL
28 FORMAT(1H-, * BALANCE ERROR THIS TIME STEP = * E15.3 / * CUMULATI
    VE ERROR = * E15.3 / * BALANCE ERROR RELATIVE TO VOL STORAGE = *
    2E15.3 //)
    WRITE(6,29) T
29 FORMAT(1H-,20X,*WATER TABLE ELEVATIONS AT TIME* F15.2//)
    DO 30 I=1,NC,10
    II=I+9
30 WRITE(6,31) (Y(J),J=I,II)
31 FORMAT(1H ,10F10.3)
32 CONTINUE
    IF(T.LE.TT) GO TO 8
    WRITE(6,33)
33 FORMAT(1H1,5X,*TIME*,8X,*Y/YO VOL DRAIN REL VOL FLOW RATE *
    1 / 5X,* (SEC)*,19X,* ML DRAINED ML/SEC * /)
    WRITE(6,34)((TTL(I),YM(I),QTT(I),TSQ(I),RAT(I)),I=1,KT)
34 FORMAT(1H ,2X, 5(E11.2))
    END

```

```

SUBROUTINE GELIM(NA,C,R)
C SUBROUTINE FOR SOLVING A TRIDIAGONAL MATRIX BY GAUSSIAN ELIMINATION. C IS THE
C COEFFICIENT MATRIX HAVING NA UNKNOWN. R IS THE SOLUTION MATRIX. NO ROW
C INTERCHANGE IS PROVIDED.
    DIMENSION C(200,3),R(200)
    C(1,1)=C(1,2)
    C(NA,3)=0.
    C(1,3)= C(1,3)/C(1,2)
    R(1)= R(1)/C(1,2)

```

```

DO 2 I= 2,NA
IF(C(I,1).EQ.0.0) GO TO 1
C(I,2)= C(I,2)/C(I,1)
C(I,3)= C(I,3)/C(I,1)
R(I)=R(I)/C(I,1)
C(I,2)= C(I-1,3)-C(I,2)
1 C(I,3)= -C(I,3)/C(I,2)
2 R(I)=(R(I-1)-R(I))/C(I,2)
DO 3 J= 2,NA
K= NA-J+1
3 R(K)=R(K)-C(K,3)*R(K+1)
RETURN
END

```

```

SUBROUTINE SKEF (PBOG,PSDI,SR)
COMMON Y(200),YP(200),YE(200),SH(250),PH(250),SE(200),SEP(200),
IRHS(200),CM(200,3),YM(500),TSQ(500),TTL(500),QTT(500),RAT(500)
DIMENSION SAT(250),PERM(250)
C SUBROUTINE TO CALCULATE EFFECTIVE SATURATED HEIGHT AND EFFECTIVE PERMEABLE
C HEIGHT WHEN INFILTRATION RATE IS ZERO.
WRITE(6,6)
DO 1 I=1,250
SAT(I)=1.0
1 PERM(I)=1.0
IPB=PBOG
FP=IPB
IF (PBOG-FP.GT.0.5) IPB=IPB+1
IP=IPB+1
DO 2 J=IP,250
FJ=J
PERM(J)= (PBOG/FJ)**(2.0+3.0*PSDI)
2 SAT(J)= SR+(1.0-SR)*(PBOG/FJ)**PSDI
DO 3 K= 1,250
FK=K
SH(K)=FK
3 PH(K)=FK
DO 4 L=IP,250
SH(L)= SH(L-1)+0.5*(SAT(L-1)+SAT(L))
4 PH(L)= PH(L-1)+0.5*(PERM(L-1)+PERM(L))
WRITE(6,5) ((I,PERM(I),SAT(I),PH(I),SH(I)),I=1,250)
5 FORMAT(1H ,13X,I3,5X,2E10.3,4X,2E10.3)
6 FORMAT(1H1,10X,*CAP PRESS REL PERM EFF SAT EFF PERM HGT EF
IF SAT HGT *//)
RETURN
END

```

```

PROGRAM EFFECT(INPUT,OUTPUT,TAPES=INPUT,TAPE6=OUTPUT)
COMMON FINT(1000),FENT(1000),FLNT(1000)
C PROGRAM EVALUATES EFFECTIVE PERMEABLE AND SATURATED HEIGHTS AS A FUNCTION OF
C ELEVATION, THEN CALCULATES SURFACE PRESSURE AND DEPTH OF AERATED ZONE FOR
C GIVEN WATER TABLE DEPTH.
  1 READ(5,2) QDOT,PETA,SLMD
  2 FORMAT(3F10.4)
  WRITE(6,500) PETA
500 FORMAT(1H1, * ETA = *,F10.1)
  QNEG= 0.00001
  EPS=1.001
  IF(QDOT.EQ.0.0) GO TO 112
  CALL INTEGR(QDOT,SLMD,PETA,EPS,QNEG)
112 ZS=1.0/(1.0-QDOT)
110 READ(5,111) H,SA
111 FORMAT(2F10.4)
  IF(H.EQ.0.0) GO TO 1
  IF(H.LE.ZS) 3,4
  3 HES=H
  HEK=H
  HS=0.
  PSUR=H/ZS
  IF(QDOT.EQ.0.0) PSUR=H
  GO TO 100
  4 IF(QDOT) 5,6,7
  6 HEK= (PETA-H**(1.0-PETA))/(PETA-1.0)
  HES= (SLMD-H**(1.0-SLMD))/(SLMD-1.0)
  HS= H-SA**(-1.0/SLMD)
  IF(HS.LT.0.0) HS=0.0
  PSUR= H
  GO TO 100
  7 EQ= (EPS*QDOT)**(-1.0/PETA)
  IEQ= 100.*EQ
  ZDP= ZS + FINT(IEQ)
  IF(ZDP.GT.H) 9,10
  9 DO 11 J=100,IEQ
  IF(FINT(J).GT.(H-ZS)) 12,11
12 FJ=J
  PSUR=FJ/100.
  HEK= ZS+FENT(J)
  HES= 7S+FLNT(J)
  GO TO 13
11 CONTINUE
  GO TO 13
10 HEK= ZS + EPS*QDOT*(H-ZDP) + FENT(IEQ)
  HES= 7S+((EPS*QDOT)**(SLMD/PETA))*(H-ZDP) + FLNT(IEQ)
  PSUR= EQ
13 SAL= SA**(-1.0/SLMD)
  ISAL=SAL*100.
  SLA= SA**(PETA/SLMD)
  IF(EPS*QDOT.GE.SLA) 15,16
15 HS=0.
  GO TO 100
16 HS= H-ZS-FINT(ISAL)
  GO TO 100
  5 ZDP= H-ZS
  PLIM=QNEG**(-1.0/PETA)
  IF(PLIM.GT.10.0) PLIM=10.0
  LIMP= PLIM*100.
  IF(ZDP.GT.FINT(LIMP)) GO TO 101
  DO 17 I=100,LIMP
  IF(FINT(I).GT.ZDP) 18,17
18 HEK= ZS + FENT(I)
  HES= ZS + FLNT(I)
  FJ=I
  PSUR= FJ/100.0

```

```

SAL= SA**(-1.0/SLMD)
ISAL=SAL*100.
HS= H-ZS-FINT(ISAL)
GO TO 100
17 CONTINUE
100 WRITE(6,20) QDOT,H,HEK,HES,PSUR,HS
20 FORMAT(1H--, * Q. = *,F10.4/ * H. = *,F10.4/ * HE(K)= *,F10.4/ *
1HE(S) = *,F10.4/ * SCALED CAP PRESS. AT SURFACE = *,F10.4/ * UPP
2ER *,F10.4. *(SCALED) IS BELOW CRITICAL SATURATION* ///)
GO TO 110
101 WRITE(6,21) QDOT,H
21 FORMAT(1H--, * Q. = *,F10.4/ * H. = *,F10.4/ * THIS FLUX RATE CANNOT
1 BE ATTAINED AT THIS DEPTH* ///)
GO TO 110
END

```

```

SUBROUTINE INTEGR(QDOT,SLMD,PETA,EPS,QNEG)
COMMON FINT(1000),FENT(1000),FLNT(1000)
C SUBROUTINE DESIGNED TO SOLVE BY SIMPSONS RULE, THE INTEGRALS NECESSARY FOR
C EVALUATION OF THE VARIOUS EFFECTIVE HEIGHTS.
C QDOT = SCALED FLUX RATE , POSITIVE DOWNWARD
C SLMD = NEG EXPONENT OF S-PC RELATION
C PETA = NEG EXPONENT OF K-PC RELATION
C FINT = AREA UNDER DP./(1-Q.P.**PETA), INCREMENTS OF P.=.01
C FENT = AREA UNDER DP./(P.**PETA(1-Q.P.**PETA))
C FLNT = AREA UNDER DP./(P.**SLMD(1-Q.P.**PETA))
C EPS = ARBITRARY COEFFICIENT TO DETERMINE HOW CLOSE Q APPROACHES CE
C BEFORE ASSUME Q=CE (IN PERCOLATION)
C QNEG = QDOT WHICH IS ASSUMED NEGLIGIBLE (IE,CUTOFF FOR UPWARD FLOW
C INTEGRATION)
IFLAG=0
DO 1 I=1,1000
FINT(I)=0.
FENT(I)=0.
1 FLNT(I)=0.
IF(QDOT) 3,3,2
2 PLIM=(EPS*QDOT)**(-1.0/PETA)
GO TO 5
3 PLIM= QNEG**(-1.0/PETA)
IF(PLIM.GT.10.)4,5
4 PLIM=10.
IFLAG=1
5 CONTINUE
DEN=1.0/(1.0-QDOT)
LIMP=1000.*PLIM
S0= DEN
P0 =DEN
F0= DEN
SS1= 0.
SF1= 0.
SK1= 0.
DO 7 I=1002,LIMP,2
FI=I
PDOT= FI/1000.
PDE = PDOT**PETA
PDE1=(PDOT-.001)**PETA
F2= 1.0/(1.0-QDOT*PDE)
F1= 1.0/(1.0-QDOT*PDE1)
P2= F2/PDE
P1= F1/PDE1
S2 =F2/(PDOT**SLMD)
S1 =F1/((PDOT-.001)**SLMD)
SF1= 0.001*(F0+4.0*F1+F2)/3.0 + SF1
SS1= 0.001*(S0+4.0*S1+S2)/3.0 + SS1
SK1=0.001*(P0+4.0*P1+P2)/3.0 + SK1
F0=F2
S0=S2
P0 =P2
J=I/10
IF(J*10.EQ.I) 6,7
6 FINT(I)= SF1

```

```

      FENT(J)= SK1
      FLNT(J)= SS1
7 CONTINUE
      WRITE(6,8)
8 FORMAT(1H-,20X,* INTEGRAL OF DP./(1-Q.P.*,2H**,*ETA) FOR VALUES 0
      IF P.*//)
      WRITE(6,12)
      LIMP=LIMP/10
      DO 9 J=100,LIMP,10
      FI=J
      FI=FI/100.0
      JJ=J+9
9 WRITE(6,10) FI,(FINT(K),K=J,JJ)
10 FORMAT(1H ,F5.1,10E12.4)
      WRITE(6,11)
11 FORMAT(1H-,20X,* INTEGRAL OF DP./(P.*,2H**,*ETA(1-Q.P.*,2H**,*ETA)
      1 FOR VALUES OF P.*//)
      WRITE(6,12)
12 FORMAT(1H ,11X,*.00*,9X,*.01*,9X,*.02*,9X,*.03*,9X,*.04*,9X,*.05*,
      19X,*.06*,9X,*.07*,9X,*.08*,9X,*.09*)
      DO 13 J=100,LIMP,10
      FI=J
      FI=FI/100.0
      JJ= J+9
13 WRITE(6,10) FI,(FENT(K),K=J,JJ)
      WRITE(6,14)
14 FORMAT(1H-,20X,* INTEGRAL OF DP./(P.*,2H**,*LAMBDA(1-Q.P.*,2H**,*E
      1TA) FOR VALUES OF P.* //)
      WRITE(6,12)
      DO 15 J=100,LIMP,10
      FI=J
      FI= FI/100.0
      JJ=J+9
15 WRITE(6,10) FI,(FLNT(K),K=J,JJ)
      IF(IFLAG.EQ.0) GO TO 17
      WRITE(6,16)
16 FORMAT(1H ,*ABOVE TABLES INCOMPLETE- MAX ELEVATION AT WHICH Q. CAN
      1 EXIST NOT REACHED* /)
17 WRITE(6,18) QDOT,SLMD,PETA
18 FORMAT(1H ,* FOR ABOVE THREE TABLES,* / * Q.  =*,F10.4 / * ETA
      1 =*,F10.4 / * LAMBDA=*,F10.4//)
      RETURN
      END

```

APPENDIX B

PHYSICAL PROPERTIES OF SOILS AND FLUID

Soil Properties

Table B-1. Properties of soils used in experimental models.

Parameter	Units	Poudre Sand	Hygiene Sand
k	μ^2	12.7	35.6
$P_b/\rho g^1$	cm	19.0	5.7
λ	none	1.6	1.6
ϕ_e	none	0.348	0.288

¹with Phillips core test fluid.

Fluid Properties

Two hydrocarbon liquids were used in the experiments. The first, Phillips core test fluid² was used in all transient experiments. This fluid is no longer available, and has been replaced by Soltrol 130³, a similar branch chain paraffin. The pertinent properties of both are presented in Table B-2.

Table B-2. Properties of hydrocarbon fluids.

Temp. °C	Core Test Fluid		Soltrol 130	
	Viscosity, μ centipoise	Density, ρ gm/ml	Viscosity, μ cp	Density, ρ gm/ml
20.0	1.589	0.7582	1.417	0.7536
22.0	1.524	.7569	1.374	.7523
24.0	1.468	.7556	1.330	.7511
26.0	1.414	.7542	1.286	.7498
28.0	1.362	.7529	1.243	.7486
30.0	1.315	.7515	1.200	.7474

^{2,3}Both are products of Special Products Division, Phillips Petroleum Company, Bartlesville, Oklahoma. Brand names are mentioned only for the convenience of the reader and do not imply endorsement by USDA, Agricultural Research Service or by Colorado State University.

APPENDIX C
COMPUTED SATURATION PROFILES

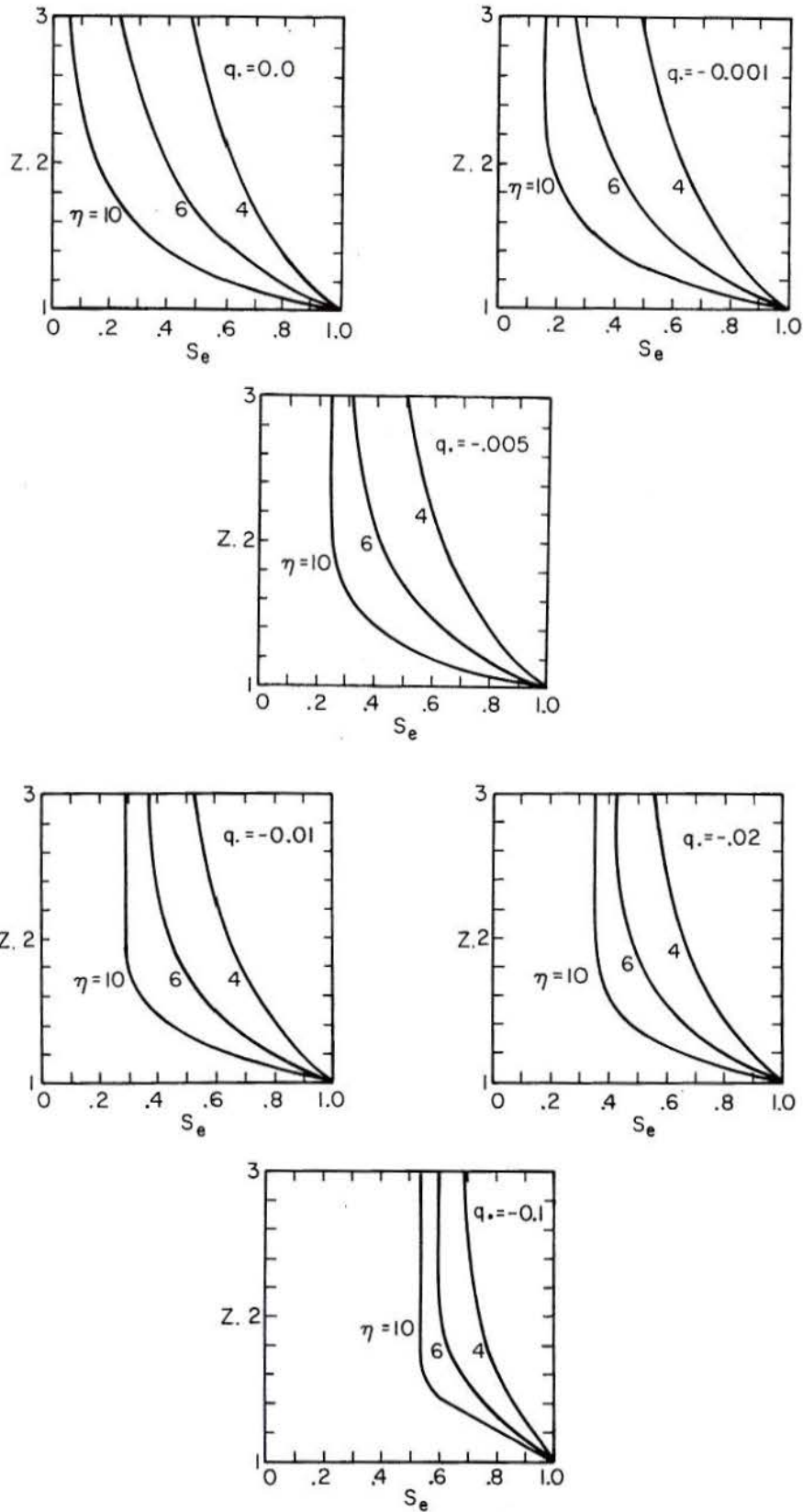


Figure C-1. Saturation profile as a function of η for a range of vertical flux.

APPENDIX D

SCALED EFFECTIVE PERMEABLE AND SATURATED HEIGHTS

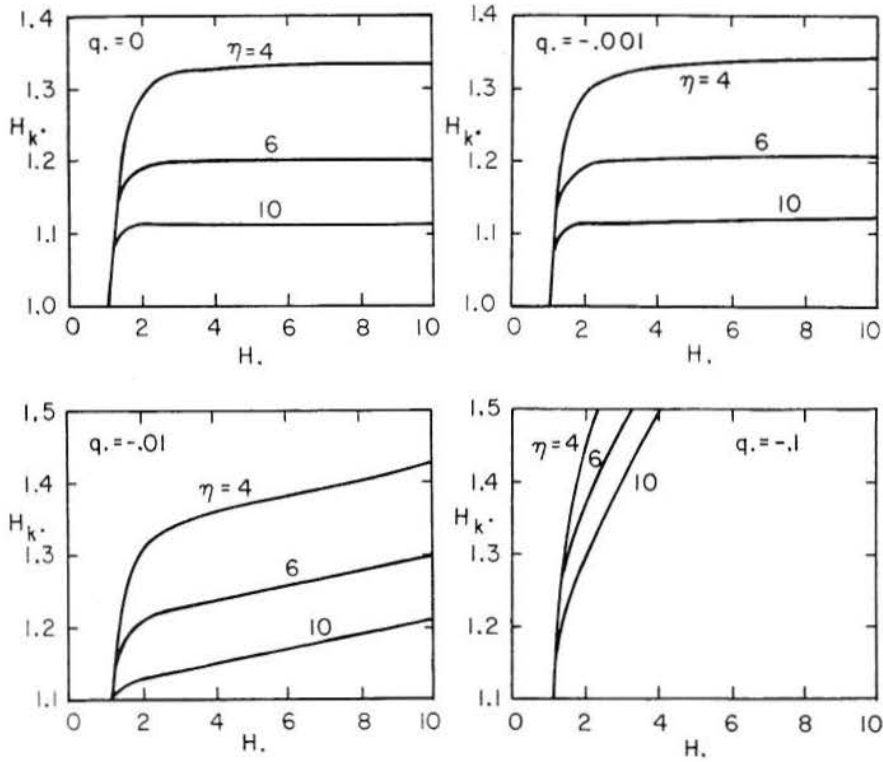


Figure D-1. Scaled effective permeable height as a function of scaled water table depth for a range of vertical flux.

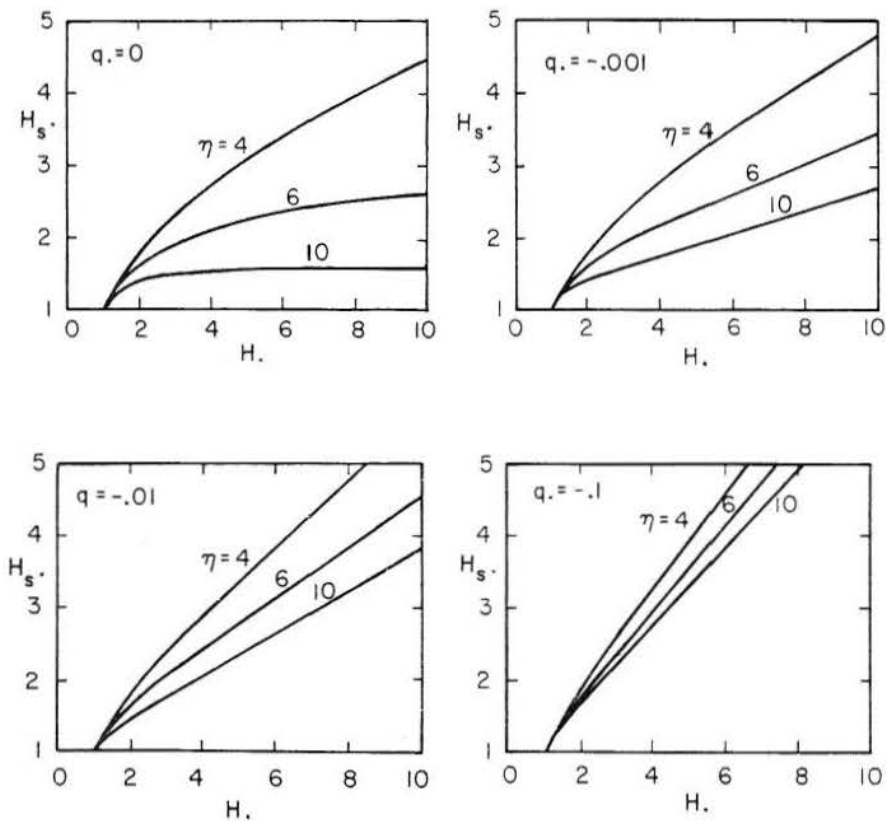


Figure D-2. Scaled effective saturated height as a function of scaled water table depth for a range of vertical flux.

APPENDIX E

COMPARISON OF EXPERIMENTAL AND NUMERICAL RESULTS

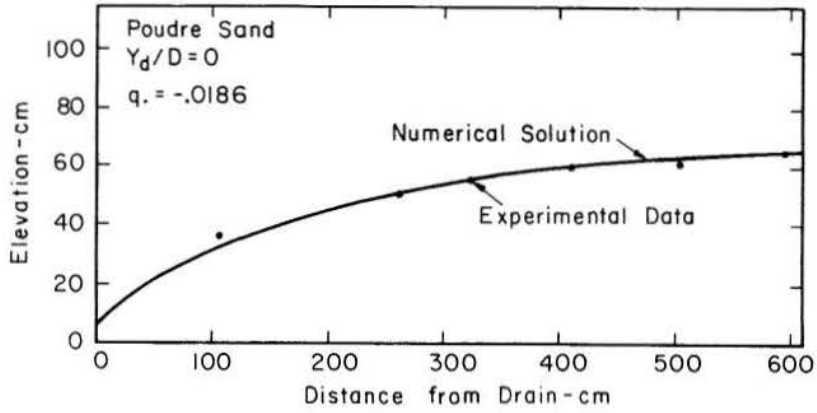


Figure E-1. Comparison of experimental data and numerical results for steady flow, $Y_d/D = 0$, $q = -0.0186$, Poudre sand.

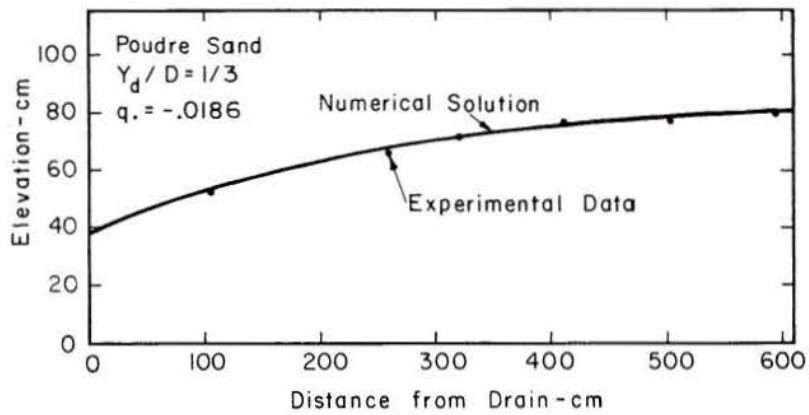


Figure E-2. Comparison of experimental data and numerical results for steady flow, $Y_d/D = 1/3$, $q = -0.0186$, Poudre sand.

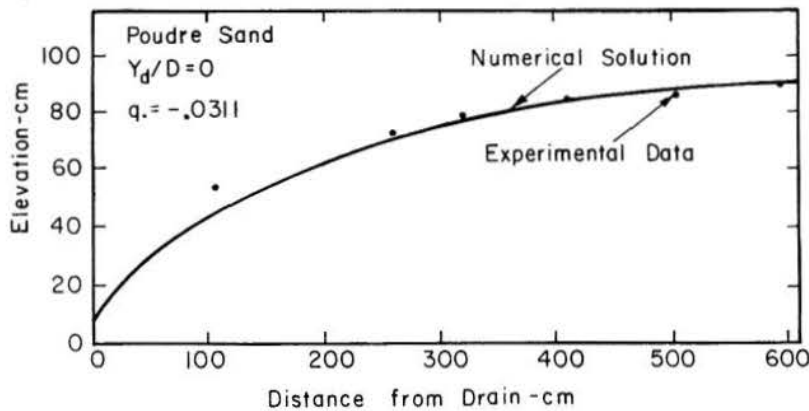


Figure E-3. Comparison of experimental data and numerical results for steady flow, $Y_d/D = 0$, $q = -0.0311$, Poudre sand.

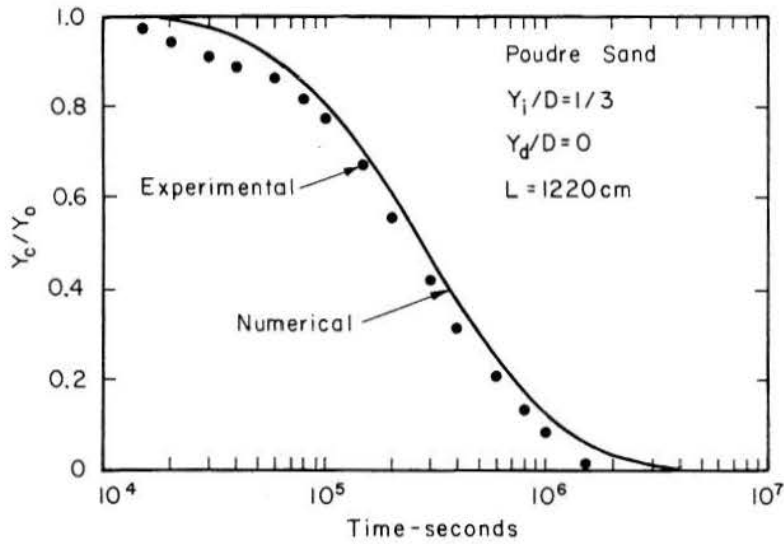


Figure E-4. Comparison of experimental data and numerical results for transient flow, $Y_i/D = 1/3$, $Y_d/D = 0$, Poudre sand.

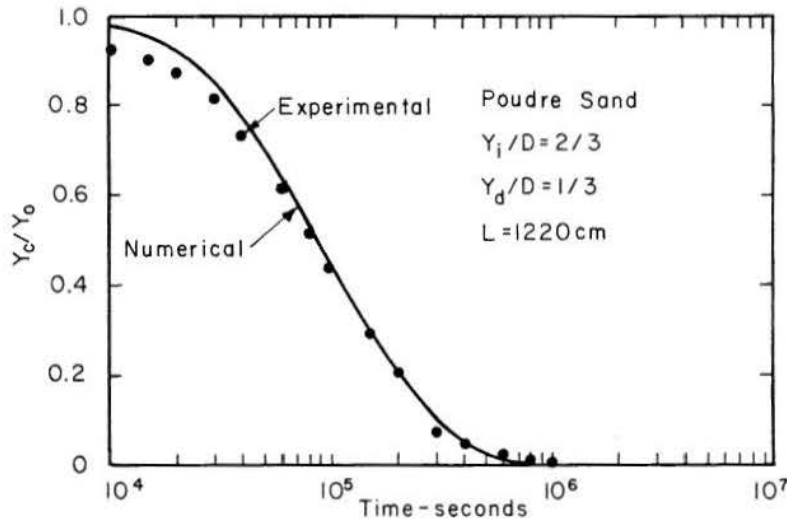


Figure E-5. Comparison of experimental data and numerical results for transient flow, $Y_i/D = 2/3$, $Y_d/D = 1/3$, Poudre sand.

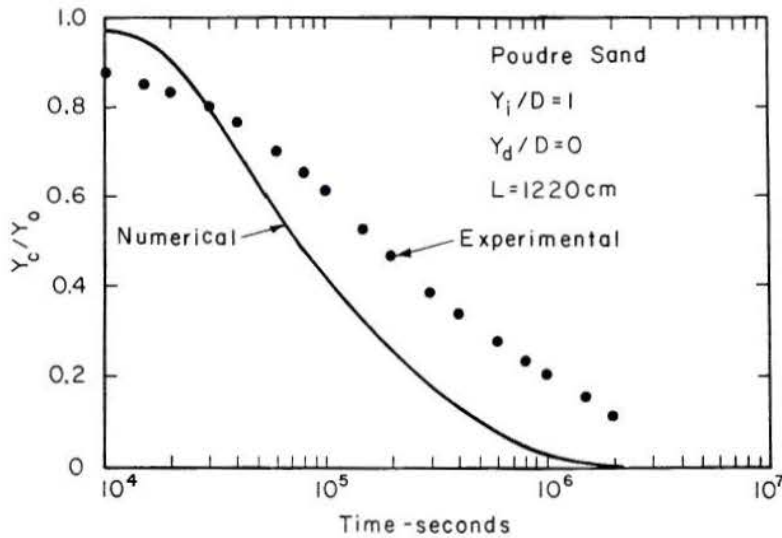


Figure E-6. Comparison of experimental data and numerical results for transient flow, $Y_i/D = 1$, $Y_d/D = 0$, Poudre sand.

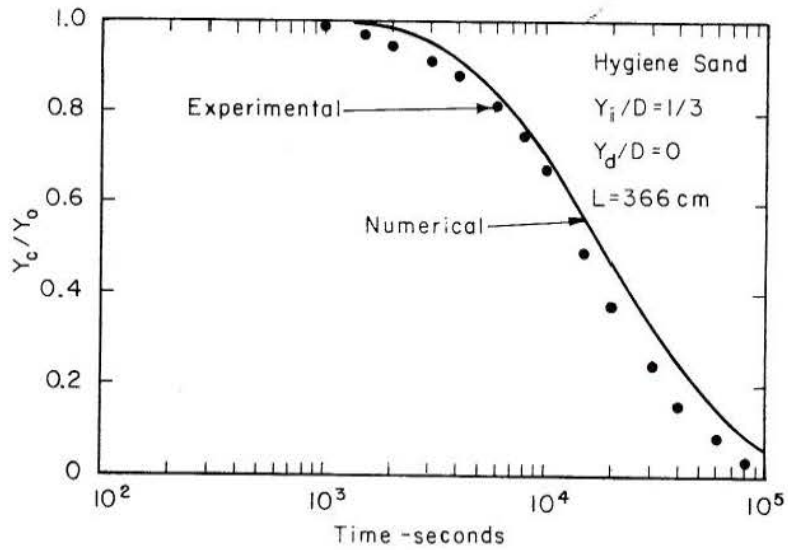


Figure E-7. Comparison of experimental data and numerical results for transient flow, $Y_i/D = 1/3$, $Y_d/D = 0$, $L = 366 \text{ cm}$, Hygiene Sand.

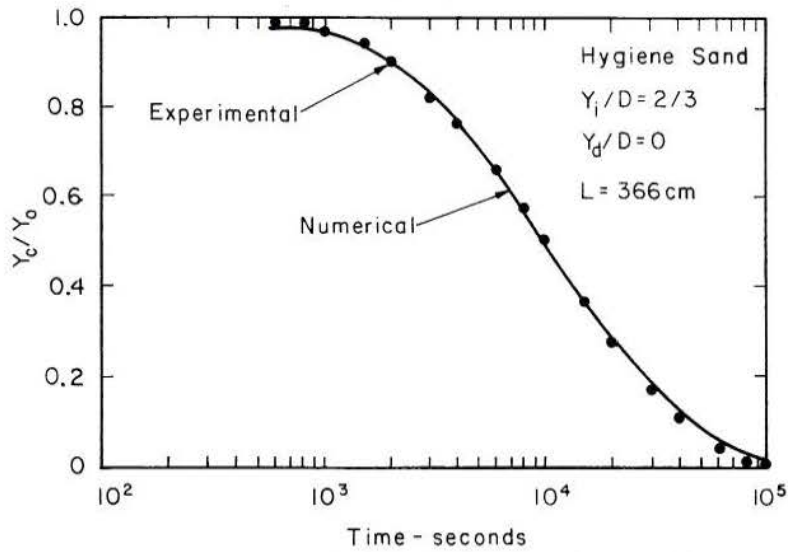


Figure E-8. Comparison of experimental data and numerical results for transient flow, $Y_i/D = 2/3$, $Y_d/D = 0$, Hygiene sand.

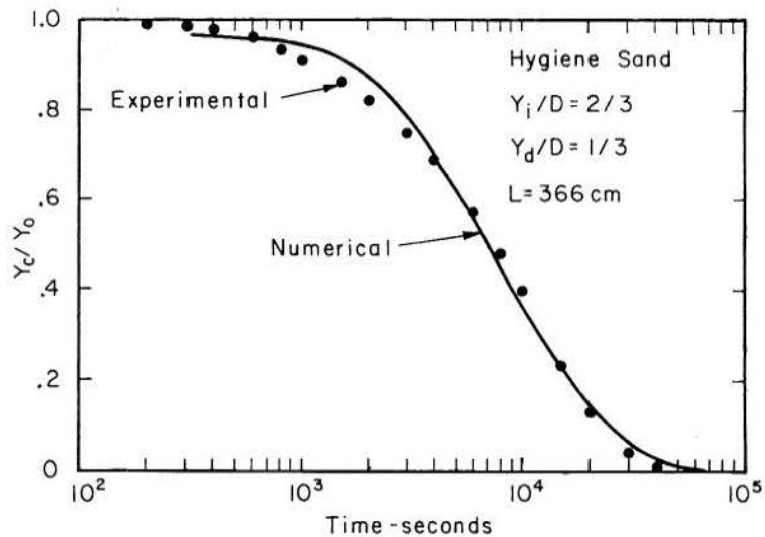


Figure E-9. Comparison of experimental data and numerical results for transient flow, $Y_i/D = 2/3$, $Y_d/D = 1/3$, Hygiene sand.

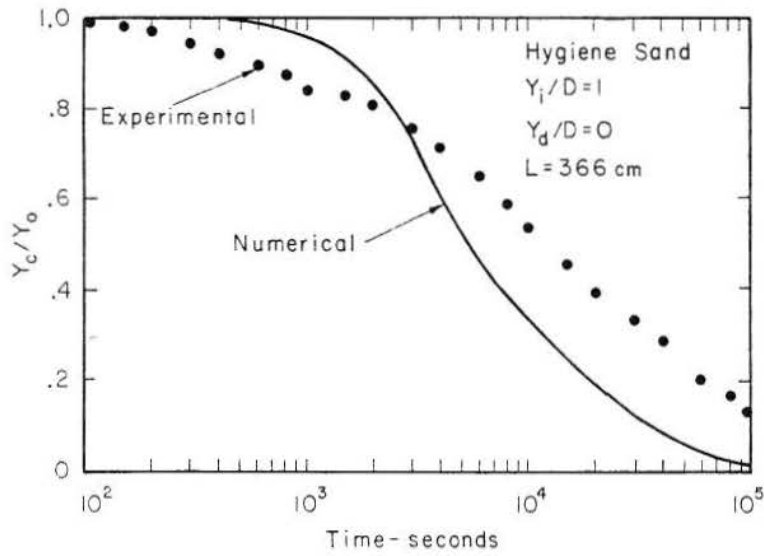


Figure E-10. Comparison of experimental data and numerical results for transient flow, $Y_i/D = 1$, $Y_d/D = 0$, Hygiene sand.

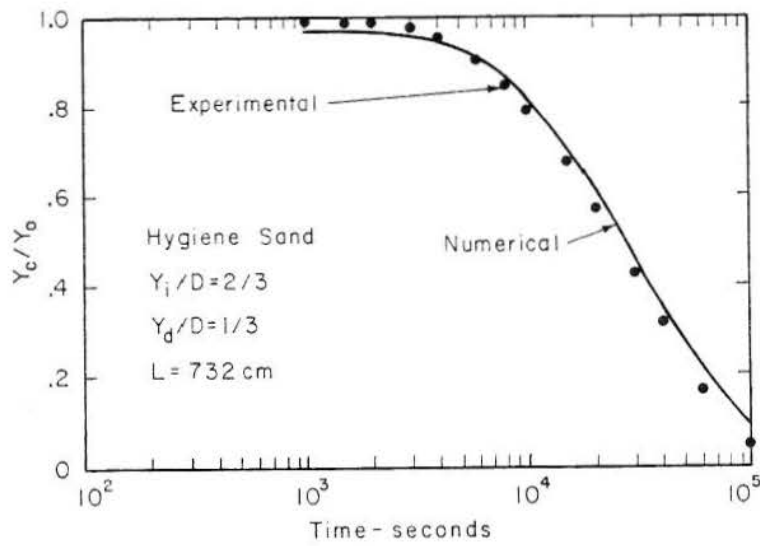


Figure E-11. Comparison of experimental data and numerical results for transient flow, $Y_i/D = 2/3$, $Y_d/D = 1/3$, $L = 732$ cm, Hygiene sand.

APPENDIX F
RESULTS OF NUMERICAL ANALYSES

Table F-1
Equilibrium Water Table Profile,
 $Y_d/D = 0, \quad q. = -.001.$

Distance from Drain	Water Table Height						
	No Cap. Flow	$\eta = 6$ $P_b/\rho g = 5$	$\eta = 6$ $P_b/\rho g = 10$	$\eta = 4$ $P_b/\rho g = 20$	$\eta = 6$ $P_b/\rho g = 20$	$\eta = 10$ $P_b/\rho g = 20$	$\eta = 6$ $P_b/\rho g = 40$
2.5	1.6	1.6	1.6	1.6	1.6	1.6	1.6
47.5	6.7	4.0	3.1	2.3	2.4	2.5	2.0
97.5	9.4	5.9	4.4	3.1	3.2	3.3	2.4
147.5	11.2	7.4	5.5	3.7	3.9	4.0	2.8
197.5	12.6	8.6	6.4	4.2	4.5	4.6	3.1
247.5	13.7	9.5	7.2	4.7	4.9	5.2	3.4
297.5	14.5	10.2	7.7	5.0	5.3	5.6	3.6
347.5	15.1	10.7	8.2	5.3	5.6	5.9	3.8
397.5	15.5	11.1	8.5	5.5	5.9	6.1	3.9
447.5	15.7	11.3	8.7	5.6	6.0	6.2	4.0
497.5	15.8	11.4	8.8	5.7	6.0	6.3	4.0
Y_a	15.8	17.3	20.5	33.7	29.4	27.7	50.8
L_e	1000	1094	1297	2131	1859	1752	3213

Table F-2
Equilibrium Water Table Profile,
 $Y_d/D = 1/3, \quad q. = -.001.$

Distance from Drain	Water Table Height						
	No Cap. Flow	$\eta = 6$ $P_b/\rho g = 5$	$\eta = 6$ $P_b/\rho g = 10$	$\eta = 4$ $P_b/\rho g = 20$	$\eta = 6$ $P_b/\rho g = 20$	$\eta = 10$ $P_b/\rho g = 20$	$\eta = 6$ $P_b/\rho g = 40$
2.5	33.4	33.4	33.4	33.4	33.4	33.4	33.4
47.5	34.0	33.9	33.8	33.7	33.7	33.8	33/6
97.5	34.6	34.4	34.3	34.1	34.1	34.1	33.9
147.5	35.2	34.9	34.7	34.4	34.4	34.5	34.1
197.5	35.6	35.3	35.0	34.7	34.7	34.8	34.3
247.5	36.0	35.6	35.3	34.9	34.9	35.0	34.5
297.5	36.3	35.9	35.6	35.1	35.1	35.2	34.6
347.5	36.6	36.1	35.8	35.2	35.3	35.3	34.7
397.5	36.8	36.3	35.9	35.3	35.4	35.4	24.9
447.5	36.9	36.4	36.0	35.4	35.5	35.5	34.9
497.5	36.9	36.4	36.0	35.4	35.5	35.5	34.9
Y_a	36.9	42.3	47.7	63.4	58.9	56.9	81.7
L_e	1000	1647	2158	3411	3071	2916	4718

Table F-3
Equilibrium Water Table Profile,
 $Y_d/D = 2/3, \quad q. = -.001.$

Distance from Drain	Water Table Height						
	No Cap. Flow	$\eta = 6$ $P_b/\rho g = 5$	$\eta = 6$ $P_b/\rho g = 10$	$\eta = 4$ $P_b/\rho g = 20$	$\eta = 6$ $P_b/\rho g = 20$	$\eta = 10$ $P_b/\rho g = 20$	$\eta = 6$ $P_b/\rho g = 40$
2.5	66.7	66.7	66.7	66.7	66.7	66.7	66.7
47.5	67.0	67.0	67.0	66.9	66.9	66.9	66.9
97.5	67.3	67.3	67.2	67.2	67.2	67.2	67.1
147.5	67.6	67.5	67.5	67.4	67.4	67.4	67.3
197.5	67.8	67.7	67.7	67.5	67.5	67.6	67.5
247.5	68.0	67.9	67.8	67.7	67.7	67.7	67.6
297.5	68.2	68.1	68.0	67.8	67.8	67.8	67.7
347.5	68.3	68.2	68.1	67.9	67.9	67.9	67.8
397.5	68.4	68.3	68.2	68.0	68.0	68.0	67.9
447.5	68.5	68.4	68.2	68.0	68.0	68.1	67.9
497.5	68.5	68.4	68.2	68.0	68.0	68.1	67.9
Y_a	68.5	74.3	79.9	96.0	91.4	89.5	100*
L_e	1000	2075	2785	4369	3954	3777	--

* Indicates no aerated zone at centerline

Table F-4
Equilibrium Water Table Profile,
 $Y_d/D = 0, \quad q. = -.005.$

Distance from Drain	Water Table Height						
	No Cap. Flow	$\eta = 6$ $P_b/\rho g = 5$	$\eta = 6$ $P_b/\rho g = 10$	$\eta = 4$ $P_b/\rho g = 20$	$\eta = 6$ $P_b/\rho g = 20$	$\eta = 10$ $P_b/\rho g = 20$	$\eta = 6$ $P_b/\rho g = 40$
2.5	3.5	3.5	3.5	3.5	3.5	3.5	3.5
47.5	15.0	11.4	9.3	6.9	7.2	7.4	5.6
97.5	21.0	16.7	13.8	9.9	10.4	10.8	7.5
147.5	25.1	20.5	17.3	12.4	13.1	13.5	9.2
197.5	28.1	23.4	19.9	14.5	15.2	15.8	10.6
247.5	30.5	25.7	22.0	16.1	16.9	17.5	11.8
297.5	32.3	27.4	23.7	17.4	18.3	18.9	12.8
347.5	33.7	28.7	24.9	18.4	19.3	20.0	13.5
397.5	34.6	29.6	25.7	19.1	20.1	20.8	14.0
447.5	35.2	30.2	26.2	19.6	20.5	21.2	14.3
497.5	25.4	30.4	26.4	19.7	20.7	21.4	14.4
Y_a	35.4	36.4	38.3	47.9	44.5	43.0	62.0
L_e	1000	1030	1083	1355	1259	1216	1754

Table F-5
 Equilibrium Water Table Profile,
 $Y_d/D = 1/3, \quad q. = -.005.$

Distance from Drain	Water Table Height						
	No Cap. Flow	$\eta = 6$ $P_b/\rho g = 5$	$\eta = 6$ $P_b/\rho g = 10$	$\eta = 4$ $P_b/\rho g = 20$	$\eta = 6$ $P_b/\rho g = 20$	$\eta = 10$ $P_b/\rho g = 20$	$\eta = 6$ $P_b/\rho g = 40$
2.5	53.5	53.5	53.5	53.5	53.5	53.5	53.5
47.5	56.6	56.1	55.8	55.3	55.3	55.4	54.8
97.5	59.4	58.6	58.0	57.0	57.1	57.2	56.1
147.5	41.7	40.7	39.8	38.4	38.6	38.8	37.2
197.5	43.6	42.4	41.4	39.7	39.9	40.1	38.2
247.5	45.2	43.8	42.7	40.7	41.0	41.2	39.0
297.5	46.4	44.9	43.7	41.6	41.9	42.1	39.7
347.5	47.4	45.8	44.5	42.2	42.6	42.8	40.2
397.5	48.0	46.4	45.0	42.7	43.0	43.3	40.6
447.5	48.4	46.8	45.4	43.0	43.3	43.6	40.8
497.5	48.6	46.9	45.5	43.1	43.4	43.7	40.9
Y_a	48.6	52.9	57.4	71.3	68.2	65.3	88.5
L_e	1000	1162	1322	1783	1683	1588	2319

Table F-6
 Equilibrium Water Table Profile,
 $Y_d/D = 2/3, \quad q. = -.005.$

Distance from Drain	Water Table Height						
	No Cap. Flow	$\eta = 6$ $P_b/\rho g = 5$	$\eta = 6$ $P_b/\rho g = 10$	$\eta = 4$ $P_b/\rho g = 20$	$\eta = 6$ $P_b/\rho g = 20$	$\eta = 10$ $P_b/\rho g = 20$	$\eta = 6$ $P_b/\rho g = 40$
2.5	66.8	66.8	66.8	66.8	66.8	66.8	66.8
47.5	68.3	68.2	68.1	67.9	67.9	68.0	67.8
97.5	69.9	69.6	69.4	69.1	69.1	69.1	68.9
147.5	71.2	70.9	70.6	70.1	70.1	70.2	69.8
197.5	72.4	71.9	71.6	70.9	71.0	71.0	70.7
247.5	73.3	72.8	72.4	71.6	71.7	71.8	71.4
297.5	74.1	73.5	73.1	72.2	72.3	72.4	71.9
347.5	74.7	74.1	73.6	72.7	72.8	72.9	72.4
397.5	75.1	74.5	74.0	73.0	73.1	73.2	72.7
447.5	75.4	74.7	74.2	73.2	73.3	73.4	72.9
497.5	75.5	74.8	74.3	73.3	73.4	73.5	72.9
Y_a	75.5	80.8	86.2	100*	97.2	95.1	100*
L_e	1000	1291	1545	--	2000	1918	--

Table F-7
 Equilibrium Water Table Profile,
 $Y_d/D = 0, \quad q_s = -.01.$

Distance from Drain	Water Table Height						
	No Cap. Flow	$\eta = 6$ $P_b/\rho g = 5$	$\eta = 6$ $P_b/\rho g = 10$	$\eta = 4$ $P_b/\rho g = 20$	$\eta = 6$ $P_b/\rho g = 20$	$\eta = 10$ $P_b/\rho g = 20$	$\eta = 6$ $P_b/\rho g = 40$
2.5	5.0	5.0	5.0	5.0	5.0	5.0	5.0
47.5	21.3	17.4	4.8	11.2	11.6	12.0	8.9
97.5	29.7	25.2	21.8	16.5	17.2	17.7	12.5
147.5	35.4	30.7	27.0	20.6	21.5	22.2	15.6
197.5	39.8	34.9	31.0	24.0	25.0	25.7	18.1
247.5	43.2	38.2	34.1	26.7	27.7	28.5	20.2
297.5	45.7	40.7	36.5	28.8	29.9	30.7	21.8
347.5	47.6	42.5	38.3	30.3	31.5	32.4	23.1
397.5	48.9	43.8	39.5	31.4	32.7	33.5	24.0
447.5	49.7	44.6	40.3	32.1	33.3	34.2	24.5
497.5	50.0	44.9	40.5	32.3	33.6	34.5	24.7
Y_a	50.0	50.9	52.5	60.7	57.5	56.6	72.5
L_e	1000	1018	1050	1214	1150	1132	1450

Table F-8
 Equilibrium Water Table Profile,
 $Y_d/D = 1/3, \quad q_s = -.01.$

Distance from Drain	Water Table Height						
	No Cap. Flow	$\eta = 6$ $P_b/\rho g = 5$	$\eta = 6$ $P_b/\rho g = 10$	$\eta = 4$ $P_b/\rho g = 20$	$\eta = 6$ $P_b/\rho g = 20$	$\eta = 10$ $P_b/\rho g = 20$	$\eta = 6$ $P_b/\rho g = 40$
2.5	33.7	33.7	33.7	33.7	33.7	33.7	33.7
47.5	39.5	38.7	38.2	37.2	37.5	37.4	36.3
97.5	44.6	43.3	42.2	40.4	40.7	40.9	38.8
147.5	48.7	47.0	45.6	43.2	43.5	43.8	41.0
197.5	51.9	50.0	48.4	45.5	45.9	46.2	42.8
247.5	54.5	52.4	50.6	47.4	47.9	48.2	44.4
297.5	56.6	54.3	52.4	48.9	49.4	49.8	45.6
347.5	58.1	55.8	53.8	50.1	50.6	51.0	46.6
397.5	59.2	56.8	54.8	50.9	51.5	51.9	47.3
447.5	59.9	57.4	55.3	51.4	52.0	52.4	47.7
497.5	60.1	57.6	55.5	51.6	52.2	52.6	47.8
Y_a	60.1	65.6	67.7	80.0	76.1	74.7	95.6
L_e	1000	1083	1178	1454	1368	1337	1792

Table F-9
 Equilibrium Water Table Profile,
 $Y_d/D = 2/3$, $q. = -.01$.

Distance from Drain	Water Table Height						
	No Cap. Flow	$\eta = 6$ $P_b/\rho g = 5$	$\eta = 6$ $P_b/\rho g = 10$	$\eta = 4$ $P_b/\rho g = 20$	$\eta = 6$ $P_b/\rho g = 20$	$\eta = 10$ $P_b/\rho g = 20$	$\eta = 6$ $P_b/\rho g = 40$
2.5	66.9	66.9	66.9	66.9	66.9	66.9	66.9
47.5	70.0	69.7	69.5	69.2	69.2	69.2	68.9
97.5	73.0	72.5	72.1	71.4	71.4	71.5	71.1
147.5	75.5	74.9	74.3	73.4	73.4	73.5	73.0
197.5	77.7	76.9	76.2	75.0	75.1	75.2	74.7
247.5	79.4	78.5	77.8	76.4	76.5	76.6	76.0
297.5	80.8	79.9	79.0	77.6	77.7	77.8	77.2
347.5	81.9	80.9	80.0	78.5	78.6	78.7	78.1
397.5	82.7	81.6	80.7	79.1	79.2	79.3	78.7
447.5	83.2	82.1	81.1	79.5	79.6	79.7	79.1
497.5	83.3	82.2	81.2	79.6	79.7	79.9	79.2
Y_a	83.3	88.2	93.2	100*	100*	100*	100*
L_e	1000	1155	1303	--	--	--	--

Table F-10
 Equilibrium Water Table Profile,
 $Y_d/D = 0$, $q. = -.02$.

Distance from Drain	Water Table Height						
	No Cap. Flow	$\eta = 6$ $P_b/\rho g = 5$	$\eta = 6$ $P_b/\rho g = 10$	$\eta = 4$ $P_b/\rho g = 20$	$\eta = 6$ $P_b/\rho g = 20$	$\eta = 10$ $P_b/\rho g = 20$	$\eta = 6$ $P_b/\rho g = 40$
2.5	7.1	7.1	7.1	7.1	7.1	7.1	7.1
47.5	30.1	26.0	22.9	18.0	18.7	19.1	14.4
97.5	42.0	37.3	33.5	26.7	27.7	28.4	20.9
147.5	50.2	45.3	41.2	33.4	34.6	35.4	26.2
197.5	56.3	51.3	47.0	38.6	39.9	40.8	30.5
247.5	61.0	55.9	51.5	42.8	44.1	45.1	34.0
297.5	64.6	59.5	55.0	46.0	47.4	48.4	36.7
347.5	67.3	62.2	57.6	48.4	49.8	50.8	38.8
397.5	69.2	64.0	59.4	50.1	51.5	52.6	40.3
447.5	70.3	65.1	60.5	51.1	52.5	53.6	41.2
497.5	70.7	65.5	60.9	51.5	52.9	54.0	41.5
Y_a	70.7	71.5	73.1	80.1	77.1	76.0	89.9
L_e	1000	1011	1034	1153	1090	1075	1271

Table F-11
 Equilibrium Water Table Profile,
 $Y_d/D = 1/3, \quad q. = -.02.$

Distance from Drain	Water Table Height						
	No Cap. Flow	$\eta = 6$ $P_b/\rho g = 5$	$\eta = 6$ $P_b/\rho g = 10$	$\eta = 4$ $P_b/\rho g = 20$	$\eta = 6$ $P_b/\rho g = 20$	$\eta = 10$ $P_b/\rho g = 20$	$\eta = 6$ $P_b/\rho g = 40$
2.5	34.1	34.1	34.1	34.1	34.1	34.1	34.1
47.5	44.9	43.6	42.6	40.8	41.0	41.2	39.2
97.5	53.6	51.6	49.9	46.9	47.3	47.6	44.0
147.5	60.2	57.8	55.7	51.8	52.4	52.8	48.1
197.5	65.4	62.7	60.4	55.9	56.6	57.1	51.5
247.5	69.5	66.6	64.1	59.2	60.0	60.5	54.4
297.5	72.7	69.7	67.1	61.9	62.6	63.2	56.7
347.5	75.1	72.0	69.3	63.9	64.7	65.2	58.5
397.5	76.8	73.6	70.8	65.3	66.1	66.7	59.7
447.5	77.8	74.6	71.8	66.2	66.9	67.6	60.5
497.5	78.2	74.9	72.1	66.5	67.2	67.9	60.8
Y_a	78.2	81.0	84.2	95.1	91.4	89.9	100*
L_e	1000	1044	1093	1260	1204	1181	--

Table F-12
 Equilibrium Water Table Profile,
 $Y_d/D = 2/3, \quad q. = -.02.$

Distance from Drain	Water Table Height						
	No Cap. Flow	$\eta = 6$ $P_b/\rho g = 5$	$\eta = 6$ $P_b/\rho g = 10$	$\eta = 4$ $P_b/\rho g = 20$	$\eta = 6$ $P_b/\rho g = 20$	$\eta = 10$ $P_b/\rho g = 20$	$\eta = 6$ $P_b/\rho g = 40$
2.5	67.0	67.0	67.0	67.0	67.0	67.0	67.0
47.5	73.1	72.7	72.3	71.6	71.6	71.7	71.3
97.5	78.8	77.9	77.2	76.0	76.1	76.2	75.6
147.5	83.4	82.3	81.3	79.8	79.9	80.0	79.4
197.5	87.3	85.9	84.8	83.0	83.1	83.2	82.6
247.5	90.4	88.9	87.6	85.8	85.9	86.0	85.4
297.5	92.9	91.3	89.9	88.1	88.2	88.3	87.7
347.5	94.8	93.1	91.7	89.9	90.0	90.0	89.5
397.5	96.1	94.4	93.0	91.1	91.2	91.3	90.7
447.5	96.9	95.1	93.7	91.9	92.0	92.1	91.5
497.5	97.2	95.4	94.0	92.2	92.3	92.4	91.8
Y_a	97.2	100*	100*	100*	100*	100*	100*
L_e	1000	--	--	--	--	--	--

Table F-13
 Equilibrium Water Table Profile,
 $Y_d/D = 0$, $q. = -.01$, $L = 500$.

Distance from Drain	Water Table Height						
	No Cap. Flow	$\eta = 6$ $P_b/\rho g = 5$	$\eta = 6$ $P_b/\rho g = 10$	$\eta = 4$ $P_b/\rho g = 20$	$\eta = 6$ $P_b/\rho g = 20$	$\eta = 10$ $P_b/\rho g = 20$	$\eta = 6$ $P_b/\rho g = 40$
1.25	2.5	2.5	2.5	2.5	2.5	2.5	2.5
23.75	10.6	7.3	5.8	4.3	4.4	4.6	3.6
48.75	14.8	10.9	8.6	6.0	6.3	6.5	4.6
73.75	17.7	13.5	10.8	7.4	7.8	8.1	5.5
98.75	19.9	15.4	12.5	8.6	9.0	9.4	6.2
123.75	21.6	17.0	13.9	9.5	10.1	10.5	6.9
148.75	22.9	18.2	14.9	10.3	10.9	11.3	7.4
173.75	23.8	19.1	15.7	10.9	11.5	12.0	7.8
198.75	24.5	19.7	16.3	11.3	12.0	12.5	8.1
223.75	24.9	20.1	16.6	11.6	12.2	12.7	8.2
248.75	25.0	20.2	16.8	11.7	12.3	12.8	8.3
Y_a	25.0	26.2	28.9	40.3	36.5	34.8	56.7
L_e	500	524	578	806	750	696	1134

Table F-14
 Equilibrium Water Table Profile,
 $Y_d/D = 0$, $q. = -.01$, $L = 1500$.

Distance from Drain	Water Table Height						
	No Cap. Flow	$\eta = 6$ $P_b/\rho g = 5$	$\eta = 6$ $P_b/\rho g = 10$	$\eta = 4$ $P_b/\rho g = 20$	$\eta = 6$ $P_b/\rho g = 20$	$\eta = 10$ $P_b/\rho g = 20$	$\eta = 6$ $P_b/\rho g = 40$
3.75	7.5	7.5	7.5	7.5	7.5	7.5	7.5
71.25	31.9	27.8	24.6	19.5	20.2	20.7	15.6
146.25	44.5	39.8	36.0	29.0	30.0	30.7	22.8
221.25	53.2	48.3	44.1	36.1	37.4	38.2	28.6
296.25	59.7	54.7	50.3	41.8	43.1	44.0	33.3
371.25	64.7	59.6	55.2	46.2	47.6	48.6	37.0
446.25	68.6	63.4	58.9	49.7	51.1	52.1	40.0
521.25	71.4	66.2	61.6	52.2	53.7	54.8	42.3
596.25	73.4	68.2	63.5	54.0	55.5	56.6	43.9
671.25	74.6	69.3	64.7	55.1	56.6	57.7	44.9
746.25	75.0	69.8	65.1	55.5	57.0	58.1	45.2
Y_a	75.0	75.8	77.3	84.1	81.2	80.1	93.6
L_e	1500	1516	1546	1682	1624	1602	1872

Table F-15
Decline of Water Table at Centerline,
 $Y_i/D = 1/3, \quad Y_d/D = 0.$

Water Table Height							
Time	No Cap. Flow	$\eta = 6$ $P_b/\rho g = 5$	$\eta = 6$ $P_b/\rho g = 10$	$\eta = 4$ $P_b/\rho g = 20$	$\eta = 6$ $P_b/\rho g = 20$	$\eta = 10$ $P_b/\rho g = 20$	$\eta = 6$ $P_b/\rho g = 40$
1×10^4	1.00	1.00	.99	.98	.99	1.00	.97
1.8	1.00	1.00	.99	.97	.99	.99	.96
3.2	1.00	.99	.99	.96	.98	.99	.94
5.6	.99	.98	.98	.92	.95	.96	.86
1×10^5	.98	.95	.92	.81	.87	.89	.71
1.8	.92	.86	.82	.64	.72	.76	.50
3.2	.82	.73	.66	.43	.53	.58	.29
5.6	.69	.56	.47	.23	.33	.38	.12
1×10^6	.53	.38	.29	.08	.16	.21	.03
1.8	.38	.22	.15	.01	.06	.09	.00
3.2	.25	.11	.06	.00	.01	.03	
5.6	.16	.05	.02		.00	.01	
1×10^7	.09	.01	.00			.00	
$t_s \times 10^{-4}$	35.0	47.0	62.5	∞	157	136	∞
L_e	1000	1140	1340	∞	2090	1940	∞

Table F-16
Decline of Water Table at Centerline,
 $Y_i/D = 2/3, \quad Y_d/D = 0.$

Water Table Height							
Time	No Cap. Flow	$\eta = 6$ $P_b/\rho g = 5$	$\eta = 6$ $P_b/\rho g = 10$	$\eta = 4$ $P_b/\rho g = 20$	$\eta = 6$ $P_b/\rho g = 20$	$\eta = 10$ $P_b/\rho g = 20$	$\eta = 6$ $P_b/\rho g = 40$
1×10^4	1.00	1.00	1.00	.98	.99	1.00	.91
1.8	1.00	1.00	.99	.98	.99	.99	.89
3.2	.99	.99	.98	.94	.96	.97	.82
5.6	.97	.95	.93	.83	.88	.91	.67
1×10^5	.90	.86	.83	.67	.74	.79	.47
1.8	.80	.73	.68	.46	.56	.62	.28
3.2	.66	.56	.50	.27	.37	.44	.14
5.6	.50	.39	.33	.12	.21	.27	.04
1×10^6	.35	.24	.18	.03	.01	.14	.00
1.8	.23	.13	.09	.00	.03	.06	
3.2	.14	.06	.03		.01	.02	
5.6	.08	.02	.01		.00	.00	
1×10^7	.05	.01	.00				
$t_s \times 10^{-4}$	17.6	19.7	22.5	23.2	26.2	29.0	44.5
L_e	1000	1040	1120	1140	1210	1280	1590

Table F-17
Decline of Water Table at Centerline,
 $Y_i/D = 2/3, \quad Y_d/D = 1/3.$

Water Table Height							
Time	No Cap. Flow	$\eta = 6$ $P_b/\rho g = 5$	$\eta = 6$ $P_b/\rho g = 10$	$\eta = 4$ $P_b/\rho g = 20$	$\eta = 6$ $P_b/\rho g = 20$	$\eta = 10$ $P_b/\rho g = 20$	$\eta = 6$ $P_b/\rho g = 40$
1×10^4	1.00	1.00	1.00	.97	.99	.99	.83
1.8	1.00	.99	.99	.96	.98	.99	.80
3.2	.99	.98	.97	.90	.94	.96	.70
5.6	.95	.92	.90	.76	.82	.87	.50
1×10^5	.86	.80	.76	.55	.64	.71	.27
1.8	.71	.62	.56	.30	.41	.50	.07
3.2	.51	.40	.34	.10	.21	.29	.00
5.6	.31	.21	.16	.00	.07	.12	
1×10^6	.15	.08	.05		.01	.03	
1.8	.05	.02	.01		.00	.00	
3.2	.01	.00	.00				
5.6	.00						
$t_{.8} \times 10^{-4}$	13.0	18.0	24.8	∞	53.5	53.5	∞
L_e	1000	1170	1360	∞	2010	2010	∞

Table F-18
Decline of Water Table at Centerline,
 $Y_i/D = 1, \quad Y_d/D = 0.$

Water Table Height							
Time	No Cap. Flow	$\eta = 6$ $P_b/\rho g = 5$	$\eta = 6$ $P_b/\rho g = 10$	$\eta = 4$ $P_b/\rho g = 20$	$\eta = 6$ $P_b/\rho g = 20$	$\eta = 10$ $P_b/\rho g = 20$	$\eta = 6$ $P_b/\rho g = 40$
1×10^4	1.00	1.00	1.00	1.00	1.00	1.00	1.00
1.8	1.00	.99	.99	.98	.98	.98	.98
3.2	.98	.95	.94	.91	.91	.92	.89
5.6	.93	.85	.80	.73	.74	.76	.67
1×10^5	.83	.72	.64	.48	.51	.54	.37
1.8	.70	.57	.49	.23	.34	.40	.12
3.2	.54	.42	.35	.13	.22	.28	.01
5.6	.39	.28	.22	.04	.12	.17	.00
1×10^6	.26	.17	.12	.00	.06	.09	
1.8	.16	.09	.06		.02	.04	
3.2	.10	.04	.02		.00	.01	
5.6	.06	.02	.00			.00	
1×10^7	.03	.00					
$t_{.8} \times 10^{-4}$	11.6	9.30	8.70	9.00	8.80	9.30	10.6
L_e	1000	880	850	870	860	880	940

Table F-19
Decline of Water Table at Centerline,
 $Y_i/D = 1, \quad Y_d/D = 1/3.$

Water Table Height							
Time	No Cap. Flow	$\eta = 6$ $P_b/\rho g = 5$	$\eta = 6$ $P_b/\rho g = 10$	$\eta = 4$ $P_b/\rho g = 20$	$\eta = 6$ $P_b/\rho g = 20$	$\eta = 10$ $P_b/\rho g = 20$	$\eta = 6$ $P_b/\rho g = 40$
1×10^4	1.00	1.00	1.00	1.00	1.00	1.00	1.00
1.8	.99	.98	.98	.97	.97	.98	.97
3.2	.97	.94	.92	.89	.89	.90	.87
5.6	.91	.80	.75	.66	.68	.69	.61
1×10^5	.78	.62	.52	.35	.38	.41	.26
1.8	.61	.45	.34	.10	.16	.23	.00
3.2	.42	.28	.19	.00	.06	.12	
5.6	.24	.14	.09		.01	.05	
1×10^6	.11	.05	.02		.00	.01	
1.8	.04	.01	.00			.00	
3.2	.00	.00					
$t_{.8} \times 10^{-4}$	9.25	7.65	7.95	9.65	8.90	8.90	14.8
L_e	1000	900	910	1005	960	960	1250

Table F-20
Decline of Water Table at Centerline,
 $Y_i/D = 1, \quad Y_d/D = 2/3.$

Water Table Height							
Time	No Cap. Flow	$\eta = 6$ $P_b/\rho g = 5$	$\eta = 6$ $P_b/\rho g = 10$	$\eta = 4$ $P_b/\rho g = 20$	$\eta = 6$ $P_b/\rho g = 20$	$\eta = 10$ $P_b/\rho g = 20$	$\eta = 6$ $P_b/\rho g = 40$
1×10^4	1.00	1.00	1.00	1.00	1.00	1.00	1.00
1.8	.99	.98	.97	.97	.97	.97	.97
3.2	.96	.91	.89	.88	.88	.88	.88
5.6	.88	.74	.69	.64	.64	.64	.63
1×10^5	.74	.49	.37	.27	.28	.29	.26
1.8	.53	.29	.14	.00	.00	.00	.00
3.2	.32	.14	.03				
5.6	.15	.05	.00				
1×10^6	.05	.01					
1.8	.01	.00					
3.2	.00						
$t_{.8} \times 10^4$	7.95	7.30	8.70	∞	15.6	14.3	∞
L_e	1000	950	1040	∞	1400	1340	∞

Table F-21
Decline of Water Table at Centerline,
 $Y_i/D = 2/3$, $Y_d/D = 1/3$, $L = 500$.

Water Table Height							
Time	No Cap. Flow	$\eta = 6$ $P_b/\rho g = 5$	$\eta = 6$ $P_b/\rho g = 10$	$\eta = 4$ $P_b/\rho g = 20$	$\eta = 6$ $P_b/\rho g = 20$	$\eta = 10$ $P_b/\rho g = 20$	$\eta = 6$ $P_b/\rho g = 40$
1×10^4	0.98	0.96	0.95	0.86	0.90	0.93	0.64
1.8	.92	.88	.85	.68	.76	.81	.41
3.2	.81	.73	.68	.44	.55	.63	.18
5.6	.63	.53	.47	.21	.32	.41	.02
1×10^5	.43	.32	.26	.04	.14	.21	.00
1.8	.24	.15	.10	.00	.03	.08	
3.2	.10	.05	.02		.00	.02	
5.6	.03	.01	.00			.00	
1×10^6	.01	.00					
1.8	.00						
$t_{.8} \times 10^{-4}$	3.25	4.50	7.10	∞	13.2	6.6	∞
L_e	500	590	750	∞	1020	720	∞

Table F-22
Decline of Water Table at Centerline,
 $Y_i/D = 2/3$, $Y_d/D = 1/3$, $L = 1500$.

Water Table Height							
Time	No Cap. Flow	$\eta = 6$ $P_b/\rho g = 5$	$\eta = 6$ $P_b/\rho g = 10$	$\eta = 4$ $P_b/\rho g = 20$	$\eta = 6$ $r_b/\rho g = 20$	$\eta = 10$ $P_b/\rho g = 20$	$\eta = 6$ $P_b/\rho g = 40$
1×10^4	1.00	1.00	1.00	0.97	0.99	0.99	0.83
1.8	1.00	1.00	1.00	.97	.99	.99	.82
3.2	1.00	1.00	.99	.96	.98	.99	.80
5.6	.99	.99	.98	.93	.96	.97	.74
1×10^5	.97	.95	.93	.83	.88	.91	.58
1.8	.91	.86	.82	.64	.72	.78	.36
3.2	.78	.70	.64	.40	.51	.59	.15
5.6	.60	.49	.43	.17	.28	.37	.08
1×10^6	.39	.28	.22	.02	.11	.18	.00
1.8	.21	.12	.08	.00	.02	.06	
3.2	.08	.03	.02		.00	.01	
5.6	.02	.00	.00			.00	
1×10^7	.00						
$t_{.8} \times 10^{-5}$	3.00	4.00	5.35	∞	12.0	6.0	∞
L_e	1500	1750	2000	∞	2900	2130	∞

Table F-23
Decline of Water Table at Centerline
 $Y_i/D = 1/3, \quad Y_d/D = 0, \quad H_s = 0.$

Water Table Height		
Time	$\eta = 6$ $P_b/\rho g = 20$	$\eta = 6$ $P_b/\rho g = 40$
1×10^4	1.00	1.00
1.8	1.00	1.00
3.2	.99	.98
5.6	.97	.94
1×10^5	.91	.83
1.8	.79	.67
3.2	.62	.47
5.6	.42	.28
1×10^6	.25	.14
1.8	.12	.06
3.2	.05	.02
5.6	.01	.01
1×10^7	.00	.00

KEY WORDS: Drainage, Aeration, Capillary Pressure, Saturation, Permeability, Steady Flow, Transient Flow, Water Table.

ABSTRACT: The effects of soil aeration requirements on permissible drain spacing were analyzed for both equilibrium and transient drainage problem. The presence of a zone of insufficient aeration above the water table required that drain spacing must be narrower than is calculated by classical techniques if the plant root zone is maintained adequately aerated. A one-dimensional model was developed to simulate drainage in soils where the flow and storage in the capillary region are significant. The contribution of the capillary region was described analytically in terms of the measureable soil properties and the rate of percolation to the water table. Drainage tests conducted in a sand-filled flume confirmed that the numerical model adequately described the total flow system. Further analyses were

KEY WORDS: Drainage, Aeration, Capillary Pressure, Saturation, Permeability, Steady Flow, Transient Flow, Water Table.

ABSTRACT: The effects of soil aeration requirements on permissible drain spacing were analyzed for both equilibrium and transient drainage problem. The presence of a zone of insufficient aeration above the water table required that drain spacing must be narrower than is calculated by classical techniques if the plant root zone is maintained adequately aerated. A one-dimensional model was developed to simulate drainage in soils where the flow and storage in the capillary region are significant. The contribution of the capillary region was described analytically in terms of the measureable soil properties and the rate of percolation to the water table. Drainage tests conducted in a sand-filled flume confirmed that the numerical model adequately described the total flow system. Further analyses were

KEY WORDS: Drainage, Aeration, Capillary Pressure, Saturation, Permeability, Steady Flow, Transient Flow, Water Table.

ABSTRACT: The effects of soil aeration requirements on permissible drain spacing were analyzed for both equilibrium and transient drainage problem. The presence of a zone of insufficient aeration above the water table required that drain spacing must be narrower than is calculated by classical techniques if the plant root zone is maintained adequately aerated. A one-dimensional model was developed to simulate drainage in soils where the flow and storage in the capillary region are significant. The contribution of the capillary region was described analytically in terms of the measureable soil properties and the rate of percolation to the water table. Drainage tests conducted in a sand-filled flume confirmed that the numerical model adequately described the total flow system. Further analyses were

KEY WORDS: Drainage, Aeration, Capillary Pressure, Saturation, Permeability, Steady Flow, Transient Flow, Water Table.

ABSTRACT: The effects of soil aeration requirements on permissible drain spacing were analyzed for both equilibrium and transient drainage problem. The presence of a zone of insufficient aeration above the water table required that drain spacing must be narrower than is calculated by classical techniques if the plant root zone is maintained adequately aerated. A one-dimensional model was developed to simulate drainage in soils where the flow and storage in the capillary region are significant. The contribution of the capillary region was described analytically in terms of the measureable soil properties and the rate of percolation to the water table. Drainage tests conducted in a sand-filled flume confirmed that the numerical model adequately described the total flow system. Further analyses were

conducted using the numerical model to determine the effects of bubbling pressure head pore-size distribution on the position of the water table. These analyses showed that the water table is always lower than predicted by methods that ignore the capillary region. The lowering of the water table by the presence of the capillary region is increased by a higher bubbling pressure, a wider distribution of pore sizes, and a larger percolation rate. It was shown that the region of inadequate aeration is always thicker than the amount by which capillary flow lowers the water table. As a result, the depth of aerated soil is always less than predicted by the classical drainage equations.

Drainage Design Based Upon Aeration
Harold Duke
Hydrology Paper #61
Colorado State University

conducted using the numerical model to determine the effects of bubbling pressure head pore-size distribution on the position of the water table. These analyses showed that the water table is always lower than predicted by methods that ignore the capillary region. The lowering of the water table by the presence of the capillary region is increased by a higher bubbling pressure, a wider distribution of pore sizes, and a larger percolation rate. It was shown that the region of inadequate aeration is always thicker than the amount by which capillary flow lowers the water table. As a result, the depth of aerated soil is always less than predicted by the classical drainage equations.

Drainage Design Based Upon Aeration
Harold Duke
Hydrology Paper #61
Colorado State University

conducted using the numerical model to determine the effects of bubbling pressure head pore-size distribution on the position of the water table. These analyses showed that the water table is always lower than predicted by methods that ignore the capillary region. The lowering of the water table by the presence of the capillary region is increased by a higher bubbling pressure, a wider distribution of pore sizes, and a larger percolation rate. It was shown that the region of inadequate aeration is always thicker than the amount by which capillary flow lowers the water table. As a result, the depth of aerated soil is always less than predicted by the classical drainage equations.

Drainage Design Based Upon Aeration
Harold Duke
Hydrology Paper #61
Colorado State University

conducted using the numerical model to determine the effects of bubbling pressure head pore-size distribution on the position of the water table. These analyses showed that the water table is always lower than predicted by methods that ignore the capillary region. The lowering of the water table by the presence of the capillary region is increased by a higher bubbling pressure, a wider distribution of pore sizes, and a larger percolation rate. It was shown that the region of inadequate aeration is always thicker than the amount by which capillary flow lowers the water table. As a result, the depth of aerated soil is always less than predicted by the classical drainage equations.

Drainage Design Based Upon Aeration
Harold Duke
Hydrology Paper #61
Colorado State University

LIST OF PREVIOUS 25 PAPERS

- No. 36 Suitability of the Upper Colorado River Basin for Precipitation Management, by Hiroshi Nakamichi and H. J. Morel-Seytoux, October 1969.
- No. 37 Regional Discrimination of Change in Runoff, by Viboon Nimmanit and Hubert J. Morel-Seytoux, November 1969.
- No. 38 Evaluation of the Effect of Impoundment on Water Quality in Cheney Reservoir, by J. C. Ward and S. Karaki, March 1970.
- No. 39 The Kinematic Cascade as a Hydrologic Model, by David F. Kibler and David A. Woolhiser, February 1970.
- No. 40 Application of Run-Lengths to Hydrologic Series, by Jaime Saldarriaga and Vujica Yevjevich, April 1970.
- No. 41 Numerical Simulation of Dispersion in Groundwater Aquifers, by Donald Lee Reddell and Daniel K. Sunada, June 1970.
- No. 42 Theoretical Probability Distribution for Flood Peaks, by Emir Zelenhasic, December 1970.
- No. 43 Flood Routing Through Storm Drains, Part I, Solution of Problems of Unsteady Free Surface Flow in a Storm Drain, by V. Yevjevich and A. H. Barnes, November 1970.
- No. 44 Flood Routing Through Storm Drains, Part II, Physical Facilities and Experiments, by V. Yevjevich and A. H. Barnes, November 1970.
- No. 45 Flood Routing Through Storm Drains, Part III, Evaluation of Geometric and Hydraulic Parameters, by V. Yevjevich and A. H. Barnes, November 1970.
- No. 46 Flood Routing Through Storm Drains, Part IV, Numerical Computer Methods of Solution, by V. Yevjevich and A. H. Barnes, November 1970.
- No. 47 Mathematical Simulation of Infiltrating Watersheds, by Roger E. Smith and David A. Woolhiser, January 1971.
- No. 48 Models for Subsurface Drainage, by W. E. Hedstrom, A. T. Corey and H. R. Duke, February 1971.
- No. 49 Infiltration Affected by Flow of Air, by David B. McWhorter, May 1971.
- No. 50 Probabilities of Observed Droughts, by Jaime Millan and Vujica Yevjevich, June 1971.
- No. 51 Amplification Criterion of Gradually Varied, Single Peaked Waves, by John Peter Jolly and Vujica Yevjevich, December 1971.
- No. 52 Stochastic Structure of Water Use Time Series, by Jose D. Salas-La Cruz and Vujica Yevjevich, June 1972.
- No. 53 Agricultural Response to Hydrologic Drought, by V. J. Bidwell, July 1972.
- No. 54 Loss of Information by Discretizing Hydrologic Series, by Mogens Dyhr-Nielsen, October 1972.
- No. 55 Drought Impact on Regional Economy, by Jaime Millan, October 1972.
- No. 56 Structural Analysis of Hydrologic Time Series, by Vujica Yevjevich, November 1972.
- No. 57 Range Analysis for Storage Problems of Periodic-Stochastic Processes, by Jose Salas-La Cruz, November 1972.
- No. 58 Applicability of Canonical Correlation in Hydrology, by Padoong Torranin, December 1972.
- No. 59 Transposition of Storms, by Vijay Kumar Gupta, December 1972.
- No. 60 Response of Karst Aquifers to Recharge, by Walter G. Knisel, December 1972.